SAND2023-10906R

GDSA Framework Development and Process Model Integration FY2023

Spent Fuel and Waste Disposition

Prepared for
U.S. Department of Energy
Spent Fuel and Waste Science and Technology

P.E. Mariner, C.J. Curry,
B.J. Debusschere, D.E. Fukuyama,
J.A. Harvey, R.C. Leone, C.M. Mendez,
J.L. Prouty, R.D. Rogers, L.P. Swiler

Sandia National Laboratories

September 20, 2023
M2SF-23SN010304082
SAND2023-xxxxx R

Sandia National Laboratories
U.S. DEPARTMENT OF ENERGY NNSA

Sandia National Laboratories is a multimission laboratory managed and operated by National Technology & Engineering Solutions of Sandia, LLC, a wholly owned subsidiary of Honeywell International Inc., for the U.S. Department of Energy's National Nuclear Security Administration under contract DE-NA0003525.

DISCLAIMER

This information was prepared as an account of work sponsored by an agency of the U.S. Government. Neither the U.S. Government nor any agency thereof, nor any of their employees, makes any warranty, expressed or implied, or assumes any legal liability or responsibility for the accuracy, completeness, or usefulness, of any information, apparatus, product, or process disclosed, or represents that its use would not infringe privately owned rights. References herein to any specific commercial product, process, or service by trade name, trade mark, manufacturer, or otherwise, does not necessarily constitute or imply its endorsement, recommendation, or favoring by the U.S. Government or any agency thereof. The views and opinions of authors expressed herein do not necessarily state or reflect those of the U.S. Government or any agency thereof.

DISCLAIMER

This is a technical report that does not take into account contractual limitations or obligations under the Standard Contract for Disposal of Spent Nuclear Fuel and/or High-Level Radioactive Waste (Standard Contract) (10 CFR Part 961). For example, under the provisions of the Standard Contract, spent nuclear fuel in multi-assembly canisters is not an acceptable waste form, absent a mutually agreed to contract amendment.

To the extent discussions or recommendations in this report conflict with the provisions of the Standard Contract, the Standard Contract governs the obligations of the parties, and this report in no manner supersedes, overrides, or amends the Standard Contract.

This report reflects technical work which could support future decision making by DOE. No inferences should be drawn from this report regarding future actions by DOE, which are limited both by the terms of the Standard Contract and Congressional appropriations for the Department to fulfill its obligations under the Nuclear Waste Policy Act including licensing and construction of a spent nuclear fuel repository.

Sandia National Laboratories is a multi-mission laboratory managed and operated by National Technology & Engineering Solutions of Sandia, LLC., a wholly owned subsidiary of Honeywell International, Inc., for the U.S. Department of Energy's National Nuclear Security Administration under contract DE-NA0003525.

U.S. DEPARTMENT OF ENERGY

Sandia National Laboratories

APPENDIX E
NFCSC DOCUMENT COVER SHEET[1]

Name/Title of Deliverable/Milestone/Revision No. GDSA Framework Development and Process Model Integration FY 2023 / M2SF-23SN010304082

Work Package Title and Number GDSA – Framework Development – SNL / SF-23SN01030408

Work Package WBS Number 1.08.01.03.04

Responsible Work Package Manager Paul Mariner
(Name/Signature)

Date Submitted

Quality Rigor Level for Deliverable/Milestone[2]	☐ QRL-1 ☐ Nuclear Data	☐ QRL-2	☒ QRL-3	☐ QRL-4 Lab QA Program[3]

This deliverable was prepared in accordance with Sandia National Laboratories
(Participant/National Laboratory Name)

QA program which meets the requirements of
☒ DOE Order 414.1 ☐ NQA-1 ☐ Other

This Deliverable was subjected to:

☒ Technical Review ☐ Peer Review

Technical Review (TR)
Review Documentation Provided
☐ Signed TR Report or,
☐ Signed TR Concurrence Sheet or,
☐ Signature of TR Reviewer(s) below

Peer Review (PR)
Review Documentation Provided
☐ Signed PR Report or,
☐ Signed PR Concurrence Sheet or,
☐ Signature of PR Reviewer(s) below

Name and Signature of Reviewers

Michael Nole

NOTE 1: *Appendix E should be filled out and submitted with the deliverable. Or, if the PICS:NE system permits, completely enter all applicable information in the PICS:NE Deliverable Form. The requirement is to ensure that all applicable information is entered either in the PICS:NE system or by using the NFCSC Document Cover Sheet.*

- *In some cases there may be a milestone where an item is being fabricated, maintenance is being performed on a facility, or a document is being issued through a formal document control process where it specifically calls out a formal review of the document. In these cases, documentation (e.g., inspection report, maintenance request, work planning package documentation or the documented review of the issued document through the document control process) of the completion of the activity, along with the Document Cover Sheet, is sufficient to demonstrate achieving the milestone.*

NOTE 2: *If QRL 1, 2, or 3 is not assigned, then the QRL 4 box must be checked, and the work is understood to be performed using laboratory QA requirements. This includes any deliverable developed in conformance with the respective National Laboratory / Participant, DOE or NNSA-approved QA Program.*

NOTE 3: *If the lab has an NQA-1 program and the work to be conducted requires an NQA-1 program, then the QRL-1 box must be checked in the work Package and on the Appendix E cover sheet and the work must be performed in accordance with the Lab's NQA-1 program. The QRL-4 box should not be checked.*

ACKNOWLEDGEMENTS

This report documents fiscal year (FY) 2023 accomplishments in GDSA Framework development and process model integration. Many of the accomplishments highlighted in this report are described in more detail in other GDSA reports (e.g., Nole et al. 2023; LaForce et al. 2023a).

Coauthors contributing written sections:

Section 4.1.5	Uncertainty and Sensitivity Analysis	Laura Swiler
Appendix B	Development of FEPS-Activity Tracking Tool for Reference	Jeralyn Prouty, Ralph Rogers
Appendix C	Fuel Matrix Degradation Process Model Code Development in Fortran	Jacob Harvey
Appendix D	Surrogate Modeling of the Fuel Matrix Degradation (FMD) Process Model with Neural Ordinary Differential Equations	Bert Debusschere Caitlin Curry

In addition, the following people are acknowledged for past contributions included in edited form in this report: Geoff Freeze (Section 2) and Glenn Hammond (Section 4.3.2).

The authors thank Michael Nole of Sandia National Laboratories (SNL) for his thoughtful technical review and thank the staff from U.S. Department of Energy Office of Nuclear Energy (DOE-NE), Prasad Nair (DOE NE-81), Tim Gunter (DOE NE-81), and Dan Fagnant (DOE NE-81) for their discussions, oversight, and guidance on topics addressed in this report.

EXECUTIVE SUMMARY

The Spent Fuel and Waste Science and Technology (SFWST) Campaign of the U.S. Department of Energy (DOE) Office of Nuclear Energy (NE), Office of Spent Fuel & Waste Disposition (SFWD) is conducting research and development (R&D) on geologic disposal of spent nuclear fuel (SNF) and high-level nuclear waste (HLW). A high priority for SFWST disposal R&D is disposal system modeling (Sassani et al. 2021). The SFWST Geologic Disposal Safety Assessment (GDSA) work package is charged with developing a disposal system modeling and analysis capability for evaluating generic disposal system performance for nuclear waste in geologic media.

Purpose: This report describes fiscal year (FY) 2023 advances of the Geologic Disposal Safety Assessment (GDSA) performance assessment (PA) development groups of the SFWST Campaign. The common mission of these groups is to develop a geologic disposal system modeling capability for nuclear waste that can be used to assess probabilistically the performance of generic disposal options and generic sites. The modeling capability under development is called GDSA Framework (pa.sandia.gov). GDSA Framework is a coordinated set of codes and databases designed for probabilistically simulating the release and transport of disposed radionuclides from a repository to the biosphere for post-closure performance assessment. Primary components of GDSA Framework include PFLOTRAN to simulate the major features, events, and processes (FEPs) over time, Dakota to propagate uncertainty and analyze sensitivities, meshing codes to define the domain, and various other software for rendering properties, processing data, and visualizing results.

FY2023 Accomplishments: The FY2023 advances in GDSA Framework development include:

- *General GDSA Framework development*. Produced an automated workflow to generate probabilistic repository reference case meshes from a Geologic Framework Model (Section 4.1.1); added needed capabilities to the meshing code VoroCrust (Section 4.1.2); developed tracers to measure quantities of interest in disposal system models (Section 4.1.3); developed performance factor analysis to quantify and communicate the contributions of features and processes to overall disposal system performance (Section 4.1.4); evaluated Variogram Analysis of Response Surfaces (VARS), developed a “grouped sensitivity analysis” method, and ran a full probabilistic analysis on an updated shale reference case (Section 4.1.5); completed repository reference case models for Task F of the international DECOVALEX project and analyzed results (Section 4.1.6); improved generic reference case models for shale, crystalline, salt, and unsaturated alluvium host rocks (Section 4.1.7); maintained archives and advanced archive systems for project milestones and GDSA calculations (Section 4.1.8)

- *PFLOTRAN model capability development*. Sharpened strategies for prioritizing and implementing new model capabilities in PFLOTRAN (Section 4.2.2.1); completed implementation of fuel matrix degradation (FMD) processes in the new Fortran FMD code (Section 4.2.2.2; Appendix C); developed and tested a new Machine Learning FMD surrogate model that uses neural Ordinary Differential Equations (Section 4.2.2.3; Appendix D); completed pre-processors needed for the buffer erosion and waste package corrosion model (Section 4.2.2.4); improved the spacer grid degradation model (Section 4.2.2.5); completed the main functionality of the biosphere model (Section 4.2.2.6); improved the Dual Continuum Disconnected Matrix multi-continuum model (Section 4.2.2.7); implemented thermal secondary continuum capability in GENERAL mode (Section 4.2.2.8); improved the salinity-dependent equations of state and proposed an innovative approach for emulating salt creep in salt repository simulations (Section 4.2.2.9)

- *Software and hardware infrastructure*. Adopted much of the Scrum software development methodology for managing, prioritizing, and tracking PFLOTRAN development requests (Section 4.2.1.1); established 46 software requirements for all flow modes and added related verification tests in the GDSA Quality Assurance test framework (Section 4.2.1.2)

- *PFLOTRAN performance improvements*. Integrated Newton Trust Region Dogleg Cauchy solver with Global Implicit Reactive Transport mode and Nuclear Waste Transport (NWT) mode (Section 4.2.3.1); solved convergence issues for NWT mode (Section 4.2.3.2); added the capability of expressing capillary pressure and relative permeability functions using cubic splines (Section 4.2.3.3)

- *Outreach*. Engaged with the international community through leadership in DECOVALEX, geologic repository clubs, conferences, and publications (Section 4.3.1); developed and shared new versions and applications of open-source and freely available software used in GDSA Framework (Sections 4.3.2 and 4.1.2); held a virtual PFLOTRAN short course (Nole et al. 2023, Section 5.1); maintained an external GDSA Framework website (Section 4.3.3)

- *Integration and planning*. Updated the SFWST Disposal Research R&D 5-Year Plan (Section 3.1.2); mapped FY2023 GDSA activities to SFWST disposal near-term GDSA thrusts (Section 3.3); developed a FEPs-activity tracker to link DR activities with FEPs for specific repository reference cases (Section 3.4)

An important responsibility of the GDSA Framework development team is to integrate with disposal R&D activities across the SFWST Campaign to ensure that R&D activities support the parts of the generic safety cases being developed. In FY2023, the GDSA team participated with other scientists and engineers at LANL, LBNL, PNNL, ORNL, INL, ANL, DOE, and SNL in the development of discrete fracture network modeling, multi-continuum modeling, Geologic Framework Models, fuel matrix degradation process modeling, machine-learning surrogate models, DECOVALEX-2023 Task F performance assessment, and advanced biosphere modeling.

The ability to simulate increasingly complex repository reference cases continues to affirm that GDSA Framework can be used to simulate important multi-physics couplings directly in a total system safety assessment demonstration. Reference case repository applications show that GDSA Framework can simulate complex coupled processes in a multi-kilometer domain while simultaneously simulating sub-meter-scale coupled behavior in the vicinity of each modeled waste package. Continued development will further enhance the preparedness of GDSA Framework for application in the future when transitioning to a program with potential sites.

Future Work: The SFWST Disposal Research R&D 5-Year Plan will continue to guide GDSA work in the development of:

- Advanced coupled process simulation capabilities,
- State-of-the-art uncertainty and sensitivity analysis,
- Traceable, user-friendly workflow for GDSA Framework,
- Repository systems analysis for various disposal concepts and selected host rocks, and
- Development of geologic models with interactive, web-based visualization.

This report fulfills the GDSA Framework Development Work Package Level 2 Milestone – *GDSA Framework Development and Process Model Integration*, M2SF-23SN010304082.

CONTENTS

FIGURES

Page

TABLES

Page

NOMENCLATURE

1D, 2D, 3D	one-, two-, and three-dimensional
ANL	Argonne National Laboratory
ANS	American Nuclear Society
ANN	artificial neural network
BWR	boiling water reactor
CLT	corrosion layer thickness
CSNF	commercial spent nuclear fuel
CTN	calculation tracking number
DCDM	Dual Continuum Disconnected Matrix
DECOVALEX	Development of COupled models and their VALidation against Experiments
DFN	discrete fracture network
DOE	U.S. Department of Energy
DPC	dual-purpose canister
DR	disposal research
EBS	engineered barrier system
ECPM	equivalent continuous porous medium
Eq.	equation
FEP	feature, event, or process
FMD	Fuel Matrix Degradation
FVs	fracture volumes
FY	fiscal year
g	gram
GDSA	Geologic Disposal Safety Assessment
GIRT	Global Implicit Reactive Transport mode
GFM	geological framework model
GP	Gaussian process
GUI	graphical user interface
GWd	gigawatt day
HDF5	hierarchical data format, version 5
HLW	high-level nuclear waste
HPC	high-performance computing
IAEA	International Atomic Energy Agency
ID	identification number
IHLRWM	International High-Level Radioactive Waste Management
INL	Idaho National Laboratory
IRF	instant release fraction
IWM	Integrated Waste Management
K	Kelvin
K_D	distribution coefficient
km	kilometer
kNNr	k Nearest-Neighbors regressor
LANL	Los Alamos National Laboratory
LBNL	Lawrence Berkeley National Laboratory

LGPL	lesser general public license
LHS	Latin hypercube sampling
m	meter
M	molar
MATLAB	programming language by MathWorks
ML	machine learning
mm	millimeter
mM	millimolar
mol	mole
MPa	megapascal
MS	Microsoft
MTHM	metric tons of heavy metal
MWd	megawatt day
NA	not applicable
NBS	natural barrier system
NE	Office of Nuclear Energy
NEA	Nuclear Energy Agency
NGW	Next-Generation Workflow
NM	New Mexico
nODE	neural ordinary differential equation
NTRDC	Newton Trust Region Dogleg-Cauchy
NWT	Nuclear Waste Transport mode
ODE	ordinary differential equation
OECD	Organization for Economic Co-operation and Development
OoR	out of reactor
ORNL	Oak Ridge National Laboratory
PA	performance assessment
Pa	Pascal
PCE	Polynomial Chaos Expansion
PETSc	Portable Extensible Toolkit for Scientific Computation
PFLOTRAN	massively parallel reactive flow and transport model for describing subsurface processes (pflotran.org)
pH	negative logarithm of hydrogen ion activity
PNNL	Pacific Northwest National Laboratory
PWR	pressurized water reactor
QA	quality assurance
QoI	quantity (or quantities) of interest
R&D	research and development
s	seconds
S&T	Storage and Transportation
SA	sensitivity analysis
SDA	SFWD Document Archive
SFWD	Spent Fuel and Waste Disposition
SFWST	Spent Fuel and Waste Science and Technology
SKB	Swedish Nuclear Fuel and Waste Management Company
SNF	spent nuclear fuel
SNL	Sandia National Laboratories

THMC	thermal-hydrologic-mechanical-chemical
UA	uncertainty analysis
UFD	Used Fuel Disposition
UO_2	uranium dioxide
UQ	uncertainty quantification
U.S.	United States of America
VARS	Variogram Analysis of Response Surfaces
W	watt
WF	waste form
WIPP	Waste Isolation Pilot Plant
WP	waste package
yr	year

1 INTRODUCTION

The Spent Fuel and Waste Science and Technology (SFWST) Campaign of the U.S. Department of Energy (DOE) Office of Nuclear Energy (NE), Office of Spent Fuel & Waste Disposition (SFWD) is conducting research and development (R&D) on geologic disposal of spent nuclear fuel (SNF) and high-level nuclear waste (HLW). A high priority for SFWST disposal R&D is disposal system modeling (Sassani et al. 2021).

The SFWST Geologic Disposal Safety Assessment (GDSA) Framework Development work package is charged with developing an open-source probabilistic modeling and analysis capability for evaluating/estimating generic disposal system post-closure performance for nuclear waste disposal concepts in a range of geologic media. The modeling capability under development is called GDSA Framework (pa.sandia.gov). GDSA Framework is a coordinated set of codes and databases designed for probabilistically simulating the release and transport of disposed radionuclides from a repository to the biosphere for post-closure performance assessment.

The primary components of GDSA Framework include PFLOTRAN to simulate the major features, events, and processes (FEPs) over time, Dakota to propagate uncertainty and analyze sensitivities, meshing codes to define the domain, and various other software for rendering properties, processing data, and visualizing results. PFLOTRAN is a multi-physics thermal-hydrologic-chemical reaction and mass transport code (pflotran.org), and Dakota (dakota.sandia.gov) is used to propagate uncertainty and variability using multiple realizations and to quantify the effects of model parameters on model outputs (see Section 2.2 for details of both). These codes are designed for massively-parallel processing in a high-performance computing (HPC) environment.

Developing GDSA Framework in an open-source environment promotes collaboration with regulators, stakeholders, and the scientific community, facilitates development of the software, and enhances communication in a regulatory environment. GDSA Framework is being developed currently for generic disposal concepts so that it is poised to be applied efficiently in future programs to specific disposal concepts being evaluated for comparison to regulatory safety criteria.

GDSA Framework defines the state-of-the-art by evolving continuously with progress of the technology and science and provides a nimble tool for application in the full range of possible future systems for more specific evaluations once a program is reinstituted for performance assessment (PA) of any potential candidate sites. The current focus is on incorporation of the most important technical processes for barrier capabilities/functions (e.g., radionuclide retention). Advances in computing speed over time are expected to enable higher resolution and higher fidelity PA modeling in any future program.

For the near term, objectives are focused on including essential FEPs in GDSA Framework and on developing a suite of probabilistic generic repository reference case applications. In addition, the products of the near-term objectives are useful for evaluating the effects of FEPs and input parameters on repository performance, which in turn can direct R&D planning.

For fiscal year (FY) 2023, seven tasks were planned and addressed:

- Use the 5-year Disposal Research R&D Plan to help identify additional capabilities needed in the short term and long term to advance GDSA Framework (e.g., multiphase processes, temperature dependencies, chemical processes, engineered barrier system (EBS) degradation processes, computational efficiency, gridding capability).

- Integrate subsystem models developed under this and other SFWST work packages into GDSA Framework software and safety assessments (e.g., waste form (WF) degradation, waste package (WP) degradation, EBS chemistry, EBS flow and transport, discrete fracture networks, thermal-hydrologic-mechanical-chemical (THMC) processes, natural system flow and transport, geologic framework models).

- Develop and implement methods for computationally efficient multi-scale, multi-physics modeling (e.g., surrogate models, reduced-order models, physics-based machine learning, nested models). This task aims to improve integration of complicated processes in probabilistic safety assessments.

- Produce updated features, events, and processes (FEPs) evaluations for each generic host rock repository concept including engineered barrier systems. These new FEP updates will be implemented online to be used to map the relevant R&D activities for the generic concepts into the FEP that they address for strategic planning/progress tracking for closure of excluded and included FEPs (into GDSA). This is the first stage of reinventing the Disposal Research R&D Roadmap.

- Demonstrate components of GDSA Framework at national and international forums and support an international DECOVALEX activity for a multi-year PA modeling comparison of reference repository systems. Plan to conduct an international workshop to promote accelerated use of PFLOTRAN and other components of GDSA Framework worldwide to expand the user base, which creates additional testing of GDSA Framework components and further development by outside contributors.

- Participate in technical training (e.g., classes/workshops in Python, simulation and analysis software, or computational and analysis methods), technical conferences, and international clubs and initiatives with direct benefit to GDSA.

- Update the 5-year Disposal Research R&D plan to reflect developments in DOE priorities.

Section 2 of this report describes the conceptual model framework and the PFLOTRAN-based computational framework for GDSA Framework. Section 3 examines how the FY2023 activities of the GDSA Framework development team align with the 5-Year Plan near-term GDSA thrusts. It also describes the development of the recent update of the 5-Year Plan and the development of a FEPs-activity tracking tool that will link work activities with FEPs. Section 4 (and its supporting appendices) highlights the team's major advances and activities in FY2023. Conclusions are summarized in Section 5.

This report fulfills the requirements of the GDSA Framework Development work package (SF-23SN01030408) Level 2 Milestone – GDSA Framework Development and Process Model Integration FY2023, M2SF-23SN010304082. The work presented herein builds on previous reports (e.g., Mariner et al. 2022a).

2 GDSA FRAMEWORK

A safety case for a deep geologic disposal facility is a comprehensive set of bases and analyses designed, in part, to assess regulatory compliance with respect to safety standards. More specifically, it is a widely accepted approach for documenting the bases for the understanding of the disposal system, describing the key justifications for its safety, and acknowledging the unresolved uncertainties and their safety significance (OECD 2004; IAEA 2006; Freeze et al. 2013). A full safety case may only be constructed for a specific site with an integrated design, but aspects of a safety case may also be developed for generic systems being evaluated in the SFWST Campaign.

Building a generic safety case focuses on three primary components related most directly to post-closure safety assessments: 1) a safety strategy for the generic disposal concept, 2) technical bases for the natural and engineered barriers, and 3) a safety assessment of system performance.

- The safety strategy provides direction and boundaries for the safety case. It guides the safety case by identifying requirements for site location, repository design, and safety objectives.
- Technical bases are the laws of nature and the physical and chemical barriers that govern the system. They address each FEP that could potentially facilitate or inhibit the transport of radionuclides from the repository to the biosphere. Development of the technical bases involves site characterization (mainly as defined/constrained characteristics for generic sites), FEPs identification, waste inventory, barriers to radionuclide release and migration, radionuclide behavior, natural analogs, model validation, code verification, and uncertainty quantification.
- Safety assessment involves the analysis of technical bases to evaluate whether the objectives of the safety strategy are met. In safety assessment, each FEP screened in the technical bases is either included/incorporated into the probabilistic performance assessment (PA) model or is excluded and addressed in separate analyses or process model simulations. In the PA model, regulatory metrics (e.g., annual dose rate) are estimated with probabilistic calculations to compare to regulatory limits.

The goals and objectives of the GDSA Framework development team focus on safety assessment and, more specifically, on the development of the GDSA Framework modeling capability and the PA models of generic reference case applications simulated using GDSA Framework.

Performance assessment for underground geologic disposal of nuclear waste is an iterative process for evaluating a comprehensive set of FEPs to determine the safety relevant FEPs to include in a PA model. Probabilistic PA model simulations are performed to estimate the full range of behavior of the system including the pertinent variability and uncertainty in the system, and results are evaluated against system performance metrics (e.g., for evaluating key sensitivities needing further constraint or for assessing performance against regulatory requirements). Uncertainty and sensitivity analyses may also be performed to inform prioritization of additional research and/or model development within a program.

A PA model has a conceptual model framework and a computational framework. These frameworks are summarized in Sections 2.1 and 2.2, respectively. An overview of PA methodology and terminology is presented in Sevougian et al. (2014, Section 2.2), Meacham et al. (2011, Section 1) and elsewhere (Rechard 2002).

2.1 Conceptual Model Framework

A conceptual model framework for a PA model requires a coherent representation of pertinent FEPs. Figure 2-1 schematically illustrates the conceptual model framework for a repository system. To calculate

a dose to a receptor in the biosphere, radionuclides released from the waste form must pass through the repository EBS and the surrounding natural barrier system (NBS).

A FEPs database like the one developed and described in Freeze et al. (2011) can be used to help identify a full set of potentially important FEPs for a specific conceptual repository model. Many of the FEPs in a FEPs database may be directly simulated in the PA model. In a comprehensive PA, excluded FEPs (i.e., FEPs not simulated in the PA model) must be addressed in separate analyses and arguments.

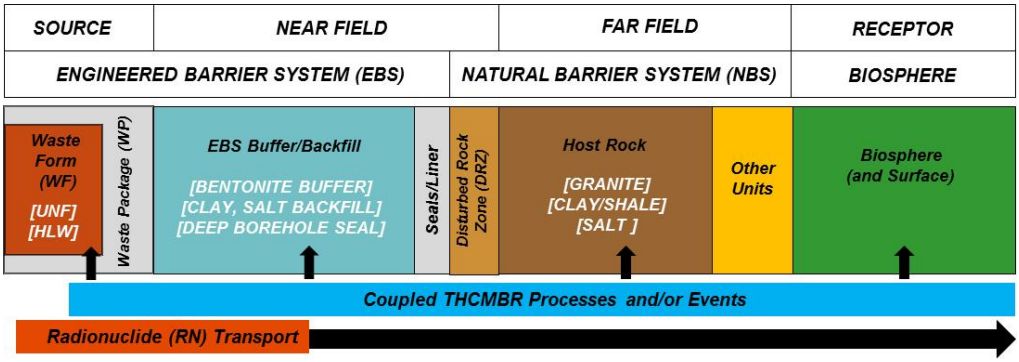

Figure 2-1 Schematic diagram of the conceptual model framework of a generic geologic disposal system PA model

2.2 Computational Framework

Performance assessment of a geologic repository is aided by directly modeling the important coupled processes in the system and executing multiple probabilistic realizations. The approach of propagating uncertainty in computational PA models is a continuation of the successful modeling approaches adopted for the Waste Isolation Pilot Plant (WIPP) PAs (Rechard 1995; Rechard 2002; Rechard and Tierney 2005) and for disposal of SNF and HLW in volcanic tuff (Rechard and Stockman 2014).

GDSA Framework is used to execute the computational PA model. GDSA Framework consists of the following components:

- Input parameter databases
- Software for sampling, sensitivity analysis, uncertainty quantification (UQ), workflow, and traceability (Dakota)
- Petascale multiphase flow and reactive transport code (PFLOTRAN), working in concert with coupled process model codes (e.g., Fuel Matrix Degradation (FMD) model)
- Computational support software and scripts for meshing, stochastic preprocessing, output processing, and visualization of results (e.g., CUBIT, VoroCrust, dfnWorks, Python, ParaView).

The two primary components of this computational framework are PFLOTRAN and Dakota. PFLOTRAN is a thermal-hydrologic-chemical multi-physics code used to simulate coupled multi-physics processes affecting waste isolation in a repository system and transport of released radionuclides to the biosphere over time. Simulated processes include heat flow, fluid flow, waste dissolution, radionuclide release, radionuclide decay and ingrowth, precipitation and dissolution of secondary phases, and radionuclide transport. Dakota is an uncertainty sampling and propagation code. Dakota is used to propagate uncertainty in PFLOTRAN simulations and to analyze PFLOTRAN results to assess sensitivities of model processes and inputs. Dakota is also used to graphically run and document the entire

workflow of probabilistic simulations. These two codes are described in more detail in Sections 2.2.1 and 2.2.2.

The flow of data and calculations through the components of GDSA Framework is illustrated in Figure 2-2. In a probabilistic simulation, Dakota's Next Gen Workflow manages the entire simulation from the generation of stochastic input for each PA realization to the execution of PFLOTRAN and production of custom output files via Python scripts. The sampled inputs are used by PFLOTRAN and its coupled process models to simulate source term release, EBS evolution, flow and transport through the EBS and NBS, and uptake in the biosphere. After the simulation, various software (e.g., Python, Matplotlib, ParaView) may be used to analyze and illustrate the output results of parameters and performance metrics. Dakota may also be used to evaluate the effects of parameter uncertainty on specific outputs.

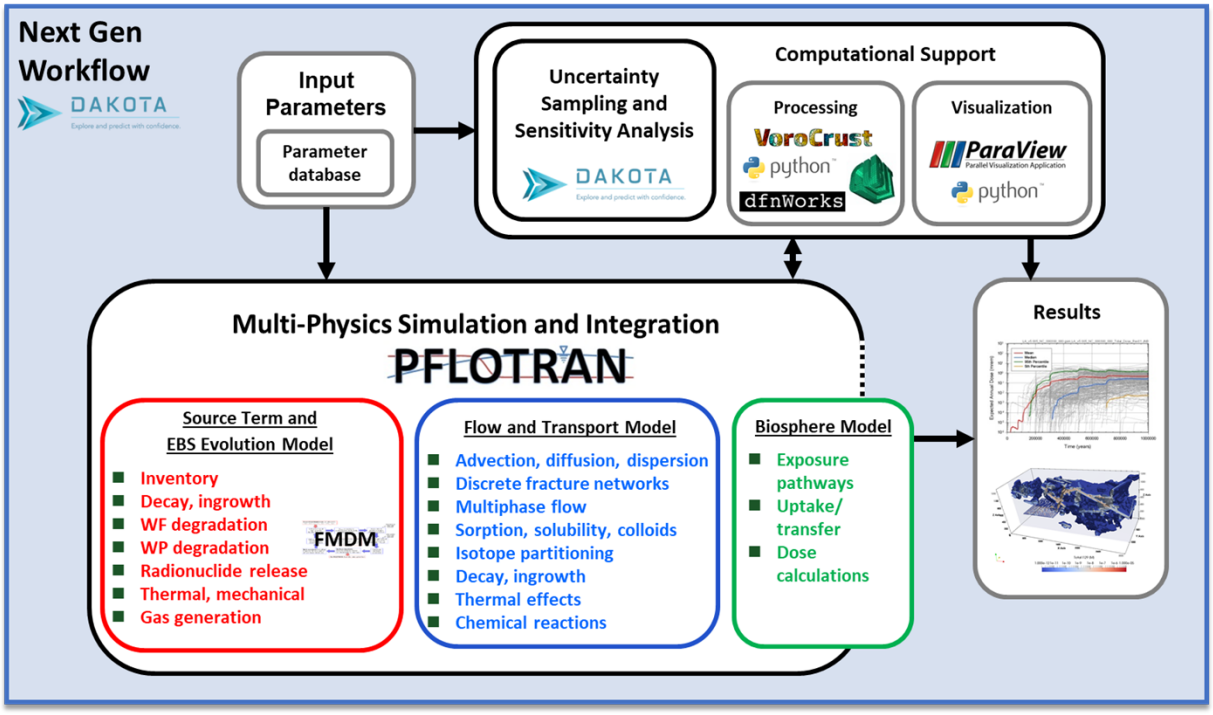

Figure 2-2 GDSA Framework structure

2.2.1 PFLOTRAN

PFLOTRAN (Hammond et al. 2011a; Lichtner and Hammond 2012) is an open source, reactive multi-phase flow and transport simulator designed to leverage massively-parallel HPC to simulate subsurface earth system processes. PFLOTRAN has been employed on petascale leadership-class DOE computing resources (e.g., Jaguar [at Oak Ridge National Laboratory (ORNL)] and Franklin/Hopper [at Lawrence Berkeley National Laboratory (LBNL)]) to simulate THC processes at the Nevada Test Site (Mills et al. 2007), multi-phase CO_2-H_2O for carbon sequestration (Lu and Lichtner 2007), CO_2 leakage within shallow aquifers (Navarre-Sitchler et al. 2013), and uranium fate and transport at the Hanford 300 Area (Hammond et al. 2007; Hammond et al. 2008; Hammond and Lichtner 2010; Hammond et al. 2011b; Chen et al. 2012; Chen et al. 2013). PFLOTRAN is also under development for use in PA at the Waste Isolation Pilot Plant (WIPP).

PFLOTRAN solves the non-linear partial differential equations describing non-isothermal multi-phase flow, reactive transport, and geomechanics in porous media. Parallelization is achieved through domain

decomposition using the Portable Extensible Toolkit for Scientific Computation (PETSc) (Balay et al. 2013). PETSc provides a flexible interface to data structures and solvers that facilitate the use of parallel computing. PFLOTRAN is written in Fortran 2003/2008 and leverages state of the art Fortran programming (i.e. Fortran classes, pointers to procedures, etc.) to support its object-oriented design. The code provides "factories" within which the developer can integrate a custom set of process models and time integrators for simulating surface and subsurface multi-physics processes. PFLOTRAN employs a single, unified framework for simulating multi-physics processes on both structured and unstructured grid discretizations (i.e., there is no duplication of the code that calculates multi-physics process model functions in support of structured and unstructured discretizations). The code requires a small, select set of third-party libraries (e.g., MPI, PETSc, BLAS/LAPACK, HDF5, Metis/Parmetis). Both the unified structured/unstructured framework and the limited number of third-party libraries greatly facilitate usability for the end user.

2.2.2 Dakota

The Dakota software toolkit is open-source software developed and supported at Sandia National Laboratories (Adams et al. 2012; Adams et al. 2013). Dakota provides deterministic codes an extensible interface for propagating uncertainty into a set of realizations and for performing sensitivity analysis and optimization. GDSA Framework uses Dakota's sampling schemes, principally Latin Hypercube Sampling (LHS), to propagate input value uncertainty into probabilistic PFLOTRAN simulations. Dakota is also used in sensitivity analyses to analyze the effects of input value uncertainty on probabilistic GDSA Framework results.

The Next Gen Workflow capability of Dakota is used to develop GDSA Workflow, a graphical workflow interface to execute and manage probabilistic GDSA Framework applications (Ridgway 2020). GDSA Workflow improves automations, reproducibility, and traceability for GDSA Framework simulations. It autonomously collects inputs from multiple sources, modifies PFLOTRAN input files based on the inputs collected, runs the PFLOTRAN simulations, and runs a post-processing script to collect and visualize results and calculate additional quantities of interest. A demonstration of GDSA Workflow is provided in Appendix C of Mariner et al. (2020a).

3 ALIGNMENT AND DIRECTION

This section identifies high priorities for the GDSA control account and the most recent Roadmap (Sections 3.1 and 3.2), how current activities align with GDSA priorities (Section 3.3), and how FEPs are being integrated into the planning process for SWFST Disposal Research R&D (Section 3.4). In addition, Section 3.1.2 addresses the new 5-Year Plan update developed in FY2023 (Sassani et al. 2023).

3.1 5-Year Plan

3.1.1 5-Year Plan Update of FY2021

GDSA priorities for FY2022 and FY2023 were guided by the FY2021 5-Year Plan Update documented in *SFWST Disposal Research R&D 5-Year Plan – FY2021 Update* (Sassani et al. 2021). In that plan, activities for each disposal research R&D technical area were evaluated and categorized in terms of near-term (1-2 years) and longer-term (3-5 years) thrusts. The objective of the GDSA technical area is "to develop and continuously maintain a state-of-the-art software framework for probabilistic post-closure performance assessment analyses of facilities for deep geologic disposal of nuclear waste."

The near-term primary thrusts for the GDSA technical area for FY2022 and FY2023 are:

- Advanced coupled process simulation capabilities (G01),
- State-of-the-art uncertainty and sensitivity analysis (G02),
- Traceable, user-friendly workflow for GDSA Framework (G03),
- Repository systems analysis for various disposal concepts and selected host rocks (G04), and
- Development of geologic models with interactive, web-based visualization (G05).

The near-term GDSA thrusts for FY2022 and FY2023 are provided verbatim in Appendix A. Longer-term (3-5 years) thrusts include multi-fidelity modeling, in-package chemistry, gas flow in the EBS, cement seal evolution, new repository designs, and preparation for site applications. An additional GDSA focus area identified in Section 3 of the plan addresses in-drift coupled chemistry modeling and major chemical reactions with materials over appropriate temperature ranges.

3.1.2 5-Year Plan Update of FY2023

One of the FY2023 tasks of the GDSA Framework Development work package is to update the 5-year Disposal Research R&D plan to reflect developments in DOE priorities. This was accomplished with the release of *SFWST Disposal Research R&D 5-Year Plan – FY2023 Update* (Sassani et al. 2023). The new update accounts for progress in the previous two years, identifies additional knowledge gaps to be investigated, and includes updates to DR R&D priorities for the next stages of activities.

Much of the wording of the near-term GDSA thrust topics is retained from the FY2021 update (Appendix A). FY2023 additions include:

- Development and implementation of advanced simulation capability to address backfill consolidation, drift convergence, waste form degradation, radionuclide release, and transport in high ionic strength solutions
- Pursuit of advanced simulator verification strategies and advanced simulator performance improvements

- Development of a FEPs-activity tracking tool to help track completeness of GDSA Framework and to aid in the prioritization of remaining DR R&D
- Addition of two classes of workflows to the GDSA Next Generation Workflow, one that performs a single loop sample study and one that supports nested sampling
- Development and implementation of new performance assessment techniques to quantify the relative contributions of specific features and processes to overall repository performance in reference case simulations

As for the longer-term thrust topics for GDSA, they were amended to include:

- Identification and prioritization of DR R&D activities using the FEPs-activity tracking tool added to the near-term GDSA thrust topics
- Continued involvement in DECOVALEX, an international collaboration comparing modeling approaches for performance assessment applications
- Development and integration of software and workflow processes to enhance traceability, computational efficiency, and the streamlining of additions of new models to GDSA Framework

3.2 2019 Roadmap Update for GDSA

Development of the FY2021 5-year plan was influenced by the 2019 Disposal Research R&D Roadmap Update (Sevougian et al. 2019a) and the 2012 Used Fuel Disposition (UFD) Campaign Roadmap (DOE 2012). The 2019 Roadmap Update highlighted progress, priorities, and remaining gaps in disposal research R&D activities.

Activities defined and tracked in the 2019 Roadmap Database are a collection of specific disposal research objectives focused on improving knowledge of FEPs and how they affect repository performance. They include:

- Collecting and measuring the properties of features (e.g., radionuclides, waste forms, waste packages, buffer, damaged rock zone, repository layout, host rock, etc.) and their associated uncertainties
- Identifying and modeling important processes (e.g., flow of heat and groundwater, waste package degradation, waste form degradation, radionuclide adsorption, buffer evolution, etc.) at small scale and/or in repository simulations
- Estimating the magnitudes, consequences, and probabilities of events that might affect repository performance (e.g., criticality, disruptive events)
- Developing tools and processes to propagate uncertainties in repository performance calculations and to enhance sensitivity analyses

A total of 17 activities were defined for GDSA PA in the 2019 Roadmap Update (Sevougian et al. 2019a). They are listed in Table 3-1. The linkages between the GDSA thrusts and the GDSA Roadmap activities are evaluated in Mariner et al. (2021, Section 5.3).

Table 3-1 GDSA PA activities in the Roadmap Database of the 2019 Disposal R&D Roadmap update

Activity	*Gap	Name
P-01		*CSNF repository argillite reference case*
P-02		*CSNF repository crystalline reference case*
P-03		*CSNF repository bedded salt reference case*
P-04		*CSNF repository unsaturated zone (alluvium) reference case*
P-05		*Disruptive events*
P-06		*(Pseudo) colloid-facilitated transport model*
P-07		*Intrinsic colloid model*
P-08	*	*Other missing FEPs (processes) in PA-GDSA*
P-09		*Surface processes and features*
P-10		*Uncertainty and sensitivity analysis*
P-11	*	*Pitzer model*
P-12		*WP degradation model framework*
P-13	*	*Full representation of chemical processes in PA*
P-14		*Generic capability development for PFLOTRAN*
P-15	*	*Species and element properties*
P-16	*	*Solid solution model*
P-17	*	*Multi-component gas transport*

3.3 GDSA Alignment with Program Priorities

GDSA Framework development activities undertaken in FY2023 are listed in Table 3-2. They are linked in Table 3-2 to FY2021 near-term GDSA thrusts (Section 3.1.1) and 2019 Roadmap activities (Section 3.2). As indicated, each GDSA near-term thrust was addressed to some degree in FY2023.

GDSA Framework development activities commonly involve careful integration between SNL GDSA work packages and other parties. The major parties involved in the FY2023 GDSA Framework development activities are also identified in Table 3-2.

Table 3-2 FY2023 GDSA Framework development activities mapped to GDSA Roadmap activities and 5-Year Plan near-term GDSA thrusts

FY2023 GDSA Framework Development Activities	FY2023 Participants	Roadmap Database PA Activity	Near-Term GDSA Thrusts
Agile/Jira code management system (Section 4.2.1.1)	SNL	-	G01, G03
Biosphere modeling (Section 4.2.2.6)	PNNL, SNL	P-08, P-09	G01, G04
Buffer evolution (Section 4.2.2.4)	SNL	P-01, P-02, P-14	G01
DECOVALEX-2023 Task F: Performance assessment (Section 4.1.6)	SNL, LBNL, LANL, International	P-02, P-03, P-05, P-12	G02, G04
dfnWorks development and integration (Section 4.1.6.1)	LANL, SNL	P-02, P-10, P-14	G01, G02
FEPs-activity tracking tool (Section 3.4, Appendix B)	SNL	P-08	G01, G02, G04, G05
Fuel matrix degradation (Sections 4.2.2.2 and 4.2.2.3, Appendix C, Appendix D)	SNL, ANL, PNNL, ORNL	P-13, P-14	G01
GDSA documentation (Section 4.1.8)	SNL	-	G01, G03
GDSA Workflow (Sections 4.1.3 and 4.1.4)	SNL	-	G02, G03
Geologic Framework Model (Section 4.1.1)	SNL, LANL, INL	P-01, P-02, P-04, P-09	G03, G04, G05
Groundwater chemistry modeling (Sections 4.2.2.4 and 4.2.2.9)	SNL	P-11, P-13, P-14	G01
Machine-learning surrogate models (Sections 4.2.2.3 and 4.1.3, Appendix D)	SNL, LBNL	P-14	G01
Material property dependency enhancements (Section 4.2.2.7, Section 5.4 of Nole et al. 2023)	SNL	P-14	G01
Multi-continuum transport development (Section 4.2.2.7)	SNL, LANL	P-02, P-14	G01
Performance factor analysis of FEPs in total system models (Section 4.1.4)	SNL	P-01, P-02, P-03, P-04, P-05	G01, G03, G04
PFLOTRAN convergence (Section 4.2.3)	SNL	P-01, P-02, P-03, P-04, P-17	G01
Process/surrogate model coupling (Sections 4.2.2.1)	SNL	P-14	G01
QA toolbox and test suite development (Section 4.2.1.2)	SNL	-	G03
Repository reference case development (Sections 4.1.6 and 4.1.7)	SNL, International	P-01, P-02, P-03, P-04, P-10	G02, G03, G04
Re-saturation modeling (Section 4.2.3.1, Section 5.2 of Nole et al. 2023)	SNL, ORNL	P-14	G01, G04
Thermal secondary continuum (Section 4.2.2.8)	SNL	P-14	G01
Uncertainty and sensitivity analysis (UQ/SA) (Section 4.1.3)	SNL, International	P-02, P-03, P-10	G02, G04
Voronoi meshing and simulation (Section 4.1.2)	SNL, LANL	P-01, P-02, P-03, P-04, P-09	G01, G04, G05
Waste package degradation (Sections 4.2.2.4 and 4.2.2.5)	SNL	P-12, P-13	G01

3.4 FEPs-Activity Tracker

A FEPs-activity tracker is being developed to aid in prioritization and planning of Disposal Research R&D. The tracker will use Excel and SharePoint to link DR activities with FEPs, 5-yr plan thrusts, and roadmap priorities. Activities will be mapped to FEPs of specific repository reference cases, e.g., shale, crystalline, and salt. These mappings will provide a framework for evaluating work activities and demonstrating progress toward program objectives for each reference case. The tracker will be online so that work package managers and technical staff across SFWST Disposal Research will be able to navigate it, populate it, and manage it. Figure 3-1 shows an example of one of the reports that can be generated.

Appendix B describes the development of the tracker and how it will work.

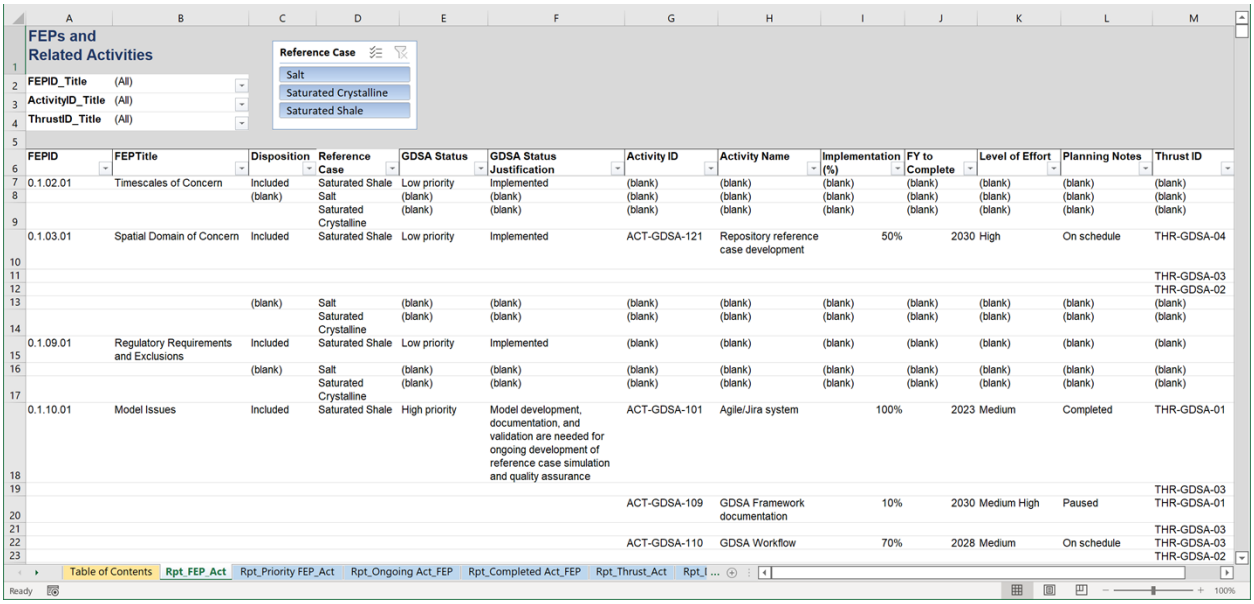

FEPs and Related Activities

Reference Case: Salt; Saturated Crystalline; Saturated Shale

FEPID_Title (All)
ActivityID_Title (All)
ThrustID_Title (All)

FEPID	FEPTitle	Disposition	Reference Case	GDSA Status	GDSA Status Justification	Activity ID	Activity Name	Implementation (%)	FY to Complete	Level of Effort	Planning Notes	Thrust ID
0.1.02.01	Timescales of Concern	Included	Saturated Shale	Low priority	Implemented	(blank)	(blank)	(blank)	(blank)	(blank)	(blank)	(blank)
		(blank)	Salt	(blank)	(blank)	(blank)	(blank)	(blank)	(blank)	(blank)	(blank)	(blank)
			Saturated Crystalline	(blank)	(blank)	(blank)	(blank)	(blank)	(blank)	(blank)	(blank)	(blank)
0.1.03.01	Spatial Domain of Concern	Included	Saturated Shale	Low priority	Implemented	ACT-GDSA-121	Repository reference case development	50%	2030	High	On schedule	THR-GDSA-04
												THR-GDSA-03
												THR-GDSA-02
		(blank)	Salt	(blank)	(blank)	(blank)	(blank)	(blank)	(blank)	(blank)	(blank)	(blank)
			Saturated Crystalline	(blank)	(blank)	(blank)	(blank)	(blank)	(blank)	(blank)	(blank)	(blank)
0.1.09.01	Regulatory Requirements and Exclusions	Included	Saturated Shale	Low priority	Implemented	(blank)	(blank)	(blank)	(blank)	(blank)	(blank)	(blank)
		(blank)	Salt	(blank)	(blank)	(blank)	(blank)	(blank)	(blank)	(blank)	(blank)	(blank)
			Saturated Crystalline	(blank)	(blank)	(blank)	(blank)	(blank)	(blank)	(blank)	(blank)	(blank)
0.1.10.01	Model Issues	Included	Saturated Shale	High priority	Model development, documentation, and validation are needed for ongoing development of reference case simulation and quality assurance	ACT-GDSA-101	Agile/Jira system	100%	2023	Medium	Completed	THR-GDSA-01
												THR-GDSA-03
						ACT-GDSA-109	GDSA Framework documentation	10%	2030	Medium High	Paused	THR-GDSA-01
												THR-GDSA-03
						ACT-GDSA-110	GDSA Workflow	70%	2028	Medium	On schedule	THR-GDSA-03
												THR-GDSA-02

Table of Contents | Rpt_FEP_Act | Rpt_Priority FEP_Act | Rpt_Ongoing Act_FEP | Rpt_Completed Act_FEP | Rpt_Thrust_Act | Rpt_I ...

Ready 100%

Figure 3-1 Example report of the FEPs-activity tracker (dummy data used in this illustration)

4 GDSA FRAMEWORK DEVELOPMENT

GDSA Framework continues to mature into a highly capable PA modeling tool for deep geologic disposal of nuclear waste. Since adoption of the PFLOTRAN-Dakota approach in 2013, many features and processes important to disposal PA have been added to the framework. Generic reference cases have been developed for different host rocks and disposal concepts, and probabilistic and sensitivity analysis tools have been refined and demonstrated on a subset of those reference cases. Advances in capabilities are aided by collaboration with other work packages in Disposal Research and by ongoing interaction with the international community. A historical summary of developments in GDSA Framework from 2010 to 2019 is documented in Mariner et al. (2019).

Guided by the *SFWST Disposal Research R&D 5-Year Plan – FY2021 Update* (Sassani et al. 2021), and more distantly by the Roadmap reevaluation exercise in FY2019 (Sevougian et al. 2019a), the GDSA Framework development team continued to make advances in FY2023. This section describes advances pertaining to general code development, meshing, uncertainty quantification, workflow, outreach, and international collaboration.

General GDSA Framework advances in FY2023 are described in Section 4.1, many of which are also covered in more detail in other reports (e.g., LaForce et al. 2023a; Swiler et al. 2023). PFLOTRAN advances are summarized in Section 4.2. Much of the PFLOTRAN development is described in detail in the recent PFLOTRAN development report (Nole et al. 2023). Section 4.3 addresses international and outreach activities.

4.1 General Development

There were many advances in FY2023 in GDSA Framework capabilities and reference cases. They include development of:

- Geologic Framework Model integration (Section 4.1.1)
- Voronoi meshing (Section 4.1.2)
- Tracer techniques (Section 4.1.3)
- Performance assessment methods (Section 4.1.4)
- Uncertainty and sensitivity analysis applications and methods (Section 4.1.5)
- International reference case development activities (Section 4.1.6)
- Generic repository reference case development (Section 4.1.7)
- Document and calculation archives (Section 4.1.8)

In addition, there was much development in the PFLOTRAN code. PFLOTRAN developments are discussed in Section 4.2.

4.1.1 Geologic Framework Model

Work on Geologic Framework Models (GFMs) focuses largely on developing specific geologic models, geologic model capabilities, and software/user capabilities. That work continues, largely at LANL and INL, and is reported elsewhere (e.g., Russell et al. 2022; Gross et al. 2022; Gross et al. 2023; LaForce et al. 2022).

This year, one of the highlights of the GFM effort is that a GFM was directly used to generate a set of geologic realizations for a shale repository reference case model to be simulated in PFLOTRAN (LaForce et al. 2023a). The workflow is illustrated in Figure 4-1. The GFM is used to build a LaGriT mesh, which in turn is used to build a VoroCrust mesh that PFLOTRAN can use. The workflow was automated using Python, and 100 realizations of the geologic model were generated for the study. Details of this new capability are presented in Section 5.1 of LaForce et al. (2023a).

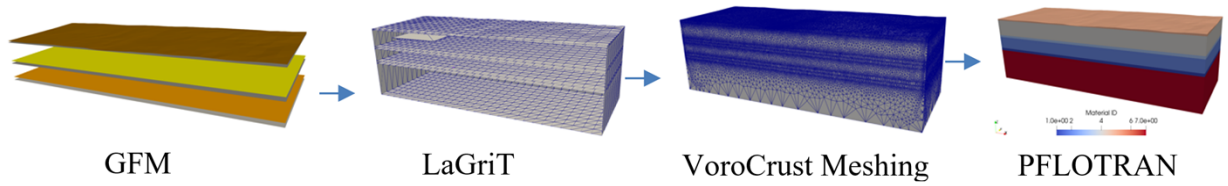

Figure 4-1 Workflow developed to integrate a GFM with GDSA Framework (LaForce et al. 2023a)

4.1.2 Voronoi Meshing

Voronoi meshes are unstructured meshes that work well with codes like PFLOTRAN that use the finite-volume approximation for fluid flow. Voronoi meshing is implemented in GDSA Framework using VoroCrust. VoroCrust is open source software that uses a sphere packing procedure to capture input surfaces as faces in a Voronoi mesh (Abdelkader, 2020). The VoroCrust website is: vorocrust.sandia.gov.

In FY2023, there were several important advances in the VoroCrust capability:

- A public Github repository was developed for releasing VoroCrust source code.
- VoroCrust classes were restructured for improved performance and easier maintenance.
- User features were added to help with Paraview integration and mesh sizing.
- User manuals were developed.
- A method was prototyped for inserting waste packages as pre-meshed elements into a random unstructured mesh. Two examples are shown in Figure 4-2.
- An option was added to return the closest seed to a monitor point if the exact monitor point cannot be captured in the final mesh.

These accomplishments are discussed in more detail in Section 6 of LaForce et al. (2023a) along with a study that compares the accuracy of Voronoi approaches against several analytical solutions and experimental data.

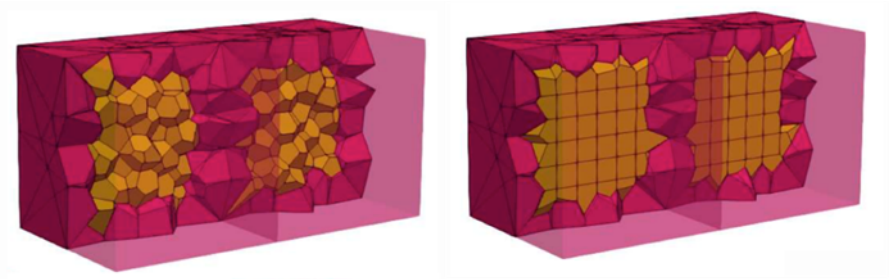

Figure 4-2 VoroCrust unstructured mesh of an interior feature (left) and structured mesh of an interior region embedded in the unstructured mesh (right) (from LaForce et al. 2023a).

4.1.3 Tracers

Tracers can be used in a repository system model to measure specific quantities of interest (QoI) such as mean travel time from the repository to the biosphere and median hydrologic retention time in the repository. They can also be used to assess the contributions of specific features and processes to overall safety performance. This section, which builds on tracer applications presented at the 2022 American Nuclear Society (ANS) International High-Level Radioactive Waste Management (IHLRWM) Conference (Mariner et al. 2022b), describes several ways tracers are being developed and used to characterize system properties and to measure the effects of features, processes, and combinations of features and processes on repository model performance.

4.1.3.1 Beyond Input Parameters

A sensitivity analysis provides useful information on how model inputs affect model outputs (Helton 1999, Helton et al. 2012). Typical sensitivity analyses involve changing model input parameter values between realizations so that the effects on model outputs can be observed. In GDSA probabilistic repository reference case simulations, inputs are generally sampled over their ranges of uncertainty, primarily using Latin Hypercube Sampling. Methods of analysis include scatterplots, correlation coefficients, and variance-based decomposition indices which measure the fraction of an output variance attributable to each input parameter.

To quantify the effects of features and processes on performance or QoI in a system model, tracers can be introduced and tracked in informative ways. A major advantage of using tracers is that the effects they interrogate are directly quantifiable for each realization, i.e., multiple realizations are not required. The tracers can be introduced as a spike in the repository at the beginning of the simulation, as a constant source over time, as fully released from a waste package upon waste package breach (i.e., not limited by slow waste form degradation), and as reactive tracers (e.g., decaying, adsorbing). Depending on how they are introduced and their properties, these tracers can be used to answer questions like:

- How well does the repository region hydrologically retain a tracer in its pore space?
- What is the mean travel time of a tracer from the repository to the receptor?
- How much does dispersion attenuate radionuclide concentrations?
- How much do specific radionuclide release mechanisms and sources affect receptor dose rates?
- How much does waste form performance reduce receptor dose rates?
- How much does waste package performance reduce receptor dose rates?

Sensitivity analyses can, in turn, be performed on tracer results to evaluate uncertainty in these measurements. The sections below describe tracer applications developed to address most of the questions above.

4.1.3.2 Hydrologic Retention in the Repository

For a simulation of a water-saturated repository, this tracer measurement captures the combined effects of advection and diffusion on the transfer of released radionuclides beyond the repository and into the host rock. Advection is controlled by water flow through the repository. Diffusion is controlled by porosity and tortuosity within and around the repository. A spike of an aqueous conservative tracer in the repository region at the beginning of the simulation can be used to directly measure repository hydrologic retention owing to the combination of advection and diffusion in the repository region.

Figure 4-3 shows the mass of initial tracer retained in the repository region over time for 20 discrete fracture network (DFN) realizations of a crystalline repository reference case (Mariner et al. 2020, Section 3.2.5). These results indicate that the hydrologic properties of the repository alone provide significant waste isolation performance. The median residence time of the tracer in this figure ranges from about 50,000 to 130,000 years. Median residence time measurements are particularly intuitive and useful in sensitivity analyses. They can be used to identify factors that affect hydrologic retention in the repository (e.g., buffer porosity) and how important hydrologic retention is to overall repository performance.

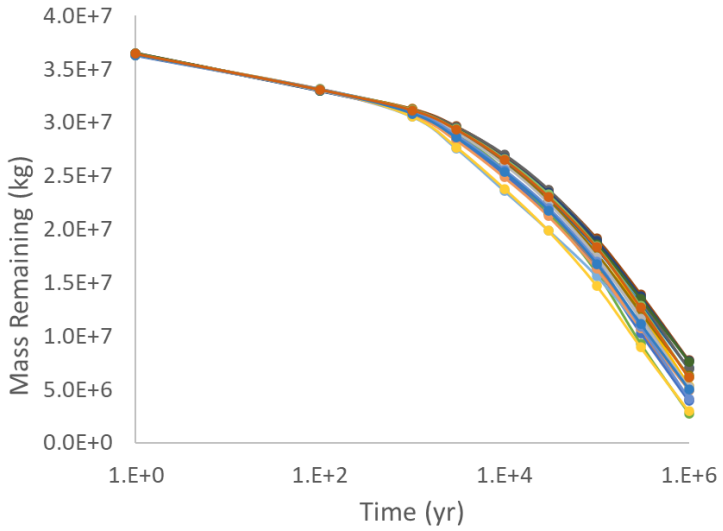

Figure 4-3 Mass of initial tracer spike remaining in a crystalline repository reference case over time for 20 realizations of a crystalline repository reference case (Mariner et al. 2020, Section 3.2.5)

4.1.3.3 Mean Travel Time

The mean travel time measurement uses two tracers; one decays or ingrows exponentially and one does not. If these two tracers are introduced at the same rate over time into the repository, the mean travel time to a distant location can be directly calculated from the concentrations at that location (Mariner et al., 2020, Section 3.2.6). Differences in mean travel time between realizations can potentially help explain why certain realizations have higher peak radionuclide concentrations at the receptor location.

4.1.3.4 Dispersion

Solute concentrations in a plume attenuate downgradient due to dispersion, decay, and non-steady-state conditions (e.g., slow diffusive exchange into and out of dead-end voids). Dispersion of a solute occurs due to mixing of the medium (water) and diffusion within the medium. Mixing is caused by the branching and merging of flow due to pore space tortuosity, intersecting fractures, and heterogeneous flow systems.

A direct way to measure the effects of transverse dispersion (lateral mixing) between a source and a receptor located in the central transport path in a simulation is to set a constant tracer concentration at the waste package source or in the repository region and run the system to steady state. At steady state, the ratio of the tracer concentration at the tracer source to that at a receptor indicates the attenuating effects of transverse dispersion in the simulation between the two locations.

Repository reference cases, clearly, are not steady state simulations. The initially high and decaying thermal output of the waste packages over time cause transient changes to the flow field, as do other processes and events that may be modeled (e.g., corrosion, buffer evolution, earthquakes, glaciation, etc.). Nevertheless, measuring the effects of transverse dispersion, e.g., at one million years, provides an additional way to interrogate bulk system properties of individual stochastic realizations so that the effects of transverse dispersion on repository performance can be better understood.

Figure 4-4 compares the concentration of a conservative tracer held at a constant aqueous concentration in a crystalline repository reference case simulation and the resulting maximum concentration at the ground surface. The ratio of these concentrations at steady state is 276. Although the regulatory period is not expected to extend beyond one million years, this steady state ratio provides a useful indicator of the effects of transverse dispersion in the geosphere between the repository and ground surface. The large difference in these concentrations clearly indicates that dispersion is an important factor in the performance of the natural barrier system in the model.

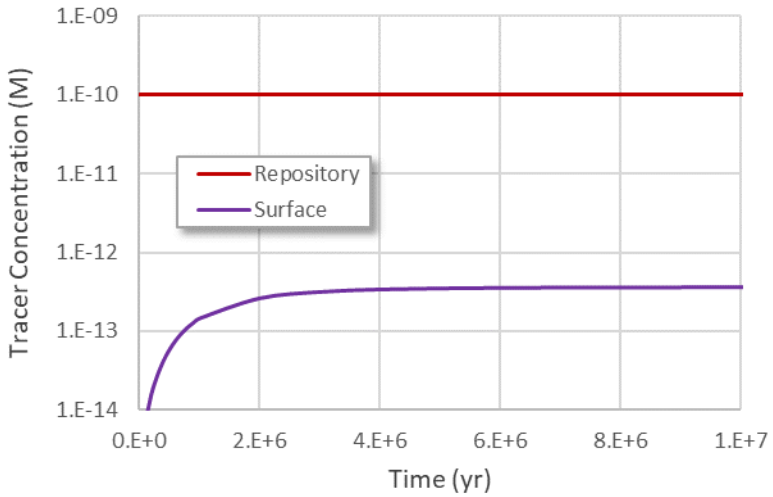

CTN: 221106-VIRTCON-01

Figure 4-4 Concentrations of a conservative tracer held constant in the repository pore space (Repository) and the resulting maximum concentration at the ground surface (Surface)

4.1.3.5 Radionuclide Release Mechanisms and Sources

The concentration of a radionuclide at a downgradient location, as typically calculated using a performance assessment model, does not provide a breakdown of the relative contributions of different sources or source mechanisms. This is unfortunate because it is useful to know how much of the resulting concentration originated from a specific source or mechanism (e.g., instantly released upon waste package breach, congruently released via slow degradation of the waste form, generated by ingrowth, released from a specific type of waste form or waste package, etc.). Such information would provide direct measures of the relative effects of the various sources and mechanisms on receptor dose.

Some of this information can be obtained through careful sensitivity analysis. However, much can be lost in the noise. If, for example, uncertainties in other aspects (e.g., waste package degradation rates or discrete fracture networks) dominate the uncertainty in radionuclide concentrations at the receptor, then the effects of different sources or source mechanisms are difficult to discern with a high degree of confidence. With the use of tracers, however, the contributions of the various sources and mechanisms can be determined precisely for each realization.

Separate tracers can be defined to represent instant release fractions, fuel matrix degradation fractions, fuel type fractions, waste package type fractions, etc. As needed, the tracers can be given the properties of the major radionuclides that contribute to dose at the receptor (e.g., radioactive decay half-lives, adsorption properties, diffusion properties). If ^{129}I is the major contributor to dose, then each tracer for this measurement must also have the same properties and distribution among the sources and source mechanisms so that the total concentration of this tracer at the receptor will be the same as the ^{129}I concentration from the same sources. That way, the relative concentrations of the tracers at the receptor will indicate the relative amounts from each source and source mechanism.

4.1.3.6 Waste Form Performance

To measure the performance of a waste form, a tracer in the waste form with a 100% instant release fraction is used. As long as this tracer is set up to mimic the behavior and amount of the important radionuclides released from the waste form, dividing the peak dose rate of this tracer at the receptor by the peak radionuclide dose rate will directly provide the dose reduction factor attributed to waste form performance.

Figure 4-5 shows results of a simulation where conservative tracers were used to determine the concentrations at the receptor over time with and without waste form performance. The tracer simulating waste form performance has a 10% instant release fraction at the time of waste package failure and is otherwise released congruently with the degradation of the waste form matrix. The matrix in this simulation degrades at a fractional rate of 10^{-7} yr^{-1}. The tracer that has no waste form performance has an instant release fraction of 100%. The results indicate that waste form performance reduces the concentration at the receptor by a factor of 10 for the first several hundred thousand years and by a factor of about 6 at one million years.

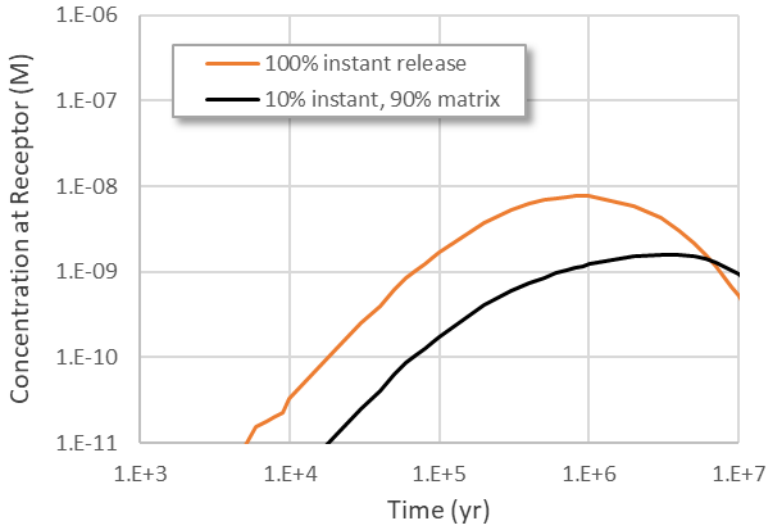

CTN: 230824-PFADCRY-01

Figure 4-5 Tracer concentration at receptor assuming no waste form performance (100% instant release) versus concentration with waste form performance (10% instant release, 90% congruent release as waste form degrades)

4.1.3.7 Waste Package Performance

The newest tracer in the suite of performance tracers is one that is released at waste package locations at time zero even when the waste package remains intact for thousands of years. This tracer allows the determination of concentrations and doses at the receptor location over time assuming no waste package and no waste form performance. An example of this tracer in action is provided in the next section on performance factor analysis (Section 4.1.4).

4.1.4 Performance Factor Analysis

As indicated in the previous section (Section 4.1.3), tracers can be used in specific ways to measure individual contributions of certain features and processes in a realization to the overall performance of a repository in a model realization. One-off realizations that exclude a feature or process can also be used to assess these individual contributions.

Quantification of performance sensitivity to features and processes can be especially useful in the early phases of a repository program because it can help with siting and design decisions. For example, if it can be shown that dispersion alone prevents receptor dose rates from exceeding safety limits, then a high degree of performance may not be needed from the waste package. For another example, if instant release fractions dominate the dose rate, then complex waste form degradation models may not be needed.

An elucidating way to quantify contributions to overall performance is in terms of performance factors. Performance factors are highly intuitive and can therefore be highly useful in identifying and communicating where performance is coming from in a repository model. Assessment of the relative contributions to performance is useful for focusing further R&D for a repository design.

A performance factor F_x for a feature or process x is defined as the ratio of the maximum annual dose in the absence of the feature or process during the regulatory period (H_x) to the maximum annual dose when it is included (H):

$$F_x = \frac{H_x}{H} \quad \text{4-1}$$

For example, a F_x value of 10 implies the feature or process causes a tenfold reduction in the maximum annual dose. A value of 1.0 implies it provides no performance benefit in terms of maximum annual dose.

The subsections below demonstrate how a suite of tracers in a single realization plus an additional one-off realization can be used to measure performance factors for three primary EBS features (waste form, waste package, buffer) and the EBS as a whole.

4.1.4.1 Crystalline Reference Case

The reference case model for this demonstration is for a repository in crystalline rock. It is nearly identical to the crystalline repository reference case developed in Task F of DECOVALEX-2023 (LaForce et al. 2023b). The model simulates spent fuel assemblies packaged in 2,500 copper waste packages in 50 drifts. Each waste package is surrounded by bentonite buffer in deposition holes in the floors of the drifts. The drifts are backfilled with buffer. In this model, approximately two-thirds of the waste packages are set to fail between 10,000 and 100,000 years; the others fail before and after that period. 10% of the ^{129}I in a waste package is instantly released upon waste package failure. The waste form degrades at a fractional rate of 10^{-7} yr^{-1} after waste package failure.

4.1.4.2 Tracers

The following tracers are included in the demonstration:

- Tracer 0. This tracer is conservative and is released at time zero in all WP regions in the model. It acts as if there is no waste package to contain it and no waste form to slowly release it.
- Tracer 1. This tracer is conservative and is released from a WP when it fails. It behaves like a 100% instant release fraction with no waste form to slowly release it.
- Tracer 2. This tracer is conservative and is released from a WP after it fails but only from the waste form matrix. It behaves like a conservative radionuclide with a 0% instant release fraction.

These tracers basically track how the instantly released (tracer 1) and slowly released (tracer 2) fractions of ^{129}I behave and how ^{129}I would behave if there is no performance from both the WP and WF (tracer 0). The only difference from ^{129}I in tracer behavior is that the tracers do not decay. To calculate performance factors there is no need to include decay because decay equivalently affects the numerator and denominator. The tracers emulate ^{129}I behavior in this demonstration because ^{129}I dominates dose calculations in the reference case model.

4.1.4.3 One-Off

A one-off simulation is a simulation that uses the same inputs as the original simulation except for a single difference so that the effects of the difference can be measured. To evaluate the performance of the buffer, a one-off realization is simulated in which the buffer is replaced with a crushed rock backfill having porosity and permeability of 0.35 and 5×10^{-16} m^2 instead of 0.46 and 1.5×10^{-20} m^2.

4.1.4.4 Concentrations at the Receptor

Figure 4-6 shows concentration breakthrough curves at the receptor location from the realization and the one-off. For this demonstration and for the purpose of calculating performance factors, concentrations at the receptor location are considered analogous to dose rate. When all features of the model are included and decay is included, the calculated ^{129}I concentration at the receptor is shown by the solid black line.

Each breakthrough curve shown in the legend below the first (^{129}I) removes one feature or process. Red removes decay, yellow additionally removes WF performance, green additionally removes WP performance, and blue additionally removes buffer performance.

The blue curve is basically controlled by the natural barrier system (NBS) though it includes the storage effects of the crushed rock backfill. It is interesting to note that replacing the crushed rock backfill with the buffer in this realization delays the peak by 500,000 years, the WP delays the peak another 200,000 years, and the WF delays it another 3 million years (excluding the effects of decay).

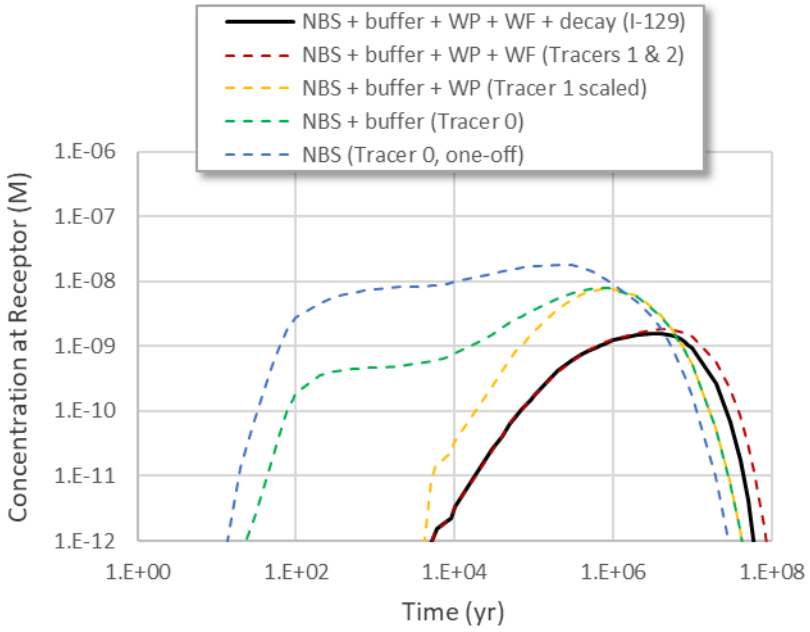

CTN: 230824-PFADCRY-01

Figure 4-6 Calculated tracer and ^{129}I concentrations at the receptor over time in the original simulation and one-off, as indicated.

4.1.4.5 Performance Factors

Figure 4-7 shows performance factors calculated for 10,000-yr and 1-million-yr time periods in the demonstration. For these time periods, the respective performance factors are 2950 and 14.39 (EBS), 12.78 and 2.32 (buffer), 23.19 and 1.02 (waste package), and 9.96 and 6.06 (waste form). The EBS performance factor is calculated directly from the ratio of the maximum concentrations of tracer 2 in the original simulation and tracer 0 in the one-off for the timeframe of interest. It can be shown that the EBS performance factor can also be calculated as the product of the performance factors of the individual EBS features.

A performance factor near 1.0 for the waste package in the 1-million-yr timeframe indicates that the waste package has little effect on overall repository performance during that timeframe for the model. Waste packages generally need to last longer than the period of interest to have a strong effect on overall performance. For the 10,000-yr timeframe in this model, waste packages indeed provide substantial performance (Figure 4-7).

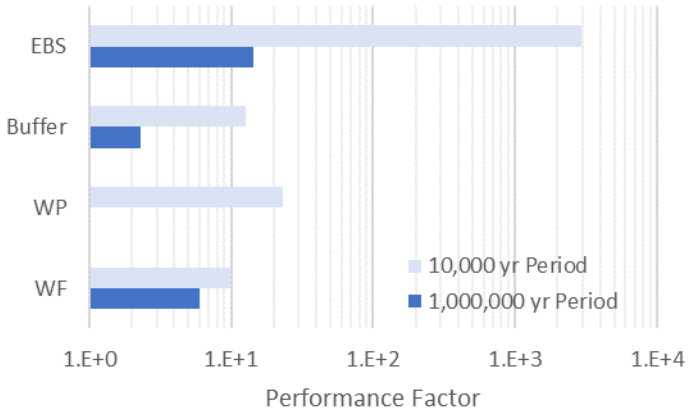

CTN: 230824-PFADCRY-01

Figure 4-7 Performance factors for the EBS and its three components in the model for two different time periods

4.1.4.6 Conclusions and Next Steps

The overall finding of this study is that performance factor analysis is an effective way to quantify and communicate a feature's importance in a repository performance assessment model. Performance factors derived from reference case simulations can be used to help prioritize additional research and development for a reference case concept.

The next steps are to add performance tracers and performance factor analysis as part of the workflow for the major repository reference cases. With performance factors calculated for each realization in a probabilistic analysis, uncertainties in calculated performance factors can then be assessed.

4.1.5 Uncertainty and Sensitivity Analysis

The report *Uncertainty and Sensitivity Analysis Methods and Applications in GDSA Framework (FY2023)* (Swiler et al. 2023) describes the work done this year on uncertainty quantification and sensitivity analysis (UQ/SA) in detail. This section provides a summary of that work.

The GDSA UQ/SA team focused on three areas: assessment of a new sensitivity analysis method, Variogram Analysis of Response Surfaces (VARS), development of a "grouped sensitivity analysis" method which accounts for the aggregate effect of groups of parameters, and analysis of an updated shale reference case. These are summarized in the sections below.

Note that we also continue to develop the GDSA Next Gen Workflow tool and capabilities. This year, we presented a tutorial at the ANS IHLRWM meeting on the GDSA Next Gen Workflow and submitted a journal article about this capability. We continue to participate in the Joint Sensitivity Analysis international working group. Finally, a main focus of the FY2023 Advanced PFLOTRAN short course was UQ/SA, which provided a great opportunity to present our UQ/SA capabilities for more widespread use and adoption.

4.1.5.1 VARS

We assessed a new sensitivity analysis method, Variogram Analysis of Response Surfaces (VARS), which has become popular in the environmental sciences community. We concluded that VARS may have some utility but a lack of maturity in the method makes it unreliable; best practices and/or diagnostics for choosing the analysis options need to be developed. This does not appear to be the focus

of the method developers since the majority of their work is for application of VARS to cases where star sampling can be applied. VARS applied to existing data also requires the use of an underlying surrogate. This does not remove the surrogate error problems we have with our current methods for estimating Sobol' indices but hides the surrogate error so it is harder to interrogate.

4.1.5.2 Grouped Sensitivity Indices

We developed a "grouped sensitivity analysis" method which accounts for the aggregate effect of groups of parameters. The grouped SA method was demonstrated on the crystalline reference case, where parameters relating to the radionuclide source were grouped together and compared with the effects of other epistemic parameters. The original problem varied seven parameters that are listed in Table 4-1. The grouped SA involved the same seven parameters, but the five at the bottom of the table were grouped together into one group representing the radionuclide source. For the grouped SA, these five parameters were combined into a single group and three groups were defined, reducing the input factors for which Sobol' indices were computed from seven to three. From a computational perspective, this means that the grouped Sobol' indices were obtained at a 44% cost reduction relative to computing Sobol' indices for each parameter individually. The greater the ratio between input parameters and groups used in grouped SA, the greater the computational benefit of grouped SA is.

Table 4-1 Uncertain parameter descriptions and probability distributions for the grouped SA case.

Parameter group	Parameter name	Parameter description	Distribution
Glacial aquifer properties	*kGlacial*	Glacial aquifer region permeability [m^2]	$\log \mathcal{U}[10^{-15},10^{-13}]$
Repository region properties	*pBuffer*	Buffer porosity [-]	$\mathcal{U}[0.3, 0.5]$
Radionuclide source	*IRF*	Instantaneous release fraction [-]	$\mathcal{U}[0.038, 0.156]$
	meanWPrate	General corrosion rate truncated log-Normal distribution mean [log(yr^{-1})]	$\mathcal{U}[-5.5, -4.5]$
	environmentalCO	CO_3^{2-} environmental concentration [mol/liter]	$\log \mathcal{U}[10^{-6},2 \cdot 10^{-5}]$
	environmentalHtwo	H_2 environmental concentration [mol/liter]	$\log \mathcal{U}[10^{-8},2 \cdot 10^{-5}]$
	burnup	Fuel burnup [GWd/MTHM]	$\mathcal{U}[40,65]$

The results are shown in Figure 4-8, where the radionuclide source indices are the largest, indicating this group is the most important input factor contributing to the variance of peak ^{129}I. The permeability of the glacial aquifer, *kGlacial* is also important. The grouped main effect index for the radionuclide source group is 0.73, while the sum of the main effects indices for each input in the group individually is 0.63. This indicates some interaction between parameters within the radionuclide source group. Further discussion of this example is found in Chapter 3 of the report (Swiler et al. 2023).

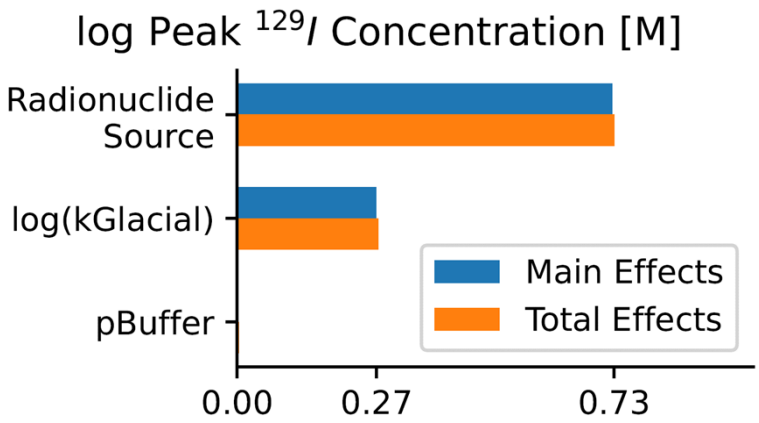

Figure 4-8. Peak ^{129}I Sobol' indices for the grouped SA.

4.1.5.3 Sensitivity Analysis of the Shale Reference Case

This year, we performed a detailed sensitivity and uncertainty analysis of the updated shale reference case. For this analysis, we examined the sensitivities of ^{129}I concentrations at different observation points in different geologic layers at the final simulation time of one million years. We analyzed the behavior of tracers and also examined a new QoI, pressure in the repository region over time (Swiler et al. 2023, Section 4).

The results show that the model is behaving as expected; the sensitivities make sense given the absence of buffer uncertainties. The *pShale*, *kLime*, and *kSand* parameters were most significant to the ^{129}I concentrations. The peak ^{129}I concentrations showed different sensitivity to these parameters depending on which rock layer was examined and where the observation point was located. An example of the sensitivity analysis for observation point 1 in the limestone layer is shown in Figure 4-9. Note that sensitivities were calculated in four ways: using a Polynomial Chaos Expansion (PCE) of order 3 or a Gaussian process (GP) surrogate. The PCE3 and GP surrogates were constructed on the original untransformed data as well as log-transformed data to see differences in rankings as some of the parameters are very small and vary by several orders of magnitude. While there are differences in the results based on these surrogates and transformations, the overall rankings are fairly consistent.

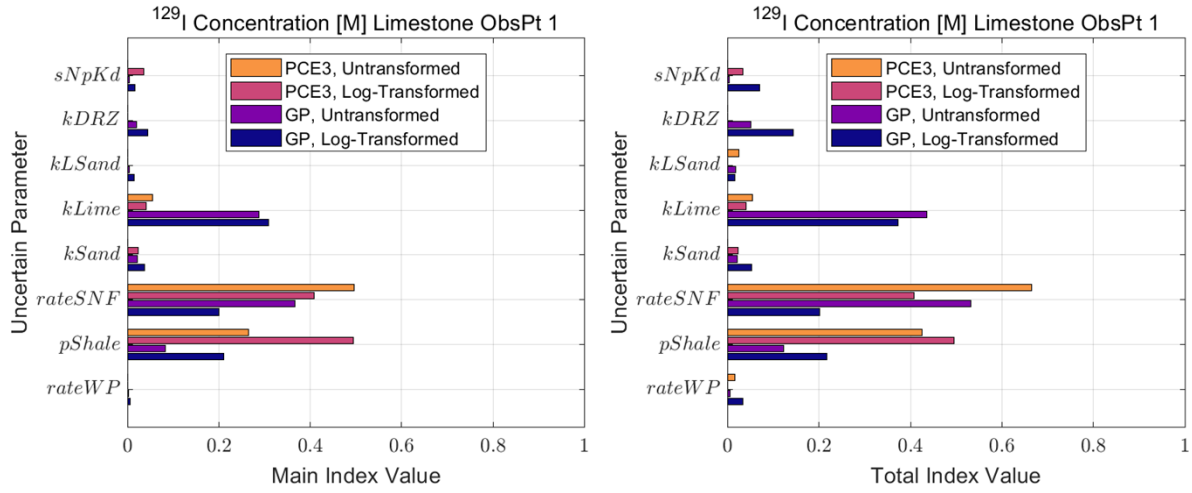

Figure 4-9. Sensitivity analysis results for the ^{129}I concentration at observation point 1 in the limestone at 1Ma

This year, we investigated pressures in the repository region (these are new Quantities of Interest) and incorporated tracers into the shale case. From the pressure plots as a function of time, we learned that the highest pressures occurred around 1000 years and were highly correlated to the *pShale* parameter. There was a complicated interaction between the liquid pressure values and the *pShale* and *kLime* parameters over time as shown in Figure 4-10 below. *pShale* is the dominant uncertainty until after 1,000 years, at which point it starts to lose importance and *kLime* becomes more important. *kLime* remains the dominant uncertainty until around 20,000 years, when *pShale* becomes important again. We discuss this behavior in the main report (Swiler et al. 2023, Section 4). This analysis has given us ideas for subsequent analyses of the pressure dynamics in the repository.

Finally, we examined the behavior of two conservative tracers in this shale case. Figure 4-11 shows the breakthrough curves for Tracer 1, which is fully released upon waste package failure. The tracer concentrations show that the earliest concentration breakthrough times occur in the limestone layer, followed by shale, sandstone, and silt layers. This is to be expected given the permeabilities of each layer and their relative locations. The parameters *kLime* and *pShale* were most important in the tracer concentrations.

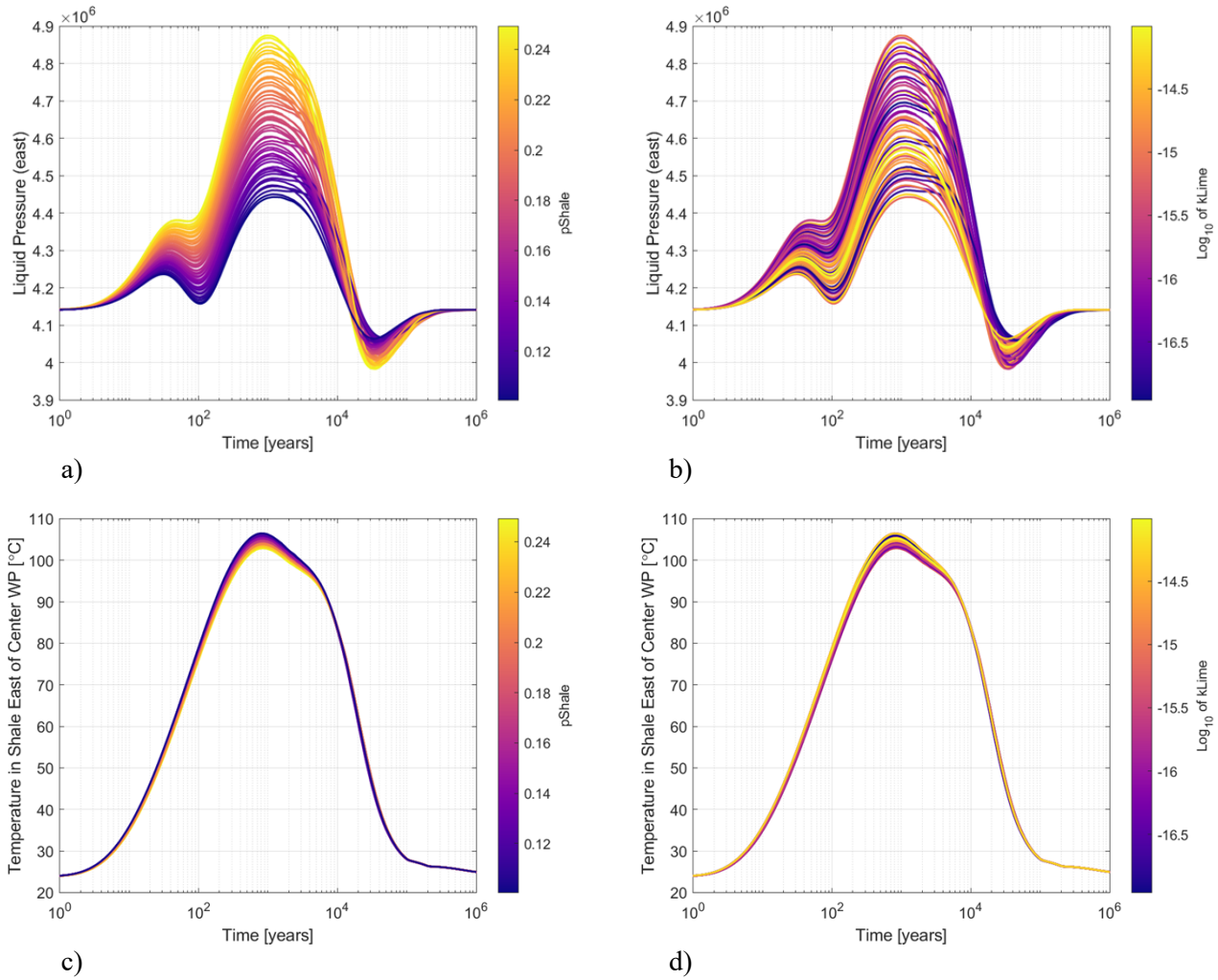

Figure 4-10. Liquid pressure [Pa] and temperature [$°C$] over time at an observation point in the shale east of the centermost waste package colored by *pShale* and *kLime*

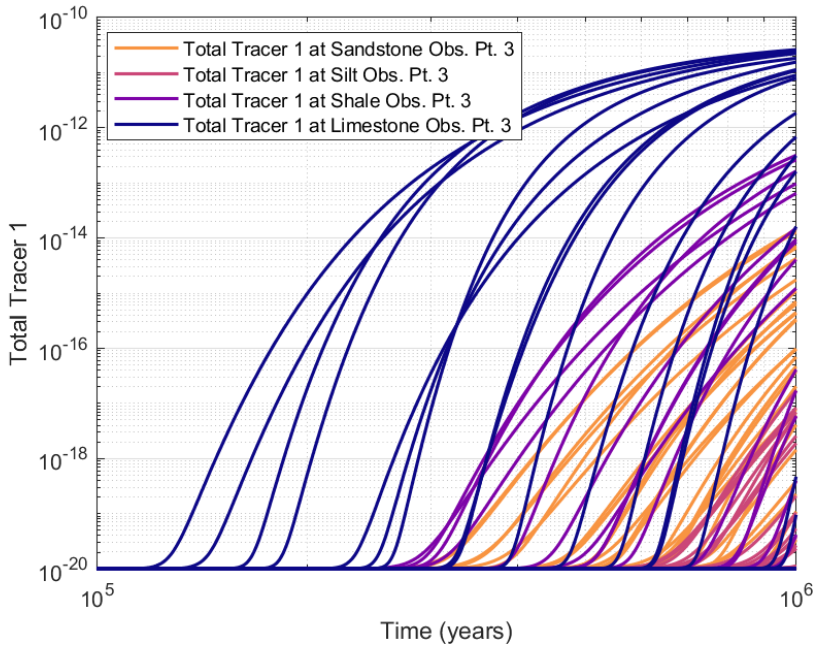

Figure 4-11. Total Tracer 1 concentration [M] over time in the different rock layers

4.1.6 DECOVALEX-2023 Task F

The DECOVALEX project is an international research and model comparison collaboration for advancing the understanding and modeling of coupled THMC processes in geological systems (decovalex.org). Task F of DECOVALEX-2023 focuses on comparison of models and methods used for post-closure PA. Members of the GDSA Framework development team at SNL are leading this effort. The goal of this work is to test and build confidence in the models, methods, and software used for post-closure PA and to identify additional research and development needed to improve PA methodologies.

In Task F, two hypothetical repositories are being developed, one in crystalline rock and one in salt. In 2020, the first year of the four-year task, nine teams from six countries participated in the crystalline repository and benchmarking exercises, and three teams from three countries defined a generic salt repository reference case. In the second year, each focus group gained one additional team.

To date, Task F has provided and will continue to provide numerous opportunities for learning new modeling approaches, developing new models for use in PA simulations, testing uncertainty and sensitivity analysis methods, comparing PA methods, and exchanging ideas with modelers in other programs. Several accomplishments in the past year are highlighted below.

4.1.6.1 Crystalline

Initially, a major focus of the crystalline group of Task F was the testing and comparison of codes used to simulate flow and transport through fractured rock. Several benchmark cases were simulated by participating teams. The exercise allowed participants to examine differences in model implementation, types of model outputs, and the influence of modeling choices. Benchmark problems included analytical solutions for single fracture problems and a 4-fracture discrete network fracture (DFN) problem with and without stochastic fractures. Several teams modeled the 4-fracture problem as an equivalent continuous porous medium (ECPM), some teams applied multiple models, and two teams applied particle tracking.

BENCHMARKS

In FY2023 a continuous point source was added to the set of 4-fracture benchmarks. Figure 4-12 shows the 4-fracture problem domain and the point source location on the inlet face. For quantitative comparisons using temporal moments, time was converted to fracture volumes (FVs), i.e., FVs = (time of simulation)/((mass of water in fractures)/(flux of water through domain)). Fracture volumes (FVs) provide a nondimensional time that normalizes for different flow rates. Figure 4-13 shows the breakthrough curves produced by the SNL team using two different approaches, discrete fracture network (DFN) and equivalent continuous porous medium (ECPM). Results indicate that the high resolution of the DFN causes earlier breakthrough of the first 68% of the tracer flux and much later breakthrough of the final 12%. Additional results are documented in LaForce et al. (2023a, Section 2.2.1). Results of other teams are similar. Full comparisons among all teams will be presented in the Task F1 final report and likely in a journal paper in 2024.

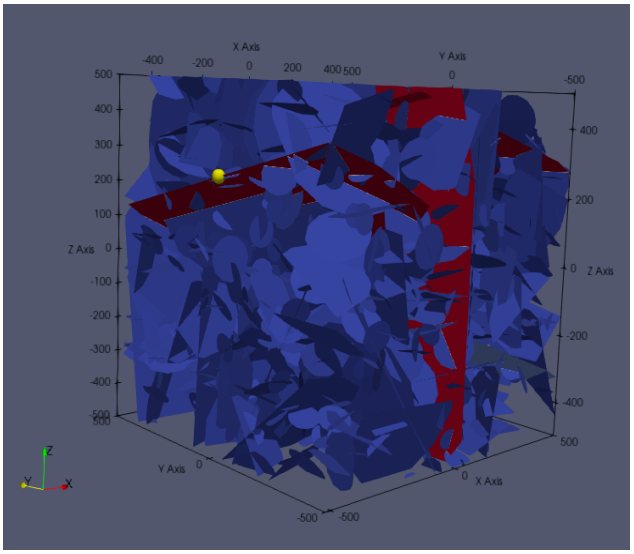

Figure 4-12 4-fracture problem domain showing the four deterministic fractures (red), the stochastically generated fractures (blue), and the location of the continuous point source (yellow) on the inlet face

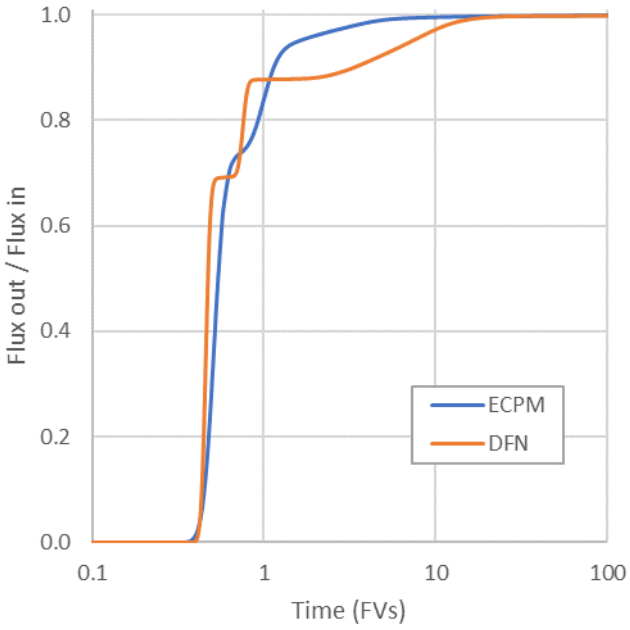

CTN: 230904-4FRACDE-01

Figure 4-13 Conservative tracer breakthrough curves for the new DECOVALEX-2023 Task F1 continuous point source benchmark. Shown here are two different model approaches, discrete fracture network (DFN) and equivalent continuous porous medium (ECPM). Curves are plotted versus fracture volumes (dimensionless time).

In addition, a radionuclide source term benchmark was developed and simulated in FY2023. It was based on the ^{245}Cm decay chain and included the effects of radioactive decay and ingrowth, waste package breach time, instant release fraction, fuel matrix degradation, and solubility limitations. A subset of the SNL team results is shown in Figure 4-14. Additional results from this benchmark are documented in LaForce et al. (2023a, Section 2.2.1.3).

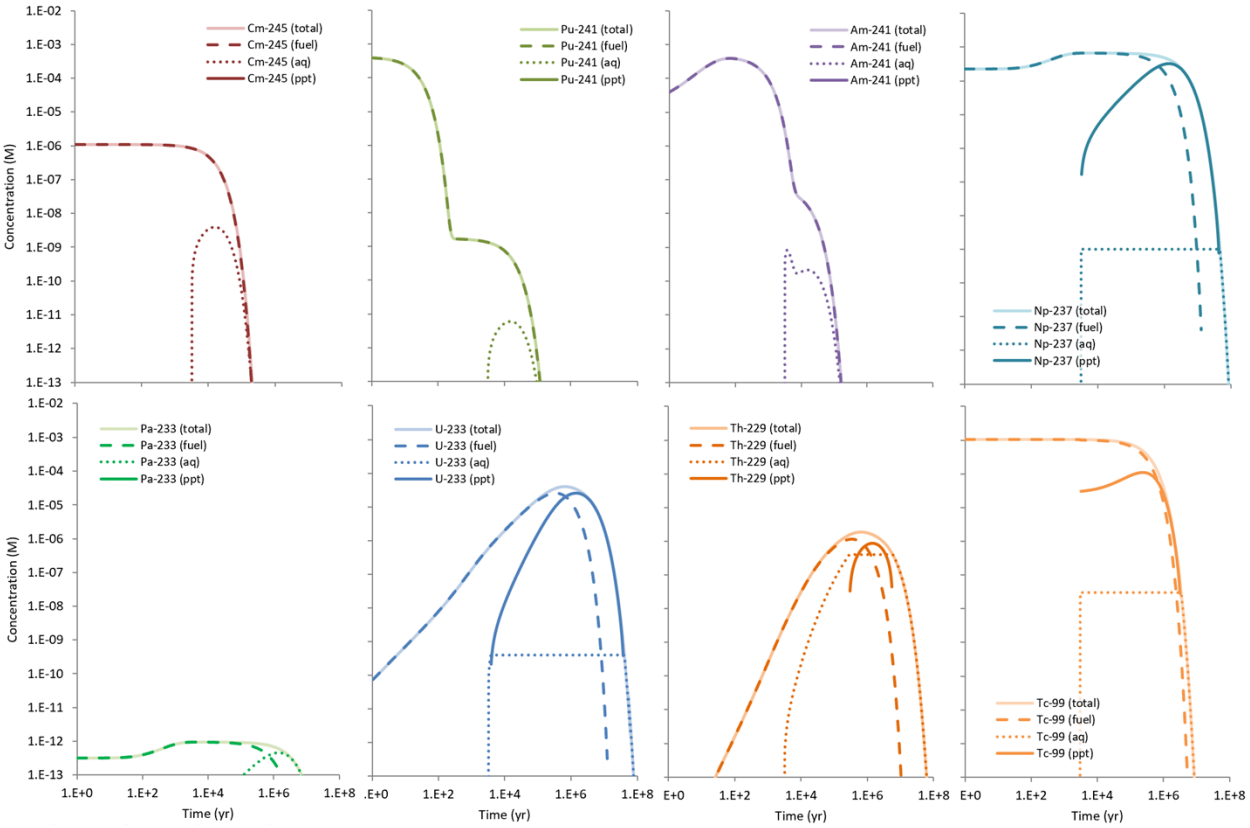

CTN: 230501-RNSOURC-01

Figure 4-14 Calculated partitioning of radionuclides in the radionuclide source term benchmark between fuel matrix (fuel), aqueous (aq), and precipitate (ppt) phases over time. Waste package breach occurs at 3,000 years. 3% of ^{99}Tc is instantly released from the fuel matrix at that time.

REFERENCE CASE

Much of the Task F1 work in FY2023 focused on the reference case. The crystalline reference case simulates a fractured rock domain with a flat top on the west, a flat top 20 m lower on the east, and a gradual hillslope connecting the two. The pressure head distribution causes groundwater to flow from west to east with a downward component on the west side and an upward component on the east side. The repository is located at a depth of 450 m on the west side. The general flow system is indicated by the Tracer 1 plume in Figure 4-15.

The reference case is based on the KBS-3V repository concept. Waste package canisters are copper, individually placed, and surrounded with bentonite in deposition holes drilled 6 m apart center-to-center into the drift floors. The repository has 50 deposition drifts of length 306 m spaced 40 m apart center-to-center. In total, the layout accommodates 2500 waste packages. Further details and figures of the repository layout and engineered barrier system are provided in LaForce et al. (2023b, Section 3).

For the tracer simulations, all waste packages are assumed to fail at the beginning of the simulations. When radionuclides are included, all waste packages are assumed to fail at 50,000 years except for one near the center of the repository, which fails at time zero due to an undetected defect. 10% of the ^{129}I in each waste package is instantly released upon waste package failure. In all simulations, the waste form degrades at a fractional rate of 10^{-7} yr^{-1} after waste package failure.

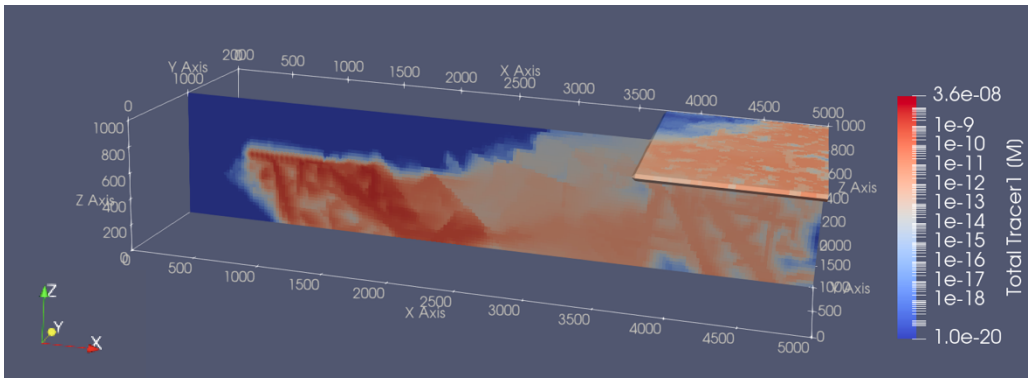

Figure 4-15 Tracer 1 plume at 100,000 years along the central vertical west-east plane and the north half of the surface boundary for Realization 1.

Five teams are implementing the reference case. All five are upscaling stochastically generated fracture networks to ECPM. Three are conforming their meshes to the deterministic deformation zones and two (including the SNL team) are including the properties of the deformation zones when upscaling to meshes composed primarily of hexahedrons.

In FY2023, the SNL team tested a dual continuum disconnected matrix (DCDM) model newly implemented in PFLOTRAN (Nole et al. 2023). The DCDM model adds matrix diffusion modeling capability to a DFN mesh. Results for the 10 DFN realizations compared well with the ECPM results, as shown in Figure 4-16. A large matrix diffusion effect is not observed in the results because the effective diffusion coefficient in the task specification is low ($10^{-13.7}$ m^2 s^{-1}) and the DCDM model inactivates cells with no fractures. All cells are active in the ECPM model. This analysis and others involving the tracers are documented in further detail in LaForce et al. (2023a, Section 2.2.1).

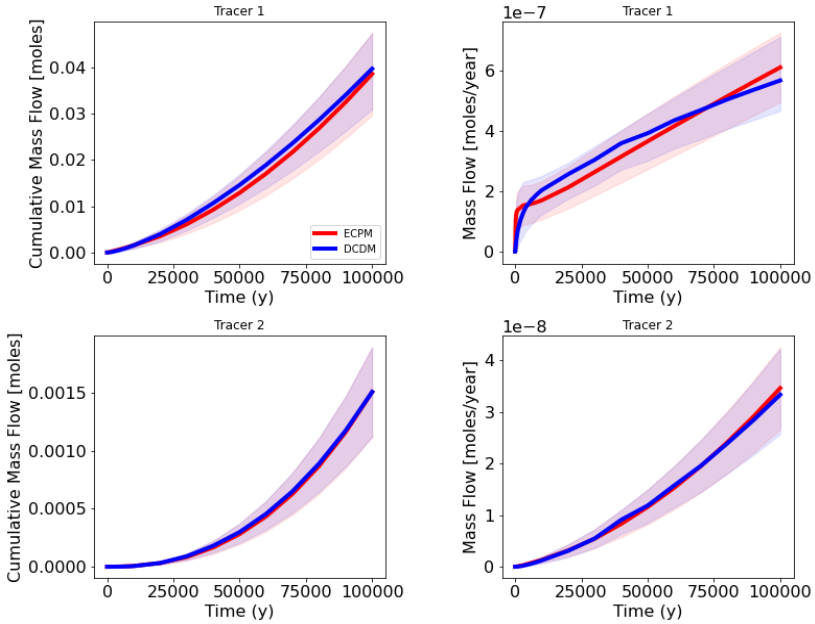

Figure 4-16 Means and 95% confidence intervals for the DCDM (blue) and ECPM (red) for the tracer fluxes at the low point.

The SNL team also completed the simulations with the waste package failure scenarios and the radionuclide source term. Concentration breakthrough curves at a location at the low point are shown in Figure 4-17. The early spike in the ^{129}I concentration is due to the 10% instant release fraction when the waste packages fail at 50,000 years.

Additional reference case results are documented in LaForce et al. (2023a, Section 2.2.1). These results and others will be compared to the results of other teams in the final report of Task F1 with the goal of learning from the approaches and results of other teams. A comparison of the reference case approaches and results among teams is expected to be published in a journal article in 2024.

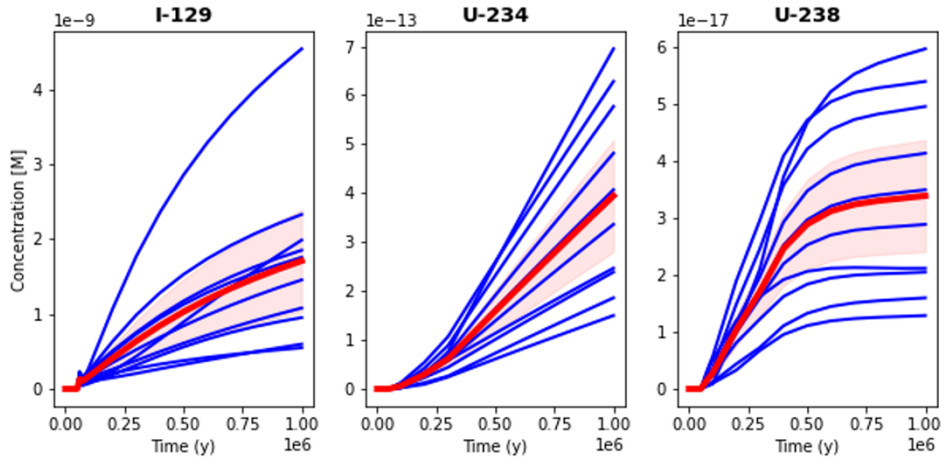

Figure 4-17 Radionuclide concentrations at an observation point (4337, 609, 1000) at the low point. Blue lines are realizations, red line is mean, pink shaded area is 95% confidence interval of the mean.

4.1.6.2 Salt

In FY2023, the salt group of DECOVALEX-2023 Task F developed a disturbed scenario for the salt repository reference case to add to the undisturbed scenarios modeled. The undisturbed scenarios show no consequential release of radiation over one million years. The disturbed scenario assumes the shaft seals fail 1,000 years after repository closure, forcing the repository to flood with water over a short time period.

The general setting is a generic salt dome with the repository located at a depth of 850 m. Figure 4-18 shows the domain, the initial water saturations of the shaft, drifts, and overburden (left) as well as the initial hydrostatic pressures within the intact salt (right). The spacing of waste was chosen to ensure that temperatures on the waste package surface do not exceed 100°C. A new cartesian mesh of 4,309,900 grid cells was developed for this scenario.

Model calculations indicate that full re-saturation of the repository takes approximately 15,000 years and that tracers and radionuclides remain within the disposal drifts and drift seals for the entire one million years simulated. Next steps are to add heat flow, temperature-dependence to drift convergence modeling, model uncertainty, and possibly gas generation. A full summary of the scenario and the results of the simulation are documented in LaForce et al. (2023a).

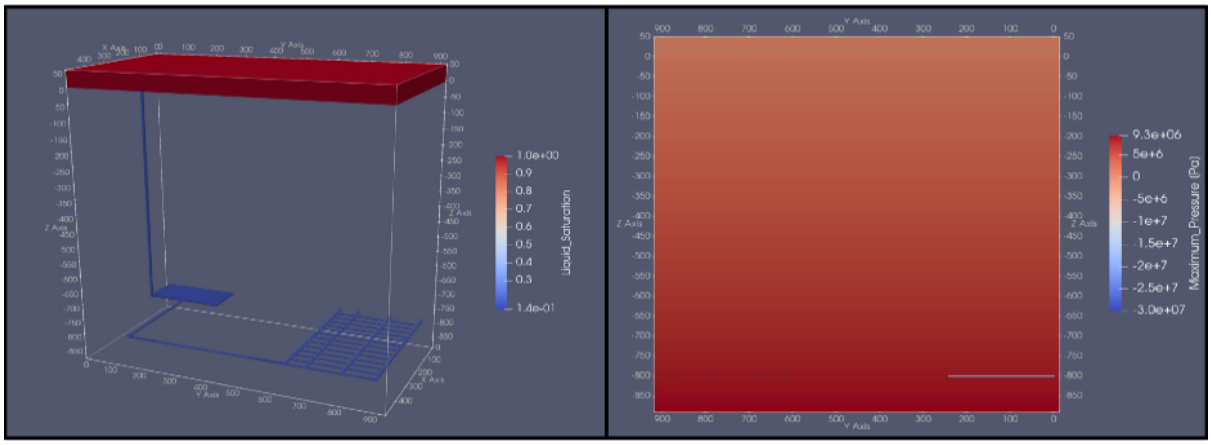

Figure 4-18 The repository, shaft, and overburden colored by initial water saturation (left) and the initial liquid pressures in the intact salt (right).

4.1.7 Repository Reference Cases

Over the past decade, generic repository reference cases have been simulated using GDSA Framework for many host rocks and repository designs. Table 4-2 identifies core reference cases, their conceptual models, and their recent applications. In FY2023, the DECOVALEX repository reference cases for crystalline rock and salt were completed. In addition, the GDSA shale reference case was updated with the GDSA Workflow, improved with more realistic DPC thermal outputs, and run probabilistically for sensitivity analyses. For a new unsaturated zone reference case, a Pierre Shale geologic framework model was used to evaluate the effects of spatial heterogeneity.

Table 4-2 Repository concepts and generic (inventory) reference cases implemented with GDSA Framework

Repository Concepts and Inventory(s)	Conceptual Models	Model Application Reports
Argillite/shale repository		
SNF ranging from 4-PWR waste packages to 37-PWR dual purpose canisters (DPCs)	Jové Colón et al. (2014); Zheng et al. (2014)	Mariner et al. (2017); Sevougian et al. (2019); LaForce et al. (2023a)
High-temperature shale repository	Stein et al. (2020)	Stein et al. (2020)
Crystalline repository		
Commercial SNF	Wang et al. (2014)	Mariner et al. (2016); Swiler et al. (2019, 2020, 2021, 2022)
DECOVALEX crystalline reference case	LaForce et al. (2023b)	LaForce et al. (2023a)
DOE managed waste (cancelled by DOE in 2017)		Sevougian et al. (2016)
Salt repository		
Commercial SNF	Sevougian et al. (2012)	Sevougian et al. (2016); LaForce et al. (2020)
DECOVALEX salt reference case	LaForce et al. (2023b)	LaForce et al. (2022, 2023a)
DOE managed waste (cancelled by DOE in 2017)		Sevougian et al. (2019)
Alluvium repository, unsaturated conditions		
SNF ranging from 12-PWR waste packages to 37-PWR DPCs	Mariner et al. (2018)	Mariner et al. (2018); Sevougian et al. (2019); LaForce et al. (2021, 2022, 2023a)
Dual purpose canister (DPC)		
24- to 37-PWR DPCs and 68- to 80-BWR DPCs	Price et al. (2019a)	Price et al. (2019b)
Deep borehole disposal		
Various waste types, including Cs/Sr capsules	Brady et al. (2009)	Freeze et al. (2016, 2019)

4.1.8 Documentation

4.1.8.1 SFWST Document Archive

The GDSA team continues to support the SFWST Document Archive (SDA), a document repository available to all SFWD participants. The SDA is a restricted-access SharePoint website that serves as an online library for reports generated in:

- NE 81, Office of SFWST
  - Disposal Research (DR)
  - Storage and Transportation (S&T)
- NE 82, Office of Integrated Waste Management (IWM)

Additionally, it contains presentations from past SFWD Annual Meetings.

4.1.8.2 GDSA Calculation Archive

The GDSA team continues to develop and support a GDSA calculation archive, a centralized repository for GDSA calculations. The archive targets all GDSA milestone calculations and their supporting input files, codes, and workflow. The main purpose is for improved internal communication and knowledge capture.

In FY2023, a tracking system was introduced. Calculation tracking numbers (CTNs) are assigned to uploaded packages of calculation files so the supporting files of a calculation can be more easily identified in reports and located in the archive. Several examples of the use of CTNs can be found in the current report.

4.2 PFLOTRAN Development

PFLOTRAN development for GDSA Framework continued at a strong pace in FY2023. Advances were made in PFLOTRAN infrastructure (Section 4.2.1), process model development (Section 4.2.2), and code performance (Section 4.2.3). Brief summaries are presented here. Most of these advances are covered in more detail in Nole et al. (2023).

4.2.1 Software and Hardware Infrastructure

4.2.1.1 Code Management System

The PFLOTRAN development team uses the Atlassian Jira issue and project tracking software to help manage code development activities. Jira issues range from major upgrades and additions to small tasks and bug corrections. Every two weeks, the team assesses progress made, categorizes newly submitted issues, re-prioritizes issues as needed, and confirms assignments for the next two weeks.

Figure 4-19 shows the status of Jira issues addressed in FY2023. PFLOTRAN development included enhancing GDSA Framework capabilities, software maintenance, developing new capabilities, improving code performance, developing new short-course material for GDSA Framework and PFLOTRAN, quality assurance, documentation, and outreach. A detailed summary is provided in Nole et al. (2023).

To improve efficiency and enhance interaction among team members, the PFLOTRAN development team adopted much of the Scrum software development methodology. The methodology establishes roles for the Product Owner (Michael Nole), Scrum Master (Heeho Park), and Development Team. Further details on how this methodology is implemented by the team is provided in Nole et al. (2023, Section 2.2.2).

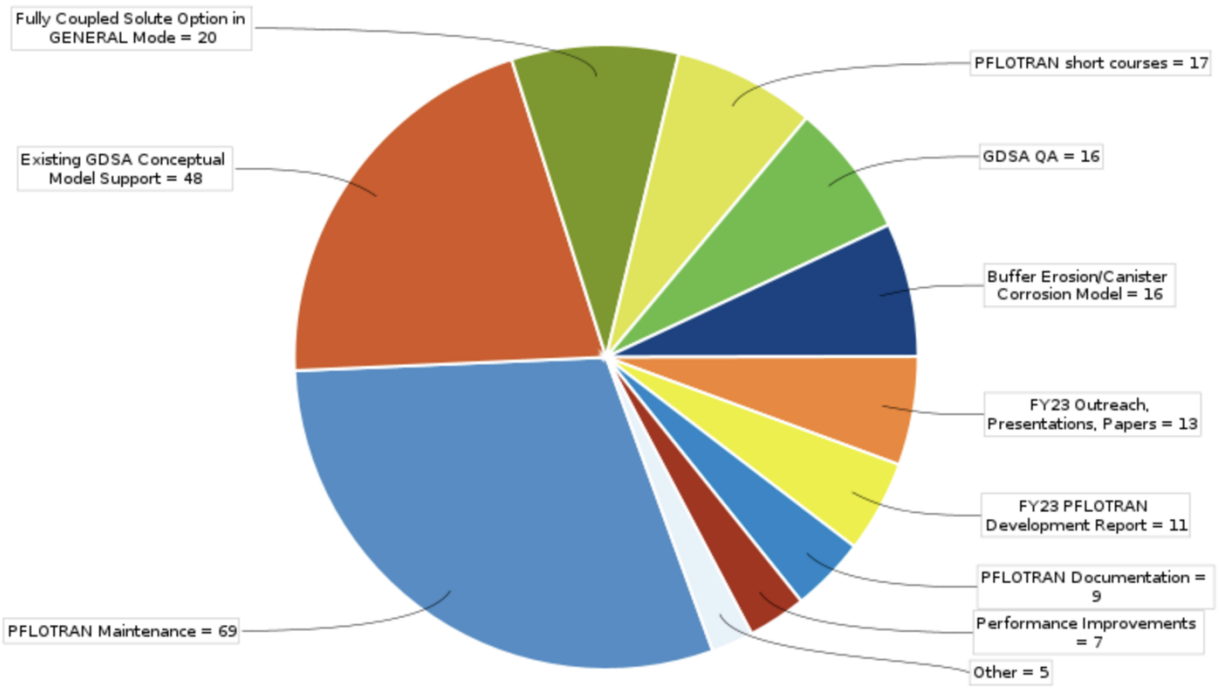

Figure 4-19 Jira issues by category (Nole et al. 2023)

4.2.1.2 Quality Assurance

In FY2023, the original 22 software requirements defined by the PFLOTRAN development team in the previous year were extended to all flow modes, reactive transport mode, and GDSA-specific process models. There are now a total of 46 requirements. To begin addressing the new requirements for TH mode, the TH mode test suite was expanded. An update on this work, including an example test case on variably saturated anisothermal flow, is provided in Nole et al. (2023, Section 2.3).

4.2.2 Model Capability Development

4.2.2.1 Strategy for Model Capability Development

A general strategy was developed to facilitate a streamlined quality-controlled process of integrating models into PFLOTRAN (Mariner et al. 2020a, Section 3.1.3). The approach uses the Jira issue and project tracking software discussed in Section 4.2.1.1. Requests for a code enhancement or a new process model implementation are submitted as Jira issues, along with details describing what is needed and the overall importance of the enhancements. A summary of the approach is provided here.

1. To prepare a Jira request for implementation of a new model or capability, requestors must:

    a. Provide a summary of the model or capability and general ideas for how it will be used

    b. Provide justification for implementation

    c. Identify all model input and output requirements including valid ranges of input values and valid combinations of input values (Detailed requirements are listed in Section 3.1.3 of Mariner et al. (2020a).)

d. State relevant model assumptions and limitations

e. Provide an example simulation/calculation of the model along with plots or tables of outputs

f. Address the following questions

i. Are all relevant model assumptions acceptable, and do the valid ranges of input values extend beyond the envelope of acceptable inputs for the intended use? If not, explain.

ii. Are there other models or approaches with more defensible assumptions that could cover the same or larger range of applicability?

iii. Does the standalone model converge and produce sensible results over the entire (potentially multi-dimensional) input sample space requested?

2. The developers must then:

a. Verify that the requestor has provided the necessary information and justification

b. Decide whether the model is ready for implementation

c. Ensure work package manager approval

d. Accept or reject request, documenting reasons (and documenting management approval as needed)

Upon acceptance, the Jira issue is prioritized and, depending on whether it is high enough priority level, the Scrum Master designs a series of tasks and assigns them to the appropriate PFLOTRAN developer(s). Once assigned, the developer works with the requestor to identify the best implementation approach. Depending on the complexity of the model, the developer may establish regular meetings with the requestor during implementation.

A good example of the process is the request for implementing a buffer erosion and waste package corrosion model (Section 4.2.2.4). The requestor prepared a Microsoft (MS) Word file that addressed in detail all the information listed above, including example simulations in Mathcad and results of the calculations. The PFLOTRAN developers were satisfied with the request, and because it would involve a significant effort, they shared it with the work package manager to ensure support for the implementation. The request was accepted and work began.

4.2.2.2 Fuel Matrix Degradation (FMD) Process Model

The FMD model is the uranium dioxide (UO_2) matrix degradation process model of GDSA Framework. It was developed collaboratively at Argonne National Laboratory and Pacific Northwest National Laboratory (Jerden et al. 2015b). The model, coded in MATLAB, calculates spent fuel degradation rates as a function of radiolysis, electro-kinetic reactions, alteration layer growth, and diffusion of reactants through the alteration layer. In more recent versions of the model, steel corrosion is included to provide a source of hydrogen (Jerden et al. 2018).

In FY2015 a version of the FMD process model that excludes steel corrosion was coded in Fortran (Jerden et al. 2015a). That Fortran code was coupled to PFLOTRAN and was successfully demonstrated (Mariner et al. 2015). Apart from the computational results, the demonstration indicated that the coupled model was highly demanding computationally. Mechanistic simulation of the FMD model processes requires many calculations at each time step. For a probabilistic repository PA calculation with thousands of WPs and hundreds of realizations, the coupled Fortran code from 2015 is too expensive. Further, 2015 Fortran code does not allow for dynamic time stepping and was not written for parallel computing.

In FY2019 and FY2020, two approaches were undertaken to include the FMD process model in GDSA Framework. One approach, described in this section, was to develop a new Fortran code utilizing rapid solvers and flexible time steps for a more powerful standalone FMD process model that smoothly couples to PFLOTRAN. The other approach, summarized in Section 4.2.2.3, was to use Machine Learning (ML) techniques to develop surrogate models of the FMD process model for accurate and rapid emulation in PFLOTRAN.

The objectives of the new Fortran FMD code are a faster design, HPC-compatible, improved convergence, and improved coupling with PFLOTRAN. Also, to make the new process model more flexible than the original MATLAB code, an additional objective is to add the capability of using dynamically changing chemical and temperature inputs over time.

The two primary objectives for FY2023 were 1) to finalize implementation of the interfacial reactions and 2) to add the corrosion layer that builds up over time. Adding these features and processes complete the model of the MATLAB code.

Appendix C summarizes the work in FY2023. The first objective, implementing the interfacial reactions of the MATLAB code, was completed early in the year. A more detailed summary of that work is presented in the proceedings of the 2022 ANS IHLRWM Conference. The title of the paper is, "Development of an Efficient Version of the Fuel Matrix Degradation Model" (Harvey et al. 2022).

The second objective, adding the buildup of the corrosion layer, was also completed. Figure 4-20 shows how the addition of the corrosion layer to the Fortran FMD code causes calculations of UO_2^{2+} to match more closely the results of the MATLAB code.

The Fortran FMD code is orders of magnitude faster than the MATLAB code for a given time step. However, the adaptive time stepping of the Fortran code and its numerical tolerance criteria force so many time step cuts that the code in most cases cannot progress beyond a few years. Work to resolve this issue is underway.

Additional future work involves an upgrade in how radiolysis is implemented. Radiolysis is currently implemented using a constant value for $G_{H_2O_2}$, the primary alpha radiolysis yield of H_2O_2. For a constant value, the implementation is working as expected. A more accurate model for $G_{H_2O_2}$ is needed when concentrations of H_2 are high and O_2 low. Implementation of the Buck et al. (2013) $G_{H_2O_2}$ model is planned to address this issue.

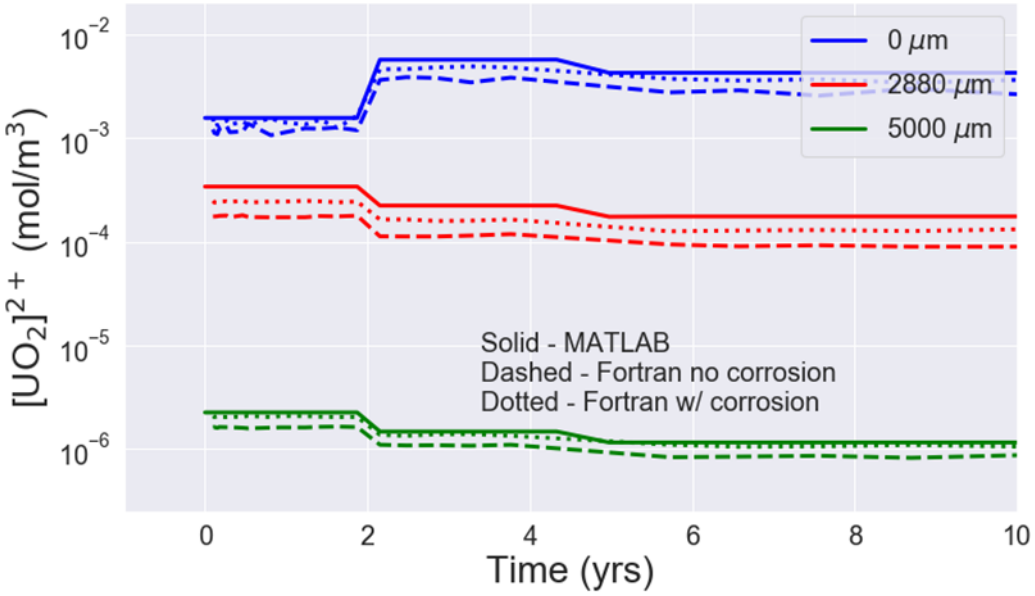

Figure 4-20 Concentration of UO_2^{2+} as a function of time for various distances from the fuel surface, calculated using the MATLAB code, Fortran code without the corrosion layer, and Fortran code with the corrosion layer.

4.2.2.3 Machine Learning FMD Surrogate Models

In FY2020, an Artificial Neural Network (ANN) machine learning (ML) surrogate model and a k-Nearest-Neighbors regression (kNNr) ML surrogate model were implemented in PFLOTRAN for the FMD process model (Mariner et al. 2020b). The ANN surrogate is a parametric model that utilizes a network of artificial neurons with nonlinear activation functions. The kNNr surrogate is a nonparametric model that uses an advanced interpolation approach to approximate a model response using the set of closest neighboring training points in a multidimensional database of training points.

In FY2022, a kNNr surrogate was developed to predict both the corrosion layer thickness (CLT) and fuel degradation rate for the current time step. It was trained on a) the inputs of the original surrogate model, b) the CLT from the previous time step, and c) the time step length. In a repository reference case simulation, the CLT provides a measure of system state. Its value at the end of the previous time step is useful as input for the surrogate model in calculating the CLT and fuel degradation rate for the current time step.

In FY2023, a new ML surrogate approach was developed: neural Ordinary Differential Equations (nODEs). nODEs are used to fit a neural network to the time-derivative of the FMD process model data. The approach is used to predict both the CLT and fuel degradation rate for the current time step, as done by the recent kNNr surrogate developed in FY2022.

Figure 4-21 and Figure 4-22 show predictions of CLT and fuel dissolution rates for 50 randomly sampled simulations of the FMD process model. These comparisons demonstrate the high accuracy of the nODE surrogate model over tens of thousands of years despite output values that vary by many orders of magnitude. Details of this work are provided in Appendix D.

In addition to surrogate model development, two papers on FMD surrogate modeling were published this year, “Machine Learning Surrogate Process Models for Efficient Performance Assessment of a Nuclear Waste Repository” (Debusschere et al. 2022) and “Machine Learning Surrogates of a Fuel Matrix

Degradation Process Model for Performance Assessment of a Nuclear Waste Repository" (Debusschere et al. 2023). The latter was published in *Nuclear Technology* in May 2023.

Future work with the neural ODE surrogate will investigate the impact of the timestep size on accuracy. Another interest is what happens when there are changes to environmental inputs such as H_2 and O_2 over time. How such changes may affect surrogate calculations will be examined.

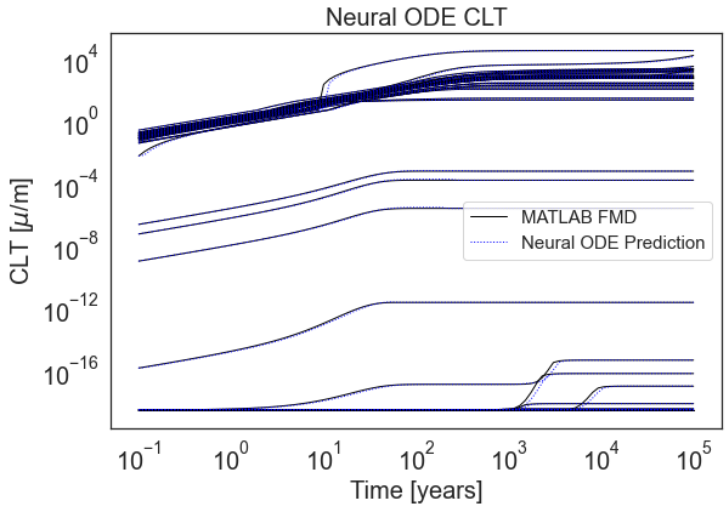

Figure 4-21 Comparison of the MATLAB testing data and neural ODE calculations of the corrosion layer thickness (CLT) for 50 randomly selected simulations.

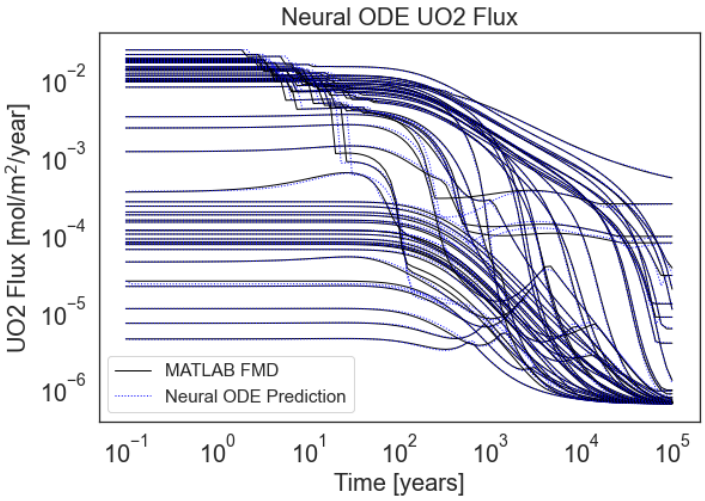

Figure 4-22 Comparison of the MATLAB testing data and neural ODE calculations of the UO_2 flux for 50 randomly selected simulations.

4.2.2.4 Buffer Erosion and Waste Package Degradation

Copper has high chemical stability under crystalline repository conditions and therefore continues to be a prime candidate as a waste package outer barrier material in the U.S. repository program and in the

programs of many countries. A plan was developed to implement buffer erosion and copper corrosion models into PFLOTRAN. The planned models, summarized in Mariner et al. (2021) and Nole et al. (2022), are based on the models developed and used by SKB and Posiva for the Forsmark and Olkiluoto repositories. The conceptual buffer erosion model is illustrated in Figure 4-23.

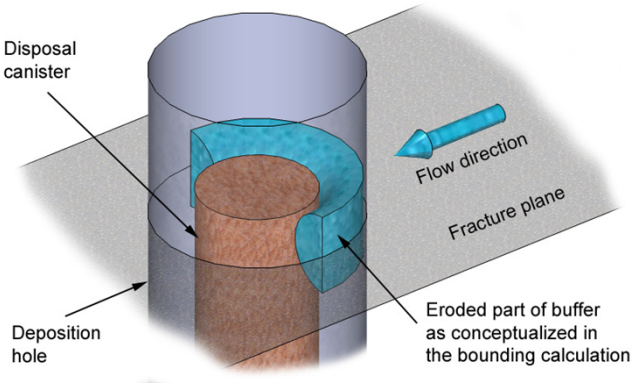

Figure 4-23 Conceptual model of buffer erosion due to a flowing fracture (Fig 6-108, Posiva 2013)

In FY2022, consistent with implementation request protocol (Section 4.2.2.1), a MS Word file was prepared to accompany the Jira request. That file carefully describes the conceptual model, inputs and outputs, the ranges of model validity for the inputs, assumptions, limitations, and the mathematical model. In addition, it provides a printout of a Mathcad model developed to show how the model works, and it provides an application that verifies the model produces the expected results.

The request was accepted, and the implementation is underway. In FY2023, a pre-processor was developed to identify all fractures where canisters are located and read the aperture sizes and angles of the fractures with the largest apertures for each canister. Within PFLOTRAN, routines were developed to read model inputs, read fracture water velocity from a separate simulation absent the deposition holes, and implement model functions affecting the materials modeled. Next steps are implementing canister failure when certain conditions are met, generating the requested output information, and testing.

4.2.2.5 Spacer Grid Degradation

PFLOTRAN's spacer grid degradation model was revised to clarify the required model inputs and improve consistency with literature data. Within the waste form process model, the spacer grid degradation model is used to track the degradation of Zircaloy spacer grids in fuel assemblies to determine when the corrosion is complete, thereby terminating the criticality. The model is described in detail in Section 3.6 of Nole et al. (2023). Scaling was changed to be based on the thickness of the Zircaloy sheets of the grid spacers.

Figure 4-24 shows the effects of the modifications on spacer grid vitality. The revised model causes complete spacer grid degradation much earlier than the previous model (Nole et al. 2023, Section 3.6).

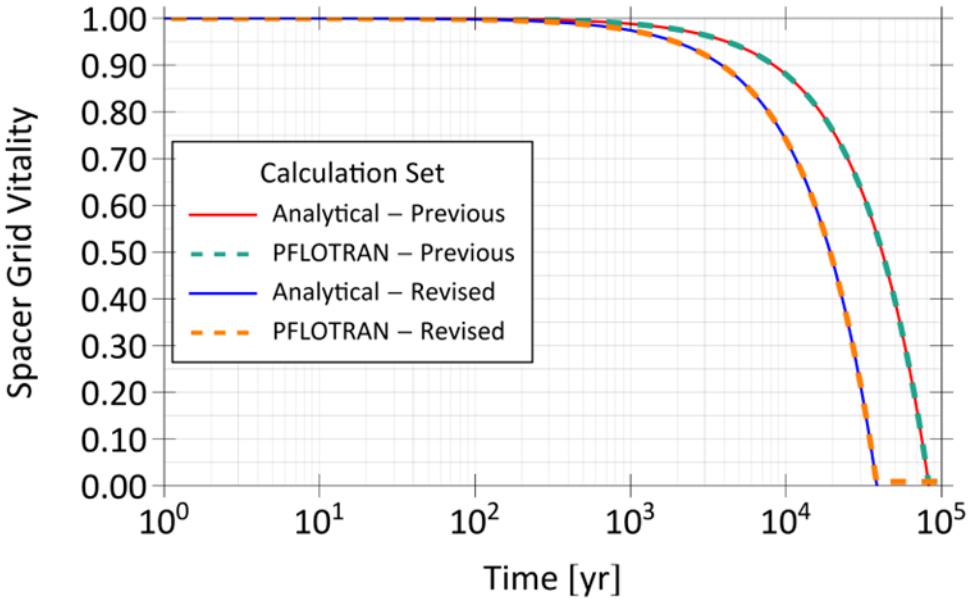

Figure 4-24 Comparison of calculated spacer grid vitality from the PFLOTRAN spacer grid models and the analytical solutions for both the previous and revised models (Nole et al. 2023, Section 3.6)

4.2.2.6 Biosphere

The current biosphere model implemented in PFLOTRAN consists of an ingestion dose model from drinking contaminated well water (Mariner et al. 2017, Section 3.2.3). That model can be used to simulate Example Reference Biospheres 1A and 1B of the International Atomic Energy Agency (IAEA 2003) and can explicitly include the special enhancement effects of highly-mobile short-lived radionuclides like Radon-222.

Pacific Northwest National Laboratory (PNNL) is developing a comprehensive biosphere model for GDSA Framework. The general requirements of the model are that it be generic, flexible, open source, compatible with PFLOTRAN, and consistent with international recommendations and guidance for such models built for deep geological repositories. Features and processes include multiple pathways, components, interactions, and radionuclide decay and ingrowth.

In FY2023, the main functionality of the biosphere model was completed and a set of verification simulations were performed to calculate dose from a large number of pathways. As indicated in Figure 4-25, calculated dose rates are consistent with those generated by GENII version 2.10, a state-of-the-art environmental dosimetry computer code also developed at PNNL. Details of the GDSA biosphere model and its development are available in Ghosh et al. (2022).

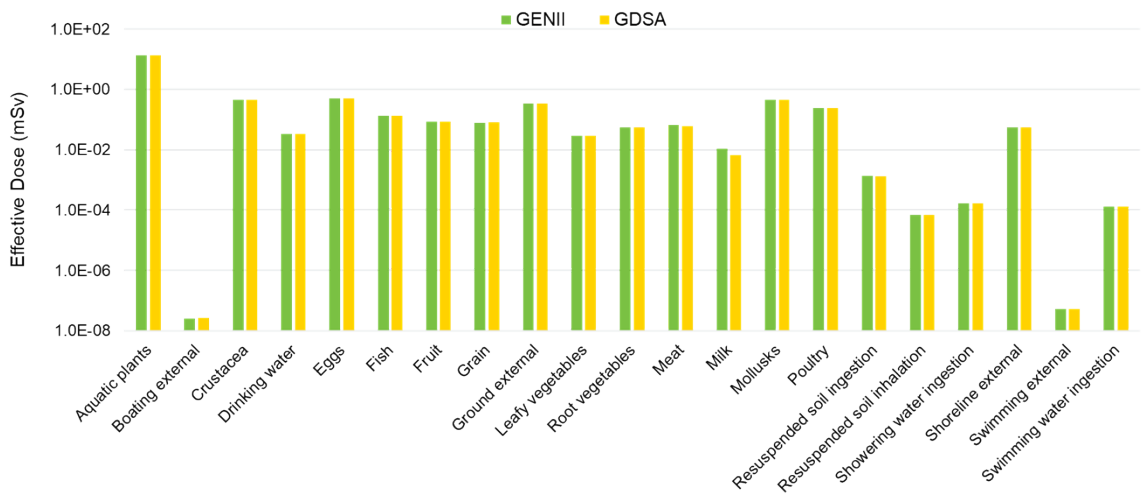

Figure 4-25 Comparison of GENII and GDSA biosphere model effective dose calculated for a unit activity (1 Bq/L) of Radium-226 in groundwater at a location. Dilution factor is used to calculate surface water concentrations (decreased activity) (graphic from Gosh et al. 2023)

4.2.2.7 Multi-Continuum Transport

PFLOTRAN's multi-continuum model simulates disconnected secondary (matrix) continua connected to a primary (fracture) continuum. It is referred to as the DCDM (Dual Continuum Disconnected Matrix) model (Lichtner, 2000). Each primary cell hosts its own disconnected one-dimensional secondary continuum.

There were several improvements to the DCDM model in FY2023:

- Extended applicability to multiple MATERIAL_PROPERTY blocks – Previously, only one MATERIAL_PROPERTY block could be used, which prevented use of the model when other materials are present in the model region. With this improvement, the secondary continua for other materials within the model region (e.g., buffer, backfill, and waste packages) can be turned off.

- Added options for the initial conditions of the secondary continuum – This improvement allows the user to opt for secondary continuum initial conditions (e.g., pressure, temperature) to be identical to the primary continuum or to be read from a file.

- Updated the reactive transport calculation of a region's total moles to properly account for both the primary and secondary continua.

Each of these improvements were tested and used in the DECOVALEX crystalline reference case simulations (Section 4.1.6.1). Additional discussion of these developments is provided in Section 3.1 of Nole et al. (2023).

4.2.2.8 Thermal Secondary Continuum

Thermal secondary continuum capability is now implemented in GENERAL mode. A limiting condition for the time being is that for thermal conduction in the secondary continuum the porosity of the secondary continuum is 0.

The conceptual model and model equations are summarized in Section 3.3 of Nole et al. (2023) along with two test problems. The first problem is for a single cell and a nested sphere geometry. The second is for a slab geometry where cool fluid flows through a fracture within a warm rock matrix. Results of both tests compare well with expected results.

4.2.2.9 Salt Effects and Salt Transport

In FY2023, there were several advances in PFLOTRAN's ability to account for salt content in the calculation of flow and transport:

- Updated equation of state – The equation of state was updated by adding a deviation function to account for density differences at low temperatures that can affect free convection.
- New boundary conditions – Mixed boundary conditions of liquid flux and dissolved components concentration are now available.
- Creep closure – Adding salt mass to grid cells may be an effective way to generate the effects of salt creep in a repository performance assessment model.

Each of these advances are addressed in the following subsections.

EQUATION OF STATE

Sodium chloride is often the dominant salt in groundwater. In FY2022, a new set of equations of state for sodium chloride solutions was built into PFLOTRAN. These equations improve the accuracy of PFLOTRAN calculations of the density, viscosity, saturation pressure, and enthalpy of sodium chloride solutions, especially for brines.

In FY2023, the Driesner equation of state was updated with a deviation function to account for density differences at low temperatures that can lead to the onset of free convection. Bugs in the previous implementation were also fixed. With these updates, test problem results using the Driesner equation of state now closely match those of Batzle and Wang (1992), as shown in Figure 4-26. Details of this update and related bug fixes are presented in Section 3.2.3.2 of Nole et al. (2023).

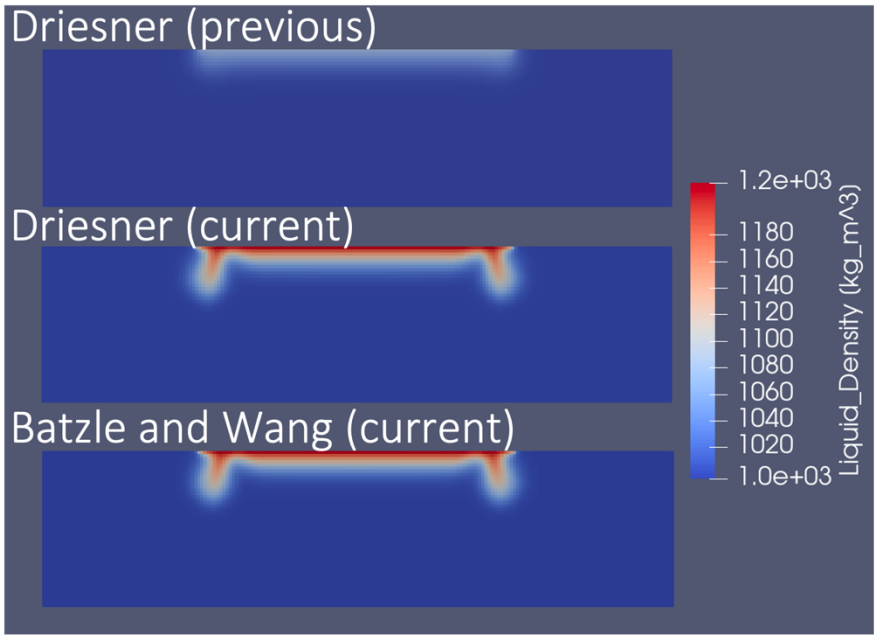

Figure 4-26 Previous and current test results using the Driesner equation of state for density of brines compared with using the Batzle and Wang equation of state

BOUNDARY CONDITIONS

Mixed boundary conditions were added so that boundary fluxes can contain dissolved components at fixed concentrations (Nole et al. 2023, Section 3.2). With this new capability, the Elder problem was rerun. Figure 4-27 compares the results at 10 years before and after implementation of the mixed boundary conditions. The results indicate that the more realistic mixed boundary conditions have notable effects on the system.

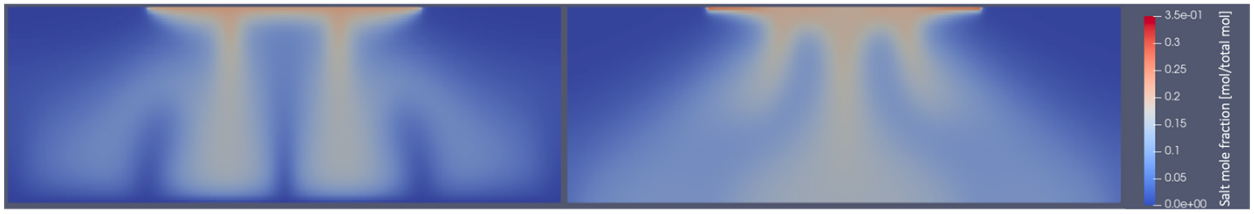

Figure 4-27 Elder problem at 10 years. Left: zero liquid flux, Dirichlet solute concentration, and Dirichlet temperature boundary conditions. Right: Dirichlet pressure, temperature, and solute concentration boundary conditions.

CREEP CLOSURE

For a salt repository model, simulating the effects of salt creep on matrix properties is a capability that would be useful to have in PFLOTRAN. Now that there is a fully coupled salt transport capability for GENERAL mode, it may be possible to emulate these effects by adding salt mass to grid cells as illustrated in Figure 4-28, as opposed to, e.g., interpolating from a porosity response surface. New salt mass reduces porosity and raises liquid pressure. With these changes, gas phase saturation decreases while liquid phase saturation increases. Permeability can be related to porosity such that it decreases with decreasing porosity. This concept is described in more detail in Section 3.2.4 of Nole et al. (2023).

This approach could be useful for total system performance assessment calculations. The appropriate amount of salt to add to each cell over time could be determined by a separate computationally expensive thermal-hydrologic-chemical-mechanical process model. Implementing the salt addition method to emulate the effects of the expensive process model would effectively include the coupled mechanical processes of salt creep in a salt repository performance assessment model.

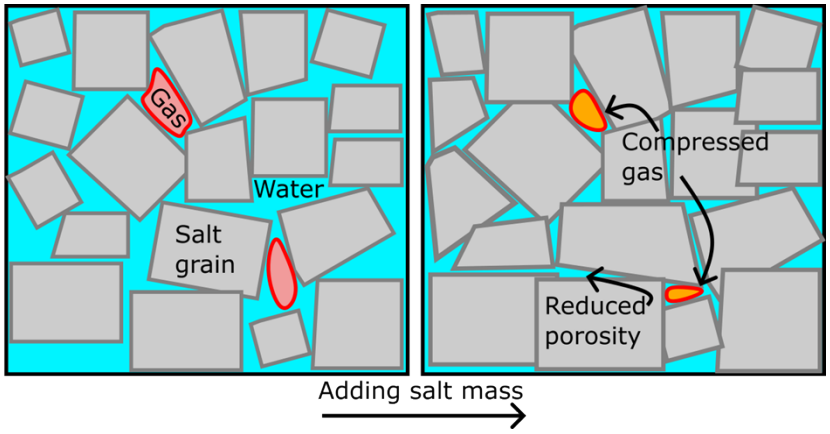

Figure 4-28 Schematic illustration of the spatial effects of adding salt mass to a grid cell

4.2.3 Code Performance Improvements

4.2.3.1 Solvers

Flow and transport calculations rely heavily on solvers and preconditioners. In FY2022, the Newton Trust Region Dogleg Cauchy solver (NTRDC) was added as an option to PFLOTRAN and PETSc. PETSc is the solver library upon which PFLOTRAN is built. The NTRDC solver code was officially released on March 30, 2022, in PETSc and on May 26, 2022, with PFLOTRAN.

In FY2023, a convergence issue was discovered by a developer. To fix the issue, the solver was updated and tested. The new modification ensures that the performance of NTRDC remains superior to Newton's method for large-scale simulations. Additional details are provided in Nole et al. (2023, Section 4.1).

In addition, NTRDC was fully integrated with Global Implicit Reactive Transport (GIRT) mode and Nuclear Waste Transport (NWT) mode in PFLOTRAN. A benchmark test case for the GIRT integration is described in full in Nole et al. (2023, Section 4.3).

4.2.3.2 Nuclear Waste Transport Mode

During the software qualification process for the Waste Isolation Pilot Plant (WIPP) program, several important bugs were discovered in the implementation of convergence criteria for the Nuclear Waste Transport (NWT) mode that caused oscillations and nonconvergence. These issues were fixed, resulting in the elimination of the output oscillations and a speedup in run times by a factor of 21. This work is discussed in more detail in Nole et al. (2023, Section 4.2).

4.2.3.3 Splines

Over the past three years, characteristic curves for media saturation in PFLOTRAN have been smoothed using various methods so that PFLOTRAN solvers can handle transitions between wet and dry conditions. In FY2023, the capability of expressing capillary pressure and relative permeability functions using cubic splines was added. Cubic splines have several advantages including the ability to emulate

complicated analytical expressions. Section 4.4 of Nole et al. (2023) explains the advantages in detail and describes difficult numerical problems during rewetting that are solved using cubic splines.

4.3 Outreach

This section reviews important outreach activities supported by the GDSA Framework development work package and how they benefit nuclear waste repository performance assessment.

4.3.1 International Involvement

Interaction and collaboration with scientists involved in international nuclear waste programs is beneficial to the US program. Opportunities for SFWST participants to interact and collaborate directly arise from participation in:

- International research projects, e.g., DECOVALEX and underground research facility studies
- International clubs, e.g., clay, salt, and crystalline clubs of the Nuclear Energy Agency (NEA)
- International conferences and journals, and technical reviews of submitted manuscripts
- International PFLOTRAN short courses (Nole et al. 2023, Section 5.1)

A detailed account of SFWST involvement in international research projects is presented in the annual report of the international collaborations work package (Birkholzer et al. 2023, in preparation).

GDSA work packages are deeply committed to international participation. In FY2023, participants in the GDSA Framework development work package (SF-23SN01030408) led Task F1 of DECOVALEX-2023 (Section 4.2.2.2), organized and led a topical session and directed a program of work at the 6th NEA Crystalline Club meeting in Korea, presented work and published papers at the 2022 International High Level Radioactive Waste Management Conference, and published a paper in *Nuclear Technology* (Section 4.2.2.3). Other GDSA work packages supported additional international research activities, club meetings, conferences, and papers.

4.3.2 Open-Source Software

GDSA Framework is being developed for DOE and its subcontractors. Most of the software components of GDSA Framework are open source, including PFLOTRAN, Dakota, VoroCrust, and dfnWorks. These codes are utilized by a community of users from around the world for work related to, and unrelated to, repository performance assessment.

Open-source software licensing governs the free distribution of source code and/or binaries among a group of software developers and users. PFLOTRAN utilizes the GNU LGPL (lesser general public license) which states that the code may be distributed and modified as desired, but any changes to the original source code must be free and publicly available. LGPL also allows anyone to link a proprietary third-party library to the code or develop a graphical user interface on top of the code for profit.

There are many benefits to open-source collaboration, especially when taxpayer funds support much of the code development. First, it encourages collaboration among a diverse team of developers. This collaboration pushes the code to the users who can help test and debug the code while providing feedback regarding user interaction. Open source provides transparency that exposes implementation details that are often critical for scientific reproducibility and quality assurance. These details are often deliberately or unintentionally omitted from user documentation, journal publications and reports. From a financial

standpoint, open source allows developers to pool funds across a diverse set of projects funded in academia, government laboratories or the private sector. In addition, funding that would be spent on licensing fees can be redirected towards development. Finally, although the most fit codes can survive under any licensing option, open source may provide a more level playing field for natural selection to run its course.

PFLOTRAN's open-source licensing and accessible distribution facilitate collaboration amongst a broader U.S. and international community. This broad user community enhances the development of PFLOTRAN by sharing conceptual models, incorporating novel physicochemical algorithms, optimizing code performance, debugging problematic issues, and generating grass-roots publicity, all of which benefit DOE in return.

The PFLOTRAN website at www.pflotran.org directs interested parties to the online documentation and the Bitbucket repository (including source code and documentation build status and code coverage). Developer and user mailing lists are managed through Google Groups.

Google Analytics can be used to estimate the size and extent of the PFLOTRAN user community. The hits on the PFLOTRAN website over the past year (Figure 4-29) demonstrates that the PFLOTRAN user base is multi-national.

Country	Acquisition			Behavior		
	Users ↓	New Users	Sessions	Bounce Rate	Pages / Session	Avg. Session Duration
	580 % of Total: 100.00% (580)	**571** % of Total: 100.18% (570)	**686** % of Total: 100.00% (686)	**85.71%** Avg for View: 85.71% (0.00%)	**1.22** Avg for View: 1.22 (0.00%)	**00:00:46** Avg for View: 00:00:46 (0.00%)
1. United States	**225** (38.59%)	218 (38.18%)	264 (38.48%)	89.39%	1.17	00:00:26
2. China	**77** (13.21%)	76 (13.31%)	95 (13.85%)	81.05%	1.34	00:01:17
3. United Kingdom	**29** (4.97%)	29 (5.08%)	35 (5.10%)	82.86%	1.26	00:00:37
4. South Korea	**28** (4.80%)	28 (4.90%)	34 (4.96%)	70.59%	1.32	00:01:18
5. Germany	**25** (4.29%)	25 (4.38%)	33 (4.81%)	87.88%	1.52	00:00:26
6. Japan	**22** (3.77%)	22 (3.85%)	25 (3.64%)	88.00%	1.12	00:00:34
7. Spain	**15** (2.57%)	15 (2.63%)	18 (2.62%)	83.33%	1.17	00:01:23
8. France	**14** (2.40%)	14 (2.45%)	14 (2.04%)	92.86%	1.21	00:00:07
9. India	**14** (2.40%)	14 (2.45%)	14 (2.04%)	92.86%	1.07	00:00:01
10. Norway	**14** (2.40%)	14 (2.45%)	18 (2.62%)	88.89%	1.11	00:00:14

Figure 4-29 Hits to the PFLOTRAN website from individual users between July 3, 2022, and July 3, 2023 from Google Analytics (Nole et al. 2023)

4.3.3 GDSA Framework Website

The GDSA team continues to maintain a public GDSA Framework website at http://pa.sandia.gov/. The home page is shown in Figure 4-30. The purpose of the website is to:

- Describe GDSA Framework, its capabilities, and the objectives behind its development
- Provide related reports for downloading
- Provide links to software used in GDSA Framework (e.g., PFLOTRAN, Dakota, dfnWorks)
- Identify collaborators involved in GDSA Framework development
- Announce events (e.g., PFLOTRAN short courses)
- Provide contact information

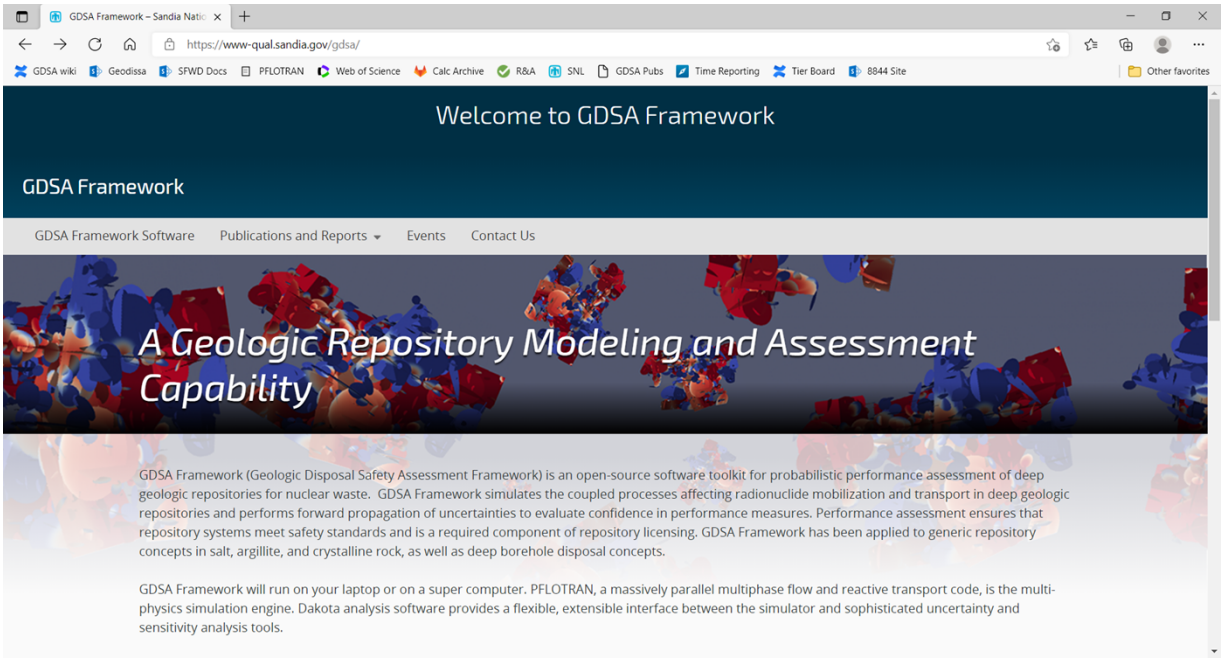

Figure 4-30 GDSA Framework website (http://pa.sandia.gov/)

5 CONCLUSIONS

This report describes FY2023 advances of the Geologic Disposal Safety Assessment (GDSA) performance assessment (PA) development groups of the SFWST Campaign. The common mission of these groups is to develop a geologic disposal system modeling capability for nuclear waste that can be used to probabilistically assess the performance of generic disposal options and generic sites. The developing capability, called GDSA Framework, employs high-performance computing codes PFLOTRAN and Dakota.

The advances in GDSA Framework modeling capabilities in FY2023 allow for improved fluid transport under saline conditions, improved emulation of fuel matrix degradation in repository simulations, material property dependencies and changes over time, improved PFLOTRAN convergence for multiphase systems and dry out, and more detailed sensitivity analysis of system performance. New methods implemented in PFLOTRAN allow for improved reactive transport of soluble porous media (salt) and improved simulation of the interactions of fractures and the rock matrix. Other new capabilities integrate Geologic Framework Models, Voronoi meshing, and biosphere modeling with GDSA Framework. Continued advances in simulation workflows, quality assurance workflows, process model coupling workflows, and other forms of supporting infrastructure are expected to further facilitate future model development and user adoption.

The GDSA reference case models for shale, crystalline rock, salt, unsaturated alluvium, and deep boreholes are enhanced by the improving capabilities of GDSA Framework. The FEPs-activity tracking tool developed this year is designed to help identify gaps in model capabilities and to help prioritize future R&D activities that support the development of these repository concepts. Understanding the relative importance of individual FEPs on post-closure safety performance in these models is also improving. As demonstrated in this report, the use of tracers and performance factors in these models to quantify contributions to safety performance by individual features and processes is expected to become common practice and can help with R&D prioritization.

An important responsibility of the GDSA Framework development team is to integrate with disposal R&D activities across the SFWST Campaign to ensure that R&D activities support the parts of the generic safety cases being developed. In FY2023, the GDSA team participated with other scientists and engineers at LANL, LBNL, PNNL, ORNL, INL, ANL, DOE, and SNL in the development of discrete fracture network modeling, multi-continuum modeling, Geologic Framework Models, fuel matrix degradation process modeling, machine-learning surrogate models, DECOVALEX-2023 Task F performance assessment, and advanced biosphere modeling.

Each year, GDSA Framework improves as additional modelers and programmers from around the world use, apply, and contribute to its development. GDSA Framework can be shared because the primary codes are open source, available for free download, and have supporting documentation online. Outreach and collaborations support a primary objective of the GDSA Framework Development work package by facilitating testing of, and feedback on, PFLOTRAN and GDSA Framework and by increasing the likelihood outside users will contribute directly to code development in the future.

The ability to simulate increasingly complex repository reference cases continues to affirm that GDSA Framework can be used to simulate important multi-physics couplings directly in a total system safety assessment demonstration. Reference case repository applications show that GDSA Framework can simulate complex coupled processes in a multi-kilometer domain while simultaneously simulating sub-meter-scale coupled behavior in the vicinity of each modeled waste package. Continued development will further enhance the preparedness of GDSA Framework for application in the future when transitioning to a program with potential sites.

6 REFERENCES

Abdelkader, A., Bajaj, C.L., Ebeida, M.S., Mahmoud, A.H., Mitchell, S.A., Owens, J.D., & Rushdi, A.A. (2020). VoroCrust: Voronoi meshing without clipping. ACM Transactions on Graphics (TOG) 39(3):1–16.

Adams, B.M., K.R. Dalbey, M.S. Eldred, L.P. Swiler, W.J. Bohnhoff, J.P. Eddy, D.M. Vigil, P.D. Hough and S. Lefantzi (2012). DAKOTA, A Multilevel Parallel Object-Oriented Framework for Design Optimization, Parameter Estimation, Uncertainty Quantification, and Sensitivity Analysis: Version 5.2+ User's Manual. Sandia National Laboratories, Albuquerque, New Mexico.

Adams, B.M., M.S. Ebeida, M.S. Eldred, J.D. Jakeman, L.P. Swiler, W.J. Bohnhoff, K.R. Dalbey, J.P. Eddy, K.T. Hu, D.M. Vigil, L.E. Baumann and P.D. Hough (2013). Dakota, a Multilevel Parallel Object-Oriented Framework for Design Optimization, Parameter Estimation, Uncertainty Quantification, and Sensitivity Analysis, Version 5.3.1+ Theory Manual. Sandia National Laboratories, Albuquerque, New Mexico.

Balay, S., J. Brown, K. Buschelman, V. Eijkhout, W.D. Gropp, D. Kaushik, M.G. Knepley, L. Curfman McInnes, B.F. Smith and H. Zhang (2013). PETSc Users Manual. Argonne, Illinois, Argonne National Laboratory.

Batzle, M., & Wang, Z. (1992). Seismic properties of pore fluids. Geophysics, 57(11), 1396–1408. https://doi.org/10.1190/1.1443207.

Birkholzer, J., B. Faybishenck, Y. Guglielme, J. Rutqvist, L. Zheng, F. Caporuscio, H. Viswanathan, C. Jove-colon, Y. Wang, M. Zavarin, and S. Asmussen (2020). International Collaboration Activities in Geologic Disposal Research: FY20 Progress. LBNL-2001353. Lawrence Berkeley National Laboratory, Berkeley, California.

Brady, P.V., B.W. Arnold, G.A. Freeze, P.N. Swift, S.J. Bauer, J.L. Kanney, R.P. Rechard, and J.S. Stein (2009). Deep borehole disposal of high-level radioactive waste. SAND2009-4401. Sandia National Laboratories, Albuquerque, New Mexico.

Buck, E., J. L. Jerden, Jr., W. L. Ebert and R. S. Wittmann (2013). Coupling the Mixed Potential and Radiolysis Models for Used Fuel Degradation. Washington D.C., U.S. Department of Energy.

Chen, X., G. Hammond, C. Murray, M. Rockhold, V. Vermeul and J. Zachara (2013). "Applications of ensemble-based data assimilation techniques for aquifer characterization using tracer data at Hanford 300 area." Water Resources Research 49: 7064-7076.

Chen, X., H. Murakami, M. Hahn, G. E. Hammond, M.L. Rockhold, J.M. Zachara and Y. Rubin (2012). "Three-Dimensional Bayesian Geostatistical Aquifer Characterization at the Hanford 300 Area using Tracer Test Data." Water Resources Research 48.

Debusschere, B.J., D.T. Seidl, T.M. Berg, K.W. Chang, R.C. Leone, L.P. Swiler, & P.E. Mariner (2022). Machine Learning Surrogate Process Models for Efficient Performance Assessment of a Nuclear Waste Repository. Proceedings of the 2022 International High-Level Radioactive Waste Management Conference, American Nuclear Society, Phoenix, Arizona (SAND2022- 10696 C.Sandia National Laboratories, Albuquerque, New Mexico).

Debusschere, B.J., D.T. Seidl, T.M. Berg, K.W. Chang, R.C. Leone, L.P. Swiler, P.E. Mariner (2023), "Machine Learning Surrogates of a Fuel Matrix Degradation Process Model for Performance Assessment of a Nuclear Waste Repository", Nuclear Technology, 209(9), pp. 1295-1318, https://doi.org/10.1080/00295450.2023.2197666

DOE (2012). Used Fuel Disposition Campaign Disposal Research and Development Roadmap. Washington, DC, Fuel Cycle Technologies, Office of Nuclear Energy, US Department of Energy.

Freeze, G., M. Voegele, P. Vaughn, J. Prouty, W. M. Nutt, E. Hardin and S. D. Sevougian (2013). Generic Deep Geologic Disposal Safety Case. Albuquerque, New Mexico, Sandia National Laboratories.

Freeze, G., P. E. Mariner, J. A. Blink, F. A. Caporuscio, J. E. Houseworth and J. C. Cunnane (2011). Disposal System Features, Events, and Processes (FEPs): FY11 Progress Report. Albuquerque, New Mexico, Sandia National Laboratories.

Freeze, G., P. Gardner, P. Vaughn, S.D. Sevougian, P. Mariner, V. Mousseau (2013). Evaluation of Advanced Performance Assessment Modeling Frameworks: Annotated Outline. SAND2013-6913P. Sandia National Laboratories, Albuquerque, New Mexico.

Freeze, G., Stein, E.R., Brady, P.V., Lopez, C., Sassani, D. (2019). Deep Borehole Disposal Safety Case SAND2019-1915. Sandia National Laboratories, Albuquerque, New Mexico.

Freeze, G., Stein, E.R., Price, L., MacKinnon, R., and Tillman, J. (2016). Deep Borehole Disposal Safety Analysis. FCRD-UFD-2016-000075, SAND2016-10949R. Sandia National Laboratories, Albuquerque, New Mexico.

Freeze, G., W.P. Gardner, P. Vaughn, S.D. Sevougian, P. Mariner, V. Mousseau and G. Hammond (2013). Enhancements to the Generic Disposal System Modeling Capabilities. Sandia National Laboratories, Albuquerque, New Mexico.

Ghosh, S. T. Hay, C. Condon, B. Napier, G. Hammond, H. Gadey (2023). GDSA Biosphere Model Development. Presented at SFWST Annual Meeting, Las Vegas, Nevada, June 26. Pacific Northwest National Laboratory, Richland, Washington.

Ghosh, S., C.A. Condon, B.A. Napier, G. Hammond, S. Snyder, and T. Bailie (2022). GDSA Biosphere Model Design Document. M3SF- 22PN010304071. PNNL-32062. Rev. 1. Pacific Northwest National Laboratory, Richland, Washington.

Gross, M., Alberts, E., Miller, T.A., Guiltinan, E., Swager, K., LaForce, T., and Stauffer, P. (2023). Prototype Workflow for 3D Geologic Modeling and Flow and Transport Simulations of a Generic Alluvial Basin for use in GDSA Repository Systems Analysis. Technical Report LA-UR-23-xxxxx. Los Alamos National Laboratories. Los Alamos, NM.

Gross, M., Guiltinan, E, Milazzo, D., Miller, T., Swanson, E., Miller, E., Lavadie-Bulnes, A., and Stauffer, P.H. (2022). Incorporating Heterogeneity into 3D Geologic Models for the Alluvial Basin Reference Case. Technical Report LA-UR-22-26137, Los Alamos National Laboratories. Los Alamos, NM.

Hammond, G., P. Lichtner and C. Lu (2007). "Subsurface multiphase flow and multicomponent reactive transport modeling using high performance computing." Journal of Physics: Conference Series 78: 1-10.

Hammond, G.E. and P. Lichtner (2010). "Field-scale modeling for the natural attenuation of uranium at the Hanford 300 area using high performance computing." Water Resources Research 46.

Hammond, G.E., P.C. Lichtner and M.L. Rockhold (2011b). "Stochastic simulation of uranium migration at the Hanford 300 Area." Journal of Contaminant Hydrology 120-121: 115-128.

Hammond, G.E., P.C. Lichtner, C. Lu and R.T. Mills (2011a). PFLOTRAN: Reactive Flow and Transport Code for Use on Laptops to Leadership-Class Supercomputers. Groundwater Reactive Transport Models. F. Zhang, G. T. Yeh and J. Parker, Bentham Science Publishers.

Hammond, G.E., P.C. Lichtner, R.T. Mills and C. Lu (2008). "Toward petascale computing in geosciences: application to the Hanford 300 Area." Journal of Physics Conference Series 125: 12051-12051.

Harvey, J.A., A.M. Taconi, & P.E. Mariner (2022). Development of an Efficient Version of the Fuel Matrix Degradation Model. Proceedings of the 2022 International High-Level Radioactive Waste Management Conference, American Nuclear Society, Phoenix, Arizona (SAND2022-8791 C, Sandia National Laboratories, Albuquerque, New Mexico).

Helton, J.C. (1999) "Uncertainty and sensitivity analysis in performance assessment for the Waste Isolation Pilot Plant," Computer Physics Communications, 117(1-2), 156-180.

Helton, J.C., C.W. Hansen, and C.J. Sallabery (2012). "Uncertainty and sensitivity analysis in performance assessment for the proposed high-level radioactive waste repository at Yucca Mountain, Nevada," Reliability Engineering & System Safety, 107, 44-63.

IAEA (2003). Reference Biospheres for Solid Radioactive Waste Disposal. Vienna, Austria, International Atomic Energy Agency.

IAEA (2006). Geological Disposal of Radioactive Waste. Safety Requirements No. WS-R-4. Vienna, Austria, International Atomic Energy Agency.

Jerden, J., G. Hammond, J. M. Copple, T. Cruse and W. Ebert (2015b). Fuel Matrix Degradation Model: Integration with Performance Assessment and Canister Corrosion Model Development. Washington, DC, US Department of Energy.

Jerden, J., J.M. Copple, K. E. Frey and W. Ebert (2015a). Mixed Potential Model for Used Fuel Dissolution - Fortran Code. O. o. U. N. F. Disposition. Washington, DC, US Department of Energy.

Jerden, J., V.K. Gattu and W. Ebert (2018). Update on Validation and Incorporationof a New Steel Corrosion Module into Fuel Matrix Degradation Model. Illinois, Argonne National Laboratory.

Jove Colon, C.F., P. Weck, L. Zheng, J. Rutqvist, C.I. Steefel, K. Kim, S. Nakagawa, J. Houseworth, J. Birkholzer, F.A. Caporuscio, M. Cheshire, M.S. Rearick, M.K. McCarney, M. Zavarin, A.B. Benedicto, M.S. Kersting, J.L. Jerden, K.E. Frey, J.M. Copple, and W.L. Ebert (2014). Evaluation of Used Fuel Disposition in Clay-Bearing Rock. FCRD-UFD-2014-000056. SAND2014-18303R. Sandia National Laboratories, Albuquerque, New Mexico.

LaForce, T., Basurto, E., Bigler, L., Chang, K.W., Ebeida, M., Jayne, R., Leone, R., Mariner, P., Sharpe, J. (2023a). GDSA Repository Systems Analysis Investigations in FY2023. M2SF-23SN010304092. SAND2023-09454R, Sandia National Laboratories, Albuquerque, NM.

LaForce, T., Basurto, E., Chang, K.W., Ebeida, M., Eymold, W., Faucett, C., Jayne, R., Kucinski, N., Leone, R., Mariner, P., Perry, F.V. (2022). GDSA Repository Systems Analysis Investigations in FY2022. SAND2022-12771 R, Sandia National Laboratories, Albuquerque, NM

LaForce, T., Chang, K.W., Perry, F.V., Lowry, T.S., Basurto, E., Jayne, R., Brooks, D., Jordan, S., Stein, E.R., Leone, R., Nole, M. (2020) GDSA Repository Systems Analysis Investigations in FY2020. SAND2020-12028 R. Sandia National Laboratories, Albuquerque, New Mexico.

LaForce, T., E. Basurto, K.W. Chang, R. Jayne, R. Leone, M. Nole, F.V. Perry, and E. Stein (2021). GDSA Repository Systems Analysis Investigations in FY2021. SAND2021-11691-R, Sandia National Laboratories, Albuquerque, New Mexico.

LaForce, T., R.S. Jayne, R. Leone, P. Mariner, E. Stein, E., S. Nguyen, T. Frank (2023b). DECOVALEX-2023 Task F Specification Revision 10. SAND2023-04005 R. Sandia National Laboratories, Albuquerque, NM.

Lichtner, P. C., Hammond, G. E., Lu C., Karra, S., Bisht, G., Andre, B., Mills, R. T., Kumar, J., Frederick, J. M. (2020) PFLOTRAN Web page. http://www.pflotran.org

Lichtner, P.C. (2000). Critique of Dual Continuum Formulations of Multicomponent Reactive Transport in Fractured Porous Media, Ed. Boris Faybishenko, Dynamics of Fluids in Fractured Rock, Geophysical Monograph 122, 281–298.

Lichtner, P.C. and G.E. Hammond (2012). Quick Reference Guide: PFLOTRAN 2.0 (LA-CC-09-047) Multiphase-Multicomponent-Multiscale Massively Parallel Reactive Transport Code. Los Alamos, New Mexico, Los Alamos National Laboratory.

Lu, C. and P. C. Lichtner (2007). "High resolution numerical investigation on the effect of convective instability on long term CO2 storage in saline aquifers." Journal of Physics Conference Series 78: U320-U325.

Mariner, P. E., E. R. Stein, J. M. Frederick, S. D. Sevougian and G. E. Hammond (2017). Advances in Geologic Disposal System Modeling and Shale Reference Cases. SFWD-SFWST-2017-000044, SAND2017-10304 R. Sandia National Laboratories, Albuquerque, New Mexico.

Mariner, P. E., E. R. Stein, J. M. Frederick, S. D. Sevougian, G. E. Hammond and D. G. Fascitelli (2016). Advances in Geologic Disposal System Modeling and Application to Crystalline Rock. FCRD-UFD-2016-000440, SAND2016-9610 R. Sandia National Laboratories, Albuquerque, New Mexico.

Mariner, P. E., E. R. Stein, S. D. Sevougian, L. J. Cunningham, J. M. Frederick, G. E. Hammond, T. S. Lowry, S. Jordan and E. Basurto (2018). Advances in Geologic Disposal Safety Assessment and an Unsaturated Alluvium Reference Case. SFWD-SFWST-2018-000509, SAND2018-11858 R. Sandia National Laboratories, Albuquerque, New Mexico.

Mariner, P. E., L. A. Connolly, L. J. Cunningham, B. J. Debusschere, D. C. Dobson, J. M. Frederick, G. E. Hammond, S. H. Jordan, T. C. LaForce, M. A. Nole, H. D. Park, F. V. Perry, R. D. Rogers, D. T. Seidl, S. D. Sevougian, E. R. Stein, P. N. Swift, L. P. Swiler, J. Vo and M. G. Wallace (2019). Progress in Deep Geologic Disposal Safety Assessment in the U.S. since 2010. SAND2019-12001 R. Sandia National Laboratories, Albuquerque, New Mexico.

Mariner, P.E., B.J. Debusschere, D.E. Fukuyama, J.A. Harvey, T.C. LaForce, R.C. Leone, F.V. Perry, L.P. Swiler, A.M. Taconi (2022a). GDSA Framework Development and Process Model Integration FY2022. M2SF-22SN010304093, SAND2022-14304 R. Sandia National Laboratories, Albuquerque, New Mexico.

Mariner, P.E., E. Basurto, D. M. Brooks, R. C. Leone, T. Portone and L. P. Swiler (2022b). Use of Virtual Tracers in Repository Performance Assessment Modeling. Proceedings of the 2022 International High-Level Radioactive Waste Management Conference Phoenix, Arizona, November 13-17 2022.

Mariner, P.E., M.A. Nole, E. Basurto, T.M. Berg, K.W. Chang, B.J. Debusschere, A.C. Eckert, M.S. Ebeida, M. Gross, G.E. Hammond, J. Harvey, S.H. Jordan, K.L. Kuhlman, T.C. LaForce, R.C. Leone, W.C. McLendon III, M.M. Mills, H.D. Park, F.V. Perry, A. Salazar III, D.T. Seidl, S.D. Sevougian, E.R. Stein, and L.P. Swiler (2020). Advances in GDSA Framework Development and Process Model Integration. M2SF-20SN010304042. SAND2020-10787 R. Sandia National Laboratories, Albuquerque, New Mexico.

Mariner, P.E., T.M. Berg, K.W. Chang, B.J. Debusschere, A.C. Eckert, J. Harvey, T.C. LaForce, R.C. Leone, M.M. Mills, M.A. Nole, H.D. Park, F.V. Perry, D.T. Seidl, L.P. Swiler (2021). GDSA Framework Development and Process Model Integration FY2021. M2SF-21SN010304053, SAND2021-12626 R. Sandia National Laboratories, Albuquerque, New Mexico.

Meacham, P. G., D. R. Anderson, E. J. Bonano and M. G. Marietta (2011). Sandia National Laboratories Performance Assessment Methodology for Long-Term Environmental Programs: The History of Nuclear Waste Management. Sandia National Laboratories, Albuquerque, New Mexico.

Mills, R., C. Lu, P. C. Lichtner and G. Hammond (2007). Simulating subsurface flow and transport on ultrascale computers using PFLOTRAN. 3rd Annual Scientific Discovery through Advanced Computing Conference (SciDAC 2007), Boston, Journal of Physics Conference Series.

Navarre-Sitchler, A., R. M. Maxwell, E. R. Siirila, G. E. Hammond and P. C. Lichtner (2013). Elucidating geochemical response of shallow heterogeneous aquifers to CO2 leakage using high-performance computing: implications for monitoring CO2 sequestration. Advances in Water Resources 53: 44-55.

Nole, M., G.D. Beskardes, D. Fukuyama, R.C. Leone, H.D. Park, M. Paul, A. Salazar, G.E. Hammond, and P.C. Lichtner (2023). Recent Advancements in PFLOTRAN Development for the GDSA Framework. M3SF-23SN010304101. SAND2023-07655. Sandia National Laboratories, Albuquerque, New Mexico.

Nole, M., G.D. Beskardes, D. Fukuyama, R.C. Leone, P. Mariner, H.D. Park, M. Paul, A. Salazar, G.E. Hammond, and P.C. Lichtner (2022). PFLOTRAN Development FY2022. M3SF-22SN010304112. SAND2022-10526 R. Sandia National Laboratories, Albuquerque, New Mexico.

Nole, M., R.C. Leone, H.D. Park, M. Paul, A. Salazar, G.E. Hammond, and P.C. Lichtner (2021). PFLOTRAN Development FY2021. M3SF-21SN010304072. SAND2021-8709 R. Sandia National Laboratories, Albuquerque, New Mexico.

OECD (2004). Post-Closure Safety Case for Geological Repositories Nature and Purpose. Paris, France, Organisation for Economic Co-Operation and Development, Nuclear Energy Agency.

Posiva (2013). Safety Case for the Disposal of Spent Nuclear Fuel at Olkiluoto - Models and Data for the Repository System 2012. POSIVA 2013-01. Posiva Oy, Eurajoki, Finland.

Price, L.L., A.A. Alsaed, A. Barela, P.V. Brady, F. Gelbard, M.B. Gross, M. Nole, J.L. Prouty, K. Banerjee, S. Bhatt, G.G. Davidson, Z. Fang, R. Howard, S.R. Johnson, S.L. Painter, and M. Swinney (2019b). Preliminary Analysis of Postclosure DPC Criticality Consequences. M2SF-20SN010305061. SAND2020-4106. Sandia National Laboratories, Albuquerque, New Mexico.

Price, L.L., A.A. Alsaed, P.V. Brady, M.B. Gross, E.L. Hardin, M. Nole, J.L. Prouty, K. Banerjee and G.G. Davidson (2019a). Postclosure Criticality Consequence Analysis—Scoping Phase. M3SF-19SN010305061. Sandia National Laboratories, Albuquerque, New Mexico.

Rechard, R.P. (1995). Performance Assessment of the Direct Disposal in Unsaturated Tuff of Spent Nuclear Fuel And High-Level Waste Owned by US Department of Energy. Sandia National Laboratories, Albuquerque, New Mexico. 1, 2, and 3.

Rechard, R.P. (2002). General approach used in the performance assessment for the Waste Isolation Pilot Plant. Scientific Basis for Nuclear Waste Management XXV, Boston, Massachussetts, Materials Research Society.

Rechard, R.P. and C.T. Stockman (2014). "Waste degradation and mobilization in performance assessments of the Yucca Mountain disposal system for spent nuclear fuel and high-level radioactive waste." Reliability Engineering and System Safety 122(2): 165-188.

Rechard, R.P. and M.S. Tierney (2005). "Assignment of probability distributions for parameters in the 1996 performance assessment for the Waste Isolation Pilot Plant, Part 1: Description of process." Reliability Engineering and System Safety 88(1): 1-32.

Ridgway, E.M. (2020). Dakota. GUI Version 6.12 User Manual – Next-Gen Workflow. https://dakota.sandia.gov/content/next-gen-workflow. Accessed August 5, 2020.

Russell, G., T. Oldemeyer, C.Davis, R. Mendadhala, D. and Thompson 2022. GDSA – Geologic Modeling – INL – Web Visualization Applications and Assessment Tools. INL/RPT-22-68204. Idaho National Laboratory, Idaho Falls, Idaho.

Sassani, D., J. Birkholzer, R. Camphouse, G. Freeze and E. Stein (2021). SFWST Disposal Research R&D 5-Year Plan – FY2021 Update. Draft Report. M2SF-21SN010304054. Draft Report - SAND2021-12491 R. Sandia National Laboratories, Albuquerque, New Mexico.

Sassani, D., J. Birkholzer, R. Camphouse, G. Freeze, C. Mendez, and L. Price (2023). SFWST Disposal Research R&D 5-Year Plan – FY2023 Update. M2SF-23SN010304083. Draft Report - SAND2023-xxxxx R. Sandia National Laboratories, Albuquerque, New Mexico.

Sevougian, S. D., E. R. Stein, T. LaForce, F. V. Perry, T. S. Lowry, L. J. Cunningham, M. Nole, C. B. Haukwa, K. W. Chang and P. E. Mariner (2019b). GDSA Repository Systems Analysis Progress Report. SAND2019-5189 R. Sandia National Laboratories, Albuquerque, New Mexico.

Sevougian, S. D., G. A. Freeze, W. P. Gardner, G. E. Hammond and P. E. Mariner (2014). Performance Assessment Modeling and Sensitivity Analyses of Generic Disposal System Concepts. Sandia National Laboratories, Albuquerque, New Mexico.

Sevougian, S. D., P. E. Mariner, L. A. Connolly, R. J. MacKinnon, R. D. Rogers, D. C. Dobson and J. L. Prouty (2019a). DOE SFWST Campaign R&D Roadmap Update, Rev. 1. SAND2019-9033R. Sandia National Laboratories, Albuquerque, New Mexico.

Sevougian, S. D., Stein, E. R., LaForce, T., Perry, F. V., Nole, M., Haukwa, C. B., and Chang, K. W. (2019c). GDSA Repository Systems Analysis FY19 Update. SAND2019-11942R. Sandia National Laboratories, Albuquerque, NM.

Sevougian, S.D., G.A. Freeze, M.B. Gross, J. Lee, C.D. Leigh, P. Mariner, R.J. MacKinnon, and P. Vaughn (2012). TSPA Model Development and Sensitivity Analysis of Processes Affecting Performance of a Salt Repository for Disposal of Heat-Generating Nuclear Waste. FCRD-UFD-2012-000320 Rev. 0. U.S. Department of Energy, Office of Nuclear Energy, Used Nuclear Fuel Disposition, Washington, D.C.

Sevougian, S.D., Stein, E.R., Gross, M.B., Hammond, G.E., Frederick, J.M., and Mariner, P.E. (2016). Status of Progress Made Toward Safety Analysis and Technical Site Evaluations for DOE Managed HLW and SNF. FCRD-UFD-2016-000082. SAND2016-11232R. Sandia National Laboratories, Albuquerque, New Mexico.

Stein, E.R., C. Bryan, D.C. Dobson, E.L. Hardin, C. Jové-Colón, C.M. Lopez, E.N. Matteo, S. Mohanty, M. Pendleton, F.V. Perry, J.L. Prouty, D.C. Sassani, Y. Wang, J. Rutqvist, L. Zheng, K.B. Sauer, F. Caporuscio, R. Howard, A. Adeniyi, K. Banerjee, and R. Josep (2020). Disposal Concepts for a High-Temperature Repository in Shale. M3SF-21SN010304064. SAND2020-12471 R. Sandia National Laboratories, Albuquerque, New Mexico.

Swiler, L. P., E. Basurto, D. M. Brooks, A. C. Eckert, P. E. Mariner, T. Portone and E. R. Stein (2020). Status Report on Uncertainty Quantification and Sensitivity Analysis Tools in the Geologic Disposal Safety Assessment (GDSA) Framework. SAND2020-10802 R. Sandia National Laboratories, Albuquerque, New Mexico.

Swiler, L. P., J. C. Helton, E. Basurto, D. M. Brooks, P. E. Mariner, L. M. Moore, S. Mohanty, S. D. Sevougian and E. R. Stein (2019). Status Report on Uncertainty Quantification and Sensitivity Analysis Tools in the Geologic Disposal Safety Assessment (GDSA) Framework. SAND2019-13835 R. Sandia National Laboratories, Albuquerque, New Mexico.

Swiler, L.P., D.M. Brooks, T. Portone, E. Basurto, R. Leone, and P.E. Mariner. Uncertainty and Sensitivity Analysis Methods and Applications in the GDSA Framework (FY2023). SAND2023-08550 R. Sandia National Laboratories, Albuquerque, New Mexico.

Swiler, L.P., E. Basurto, D.M. Brooks, A.C. Eckert, R. Leone, P.E. Mariner, T. Portone, M. L. Smith and E.R. Stein (2021). Uncertainty and Sensitivity Analysis Methods and Applications in the GDSA Framework (FY2021). M3SF-21SN010304042. SAND2021-9903R. Sandia National Laboratories, Albuquerque, New Mexico.

Swiler, L.P., E. Basurto, D.M. Brooks, A.C. Eckert, R. Leone, P.E. Mariner, T. Portone, and M. L. Smith. "Uncertainty and Sensitivity Analysis Methods and Applications in the GDSA Framework (FY2022)." M3SF- 22SN010304082. SAND2022-11220 R. Sandia National Laboratories, Albuquerque, New Mexico

Wang, Y., E. N. Matteo, J. Rutqvist, J. A. Davis, L. Zheng, J. Houseworth, J. Birkholzer, T. Dittrich, C. W. Gable, S. Karra, N. Makedonska, S. Chu, D. Harp, S. L. Painter, P. W. Reimus, F. V. Perry, P. Zhao, J. Begg, M. Zavarin, S. J. Tumey, Z. Dai, A. B. Kersting, J. L. Jerden, K. E. Frey, J. M. Copple, and W. L. Ebert (2014). Used Fuel Disposal in Crystalline Rocks Status and FY14 Progress. FCRD-UFD-2014-000060. SAND2014-17992 R. Sandia National Laboratories, Albuquerque, New Mexico.

Zheng, L. C. Jové Colón, M. Bianchi, and J. Birkholzer (2014). Generic Argillite/Shale Disposal Reference Case. FCRD-UFDC-2014-000319. LBNL-6709E. Lawrence Berkeley National Laboratory, Berkeley, California.

Appendix A. NEAR-TERM GDSA THRUSTS IN THE FY2021 DISPOSAL RESEARCH R&D 5-YEAR PLAN UPDATE

NEAR-TERM GDSA THRUSTS IN THE FY2021 DISPOSAL RESEARCH R&D 5-YEAR PLAN UPDATE

Disposal Research 5-Year Plan Thrusts: Near Term FY21

Thrust	Description	Tech. Area	Term
	Geologic Disposal Safety Assessment		
G01	*Advanced simulation capability*	*GDSA*	*Near*
	Near term advancements in PFLOTRAN capability will continue to focus on high priority topical areas identified in the 2019 Disposal Research R&D Roadmap Reassessment while building on previous accomplishments. These efforts will include continuing to advance high-temperature simulation capability, implementing material-specific waste package degradation models, and addressing the coupled thermo-hydro-mechanical (THM) processes affecting buffer evolution, and the coupled thermo-hydro-chemical (THC) processes affecting radionuclide transport. Multi-fidelity model implementation, including mechanistic models derived from detailed process understanding, reduced order models, and machine learning emulators, enhances computational efficiency and dovetails with integration of advanced UQ/SA methods. Other software development tasks will include ongoing development of open-source biosphere simulation software; addition of capability to dfnWorks (Hyman et al. 2015), software for generating discrete fracture networks and simulating particle transport; and release of an open source version of Vorocrust (Abdelkader et al. 2020), an automated meshing tool for generating conforming meshes of complex engineered and geologic features.		
G02	*Uncertainty and sensitivity analysis*	*GDSA*	*Near*
	Uncertainty quantification and sensitivity analysis (UQ/SA) methods in GDSA Framework will be advanced in two ways. First, the team will continue to identify and demonstrate methods consistent with the current standard of practice that add value to deep geologic repository performance assessment such as surrogate (meta) modeling, variance decomposition, multifidelity analysis, and evaluation of model form uncertainty. The team will continue to take a leadership role in international collaboration on these topics. Second, the team will begin to evaluate the reliability of methods dependent on surrogate models through techniques such as cross-validation and development of quantitative metrics for assessing goodness of surrogates.		

Thrust	Description	Tech. Area	Term
	Geologic Disposal Safety Assessment		
G03	*Workflow* Transparent, traceable workflows increase stakeholder confidence and user-friendliness. In the next 1 to 2 years, GDSA automation will be further developed using NGW and two additional important workflows will be established: an open source framework (scripted in Python) that automates software (PFLOTRAN) verification testing; and a workflow that streamlines data transfer from the geologic model to the meshing software and ultimately to the simulator. Integration of GDSA Framework with the Online Waste Library will be initiated. This integration will provide quality-assured radionuclide inventories for simulations involving defense-related waste streams.	*GDSA*	*Near*
G04	*Repository systems analysis* In the next 1 to 2 years, a main priority will be simulation and analysis of the salt and crystalline reference cases developed for the DECOVALEX2023 task. This task will drive development of models of bentonite backfill evolution and waste package degradation (crystalline) and of salt consolidation and creep; and advance understanding of uncertainties associated with simulation and analysis methods. GDSA will continue to integrate with other technical areas to advance analyses of direct disposal of DPCs, understanding of high-temperature FEPs, and scenario development methodology.	*GDSA*	*Near*
G05	*Geologic modeling* Geologic modeling involves two primary efforts: generation of representative 3-dimensional (3D) regional geology models that inform reference case concepts and simulations, and development of an interactive web-based application (https://gis1.inl.gov/regionalgeology/) for visualizing argillite, salt, and crystalline formations in the US. In the next 1 to 2 years, geologic models of a generic unsaturated alluvial basin and of regional argillite stratigraphy will be linked into the meshing workflow described above; and 3D subsurface visualization tools will be developed within the web application.	*GDSA*	*Near*

(This page is intentionally blank.)

Appendix B. DEVELOPMENT OF FEPS-ACTIVITY TRACKING TOOL FOR REFERENCE CASES

DEVELOPMENT OF FEPS-ACTIVITY TRACKING TOOL FOR REFERENCE CASES

B.1 Objectives

The FEPs-Activity Tracking Tool is being developed to systematize and focus annual planning within the SFWST. The tool will utilize the functionality of Excel and SharePoint to create an environment where members of the technical staff can define work activities and incorporate them into the annual planning effort. The tool will be completely on-line and, eventually, will be migrated to the cloud.

The basic inputs for planning will be work activities developed by the technical staff. These work activities will be mapped to generic FEPs and GDSA reference cases. The activities will also be mapped to broader SFWST objectives, i.e., program thrusts and Roadmap Updates. These mappings will provide a framework for evaluating work activities and demonstrating progress toward program objectives.

The tool will generate reports that synthesize the information provided by the technical staff and the GDSA management team. The synthesized information will provide managers with a technical basis to support decision making. Establishing meaningful goals and priorities requires a solid technical basis. Incorporating FEPs into the framework of the tool facilitates the evaluation of the completeness of the overall program and provides a technical basis for identifying knowledge gaps.

B.2 Approach

The design of the tracking tool emphasizes flexibility for the technical staff who provide inputs and focused information for managers. The tool takes the generic FEPs (Freeze et. al., 2011) as a starting point. The FEPs provide a framework for organizing work activities and a basis for evaluating the development of the GDSA model, i.e., a completeness check. The GDSA reference cases are also used to refine the evaluation of work activities. In some cases, the importance of a FEP will change depending on the reference case being considered. This observation is especially true for the natural system FEPs.

Initially, three reference cases are being included: saturated shale, saturated crystalline, and salt. These reference cases were chosen because they are currently being implemented in the GDSA model. The generic FEPs will be mapped to each of these reference cases. An initial mapping has been completed for

the saturated shale reference case. This initial mapping was completed to support tool development and will be updated during the continued development of the tool. This mapping of FEP to reference case produces the fundamental identifier used for much of the reporting in the tool.

As work on the tool has progressed, it has become evident that FEPs are a coarse framework for evaluating work activities. This situation becomes evident when considering things like gap analyses. Consider FEP 2.1.04.01 Evolution and Degradation of Backfill. The GDSA model currently includes the smectite to illite transition. This is clearly part of FEP 2.1.04.01. However, the model does not include the increase in porosity due to formation of denser mineral phases (e.g., zeolites). This is also part of FEP 2.1.04.01. So, is the FEP included in the GDSA model or excluded? Is there a GAP related to this FEP? This type of question has led the GDSA management team to conclude that the FEPs are a good starting point, but a more detailed discretization will be required for effective work planning. The exact nature of this improvement is under discussion. The description of the FEP may be divided into sub-FEPs. Processes associated with each FEP may be used to provide the further discretization.

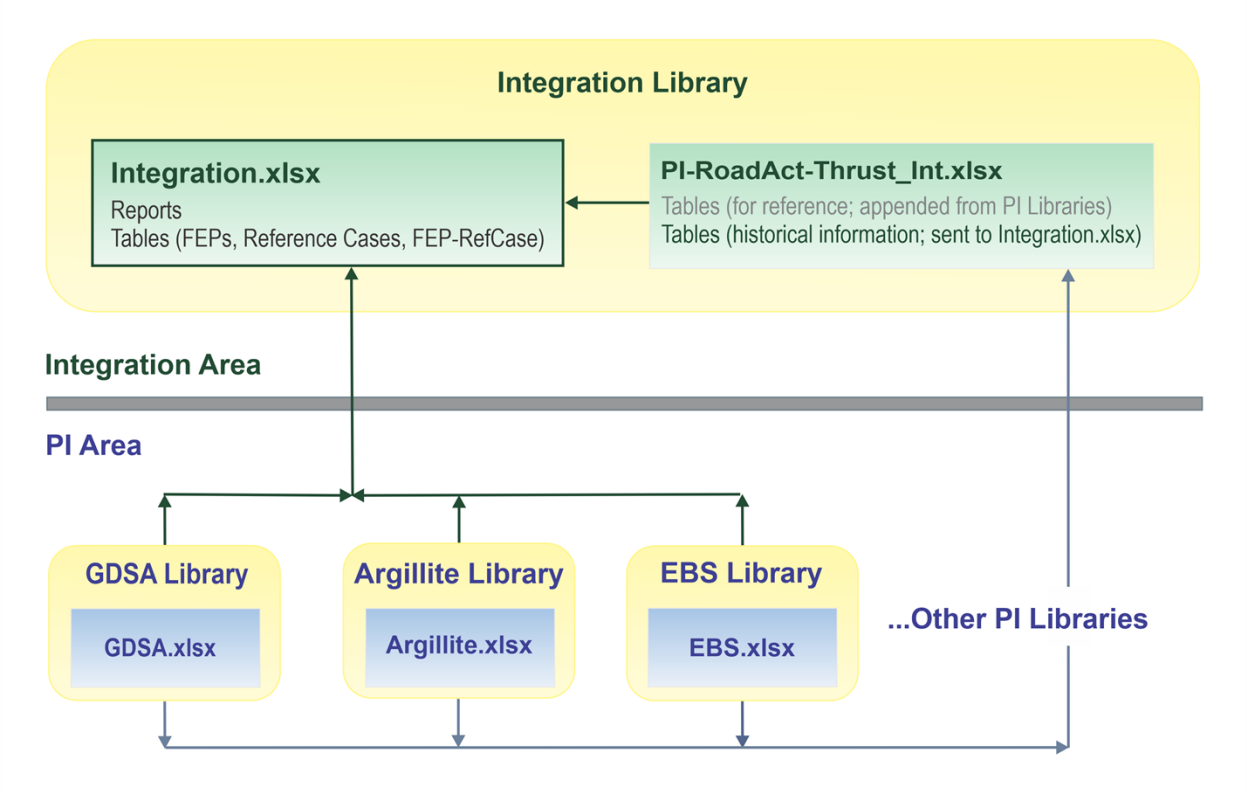

NOTE: EBS = engineered barrier system
FEP = feature, event and/or process
GDSA = Geologic Disposal Safety Assessment
PI = principal investigator

Fig. B-1 Database System Architecture

The system architecture of the tracking tool (Fig. B-1) includes a high-level division between an Integration Area with an Integration Library and a Principal Investigator (PI) Area with multiple PI or technical area libraries. This division is basic to the development and use of the tool. The division also has implications for how the tool will be populated and used. The Integration Library is the portion of the tool that will provide information for decision making. Everyone will have read access to this area, but only

the GDSA management team will have the permissions needed to make changes to information in this area. The PI Area includes a library for each of the program technical areas. The Excel files in these libraries are where information about work activities will be entered into the tool. Everyone will have read access to this area. Control account managers and their designated PIs will have the permissions needed to enter information and make changes to content in their individual libraries.

The Integration Library includes information on FEPs and reference cases as well as historical information and database reports generated from the information available throughout the tracking tool. The information and reports are included in Excel files located in the Integration Library section of the SharePoint site. Historical information that has been entered includes activities from the 2019 Roadmap Update project (Sevougian et. al., 2019), program thrusts (Sassani et. al., 2021), FEPs lists from the Yucca Mountain Project (YMP) and the Waste Isolation Pilot Plant (WIPP), and information on FEP disposition for GDSA reference cases from earlier reports (Hansen et al., 2010; Mariner et al., 2011; Sevougian et al., 2012). Relevant supporting documents for the historical information have also been included. Additional historical information can be added as needed. The Integration Library includes reports generated from the information on work activities entered by project PIs. Detailed information on these reports is provided in Section B.3.3.

The plan for the PI Area includes a SharePoint library for each of the program technical areas. Each library will include an Excel file for information about the work activities in that area. The control account managers will control the content of the libraries for their areas. The control account managers will determine who can enter information into their Excel files, i.e., who are the PIs. The control account managers can also add information to their libraries as they see fit. Additional information might include more detailed discussion of work activities or reports providing supporting information for proposed work activities. Note that the GDSA team will have a library in the PI Area for GDSA activities in addition to providing support for the Integration Library. Details about the information that will be entered into the Excel files in the PI Area are provided in Section B.3.2.

B.3 Preliminary Results

The development activities during FY2023 were designed to accomplish two goals: (1) conduct scoping tests to evaluate potential software and computing environment options for the tracking tool, and (2) establish a preliminary partial version of the tracking tool to serve as a foundation on which to build the full system.

After consideration of various options, the development team decided to use Excel and SharePoint for the tracking tool (Section B.2). These software applications are readily available and familiar to end users. They support collaborative efforts from multiple users, and they are well suited for use in a cloud environment. While tool development is not in a cloud environment at present due to an initial limitation of accepting only unclassified, unlimited release (UUR) information, the expectation is that the tool will eventually be migrated to a cloud environment.

The system structure reflects concepts used in a traditional relational database in that there are a series of tables for different types of information. Each table has a primary key; mapping tables use foreign keys that make it possible to form relationships between information in different tables.

Excel offers several features that allow the tables to operate as a database. The table function provides for the use of table names, which facilitates the process of making connections and queries involving the tables. Excel tables also support dynamic ranging, meaning that the table range expands automatically when a new row or column is added. Instead of having a database with all of the tables in a single file, this system has tables in multiple files hosted in different SharePoint libraries. However, Power Query, one of

the standard Excel features, can make logical connections and process queries for multiple files, multiple file types, and multiple locations. In this case, however, multiple file types are not involved given that there are only Excel files. The query results can be loaded into an actual table or a virtual table. Typically, the virtual option is selected to reduce the load on the file and speed refresh times. The Refresh All option allows new information saved into one or more tables to be accessed as the queries are rerun. It is also possible to refresh specific queries, which is useful when constructing or troubleshooting queries.

The system architecture (Fig. B-2) relies on multiple SharePoint libraries, which provides a means to independently control permissions for each library depending on whether the user is simply viewing information or actively entering and maintaining content. As mentioned in Section B.2, the GDSA management team oversees the operation of the tracking tool as a whole, including the SharePoint permissions, though control account managers will specify the desired permissions for their specific library. The GDSA management team is also responsible for entering and maintaining the content of the Integration Library, as is described in Section B.3.1.

As discussed in Section B.2, the information in the different PI or technical area libraries is focused on characterizing activities for a specific technical area and mapping those activities to other information. While the table structure is controlled by the GDSA management team, the content is the responsibility of the control account manager and/or technical staff assigned by the control account manager. For FY2023, the focus for the PI libraries was primarily on the GDSA Library. Section B.3.2 provides further details on the information in the PI libraries.

The Integration.xlsx file in the Integration Library is where Power Query is used to connect to tables throughout the system and run queries to establish the relationships between information in different tables. Once all the information is combined in the virtual query space, pivot tables can be created to act as database reports. By selecting the Refresh All option, the user can ensure that the reports contain the latest saved information. Section B.3.3 addresses the various types of database reports designed and tested during FY2023.

B.3.1 GDSA Management Team Input into Integration Library (Integration Area)

The Integration Library shown in Fig. B-1 contains two Excel files: Integration.xlsx and PI-RoadAct-Thrust_Int.xlsx. As the name implies, Integration.xlsx serves to integrate all the information in the various tables through the use of Power Query. There are also three tables of content: (1) a table identifying the 208 generic FEPs, (2) a table identifying saturated shale, saturated crystalline, and salt as reference cases, and (3) a table mapping the generic FEPs to the reference cases. The mapping table uses a unique FEPRef ID as a primary key that is also used as a foreign key in a number of other mapping tables in the tracking tool. Besides mapping the FEP to the reference case, the table indicates the GDSA status and the status justification, the 2012 R&D priority and its justification, and the FEP disposition (i.e., include, include?, exclude, and exclude?) and disposition notes. For FY2023 the primary focus was on mapping the FEPs to the saturated shale reference case. Some minor dummy mapping was done to the other two reference cases to ensure that the table structure, queries, and reporting designs would be adequate to handle the additional content generated by a future effort to fully map FEPs to all identified reference cases. The database reports in the file are addressed in Section B.3.3.

The file PI-RoadAct-Thrust_Int.xlsx contains a variety of tables. One set of tables was designed to show the results of appending corresponding tables from the different PI libraries. For example, eventually there will be a table characterizing activities in the Excel file in each PI library. One of the appended tables in PI-RoadAct-Thrust_Int.xlsx will display the results of a query that appends the contents of each activity table. Currently, the suite of appended tables only has results from the GDSA Library since that library

was the focus of FY2023 efforts. These tables are optional and still under consideration in terms of their usefulness. They serve as a convenience to display the information, but they are not used in the integration queries in Integration.xlsx. The integration queries will access and append the same information but will store that information virtually making it available for use in database reports.

PI-RoadAct-Thrust_Int.xlsx also contains tables of historical information as well as tables mapping the combination of the historical FEP-reference case information to the current FEP-reference case information. In addition, there is a table identifying program thrusts from the 5-year plan (Sassani et. al., 2021) and a table bibliographic information on documents cited in other tables. The information in PI-RoadAct-Thrust_Int.xlsx is considered supplemental information and can be augmented based on suggestions from PIs or management.

B.3.2 Technical Staff Input to Technical Area Library (PI Area)

The PI Area of the system architecture (Fig. B-1) is the area where detailed information on proposed, ongoing, and completed work activities is provided. The information will be entered into the Excel file in the library for the appropriate technical area. The information will provide details about the individual work activity and how the activity fits into the broader SFWST objectives.

As discussed above, the PI Area will be divided into several libraries. There will be one library for each program technical area. Each library will include an Excel file and any other information the control account manager wants to include. The Excel file will include several tables where the PI will enter information about work activities. The GDSA team will develop the initial set of tables. But this should be viewed as an initial draft. Suggestions for additional tables or modifications to the initial set of tables are encouraged.

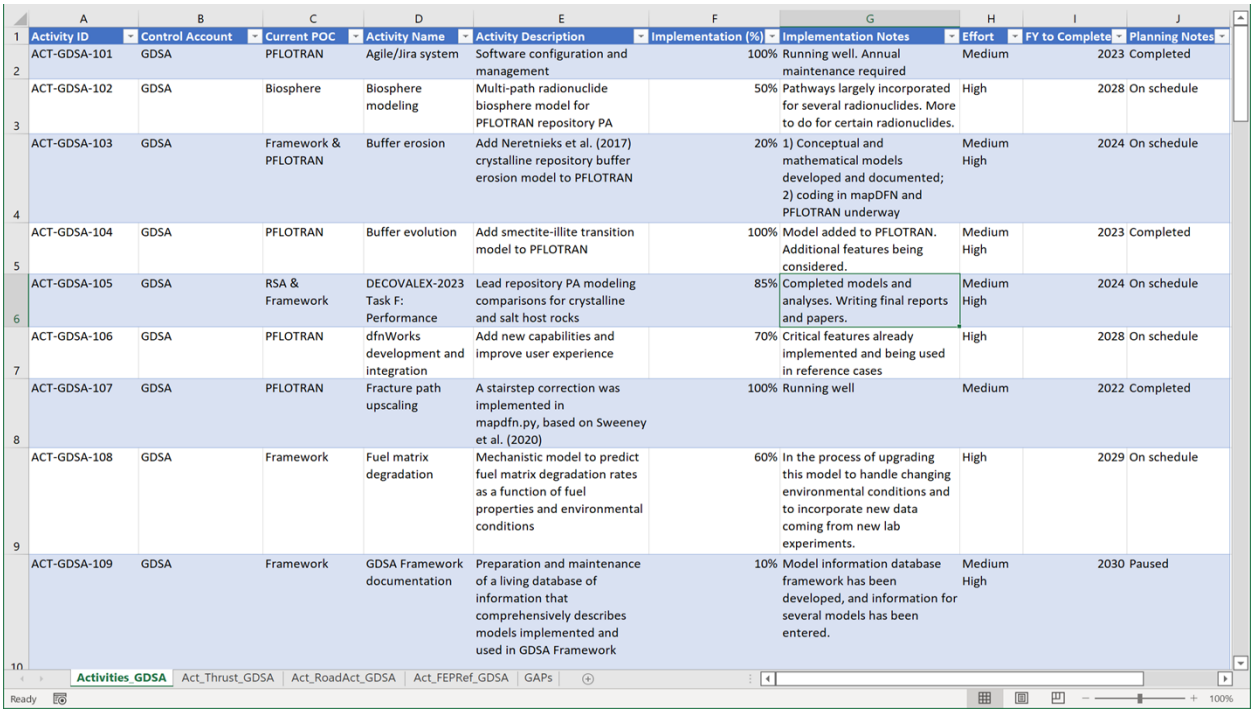

Activity ID	Control Account	Current POC	Activity Name	Activity Description	Implementation (%)	Implementation Notes	Effort	FY to Complete	Planning Notes
ACT-GDSA-101	GDSA	PFLOTRAN	Agile/Jira system	Software configuration and management	100%	Running well. Annual maintenance required	Medium	2023	Completed
ACT-GDSA-102	GDSA	Biosphere	Biosphere modeling	Multi-path radionuclide biosphere model for PFLOTRAN repository PA	50%	Pathways largely incorporated for several radionuclides. More to do for certain radionuclides.	High	2028	On schedule
ACT-GDSA-103	GDSA	Framework & PFLOTRAN	Buffer erosion	Add Neretnieks et al. (2017) crystalline repository buffer erosion model to PFLOTRAN	20%	1) Conceptual and mathematical models developed and documented; 2) coding in mapDFN and PFLOTRAN underway	Medium High	2024	On schedule
ACT-GDSA-104	GDSA	PFLOTRAN	Buffer evolution	Add smectite-illite transition model to PFLOTRAN	100%	Model added to PFLOTRAN. Additional features being considered.	Medium High	2023	Completed
ACT-GDSA-105	GDSA	RSA & Framework	DECOVALEX-2023 Task F: Performance	Lead repository PA modeling comparisons for crystalline and salt host rocks	85%	Completed models and analyses. Writing final reports and papers.	Medium High	2024	On schedule
ACT-GDSA-106	GDSA	PFLOTRAN	dfnWorks development and integration	Add new capabilities and improve user experience	70%	Critical features already implemented and being used in reference cases	High	2028	On schedule
ACT-GDSA-107	GDSA	PFLOTRAN	Fracture path upscaling	A stairstep correction was implemented in mapdfn.py, based on Sweeney et al. (2020)	100%	Running well	Medium	2022	Completed
ACT-GDSA-108	GDSA	Framework	Fuel matrix degradation	Mechanistic model to predict fuel matrix degradation rates as a function of fuel properties and environmental conditions	60%	In the process of upgrading this model to handle changing environmental conditions and to incorporate new data coming from new lab experiments.	High	2029	On schedule
ACT-GDSA-109	GDSA	Framework	GDSA Framework documentation	Preparation and maintenance of a living database of information that comprehensively describes models implemented and used in GDSA Framework	10%	Model information database framework has been developed, and information for several models has been entered.	Medium High	2030	Paused

Fig. B-2 Example Database Input Table

Fig. B-2 is an example of the basic information that PIs will enter for their work activities. PIs will also provide information on how a work activity maps to broader project objectives. The tabs at the bottom of

the figure suggest some of these mappings, e.g., program thrusts and Roadmap Update activities from 2019.

While several of the columns on Fig. B-2 are self-evident, others will benefit from some discussion:

- Activity Description should be brief but capture the important aspects of the work included in the activity.

- Implementation % can be from 0% to 100% depending on whether the activity is proposed, in progress, or complete.

- Implementation Notes provide information that is important for understanding the present status of the activity.

In the future, two more columns will be added to the table in Fig. B-2:

- ISC (Importance to the Safety Case) provides the PI with an opportunity to explain why this work is needed and provides management with a basis for evaluating the work activity. Note that the work activity may be important because it provides a technical basis for excluding a FEP, or portion of a FEP, from the GDSA model.

- ISC Rationale provides a description of the basis for the assigned importance and can be as detailed as needed to make the importance of the activity clear.

In addition to the basic information about work activities the PIs will be required to map the work activities to FEPs. Of course, the relevance and importance of a work activity to a FEP can vary depending on the reference case that is being modeled. Consequently, the mapping will be to the combination of FEP and reference case. Within the tool this combination is captured by the FEPRef ID designator. The PI will identify all FEPRef IDs that are supported by each work activity. The PI will also provide a suggested disposition, e.g., included or excluded, and a disposition justification for each FEPRef ID.

The FEPRef IDs will be defined in a table in the Integration Library (Section B.3.1). This table will include current GDSA status, status justification, and priority information for each ID. The table will be developed by the GDSA team. It will be important for all PIs to review this table and provide comments to the GDSA team. These comments should include any errors identified by the PI and any suggestions for improvement of information provided in the table.

PIs will also provide information on how each work activity supports broader SFWST objectives. This information will be provided by mapping the activities to Program Thrusts, Roadmap Update activities, and possibly other types of mapping. Tabs for these tables can be seen along the bottom of Figure B-2.

PIs will also be tasked with identifying GAPs. A gap could be information that is available but has not been included in the GDSA model. A gap could be a weakness in the state-of-the-art understanding of a process that impacts the results of the GDSA model. PIs will have broad leeway in identifying GAPs. PIs can use this aspect of the planning tool to communicate new ideas and concerns to management. Management will review all identified GAPs and will make the final decisions on how they will be addressed.

GAPs will be identified as part of the mapping of activities to FEPRef IDs. Note that FEPRef IDs are currently defined at the FEP level, but in the future they may be defined at a SubFEP or associated process level, as discussed above.

B.3.3 Database Reports in Integration File in Integration Library

As previously mentioned, the database reports are generated using the pivot table functionality in the file Integration.xlsx in the Integration Library (Fig. B-1). The development effort during FY2023 involved determining the reporting capabilities of Excel and testing potential report designs with consideration of flexibility, user interaction controls, and exportability. The information in the entire tracking tool is made available for inclusion in predetermined reports through the use of Power Query. Depending on the needs of the report, Power Query can be used to generate custom columns, e.g., a column that concatenates cell values from other columns or a column that compares values of other columns.

Fig. B-3 is an example of a potential database report. This report displays information for a particular combination of FEP and reference case (designated internally by a FEPRef ID) along with the related activity information mapped to that FEPRef ID. The white cells under the report title labelled as FEPID_Title, ActivityID_Title, and ThrustID_Title are filters providing the user additional control in analyzing the data. The filters operate similarly to the standard Excel filters available through the down arrows on the column headers. Specific items can be selected among the population of cell values or a text string can be entered into a search box. To make the filters more user-friendly, the cell values are a combination of the ID number and the related title. For example, the filter for FEPs has the FEP ID and FEP title. The other user control provided is a slicer (i.e., the box on the right with the blue rectangular buttons) for reference cases. A slicer has similar functionality to a filter except that there is no search capability. The table design in the report mimics the standard table design used for SFWST reports. A full or a filtered report can be exported into Word using a simple copy and paste process. The basic formatting is also transferred into Word. The report can also be exported into PowerPoint in the same manner, though the formatting will change according to PowerPoint's default table design. Note that the report design shown in Fig. B-3 is preliminary and subject to change as the tracking tool undergoes further development.

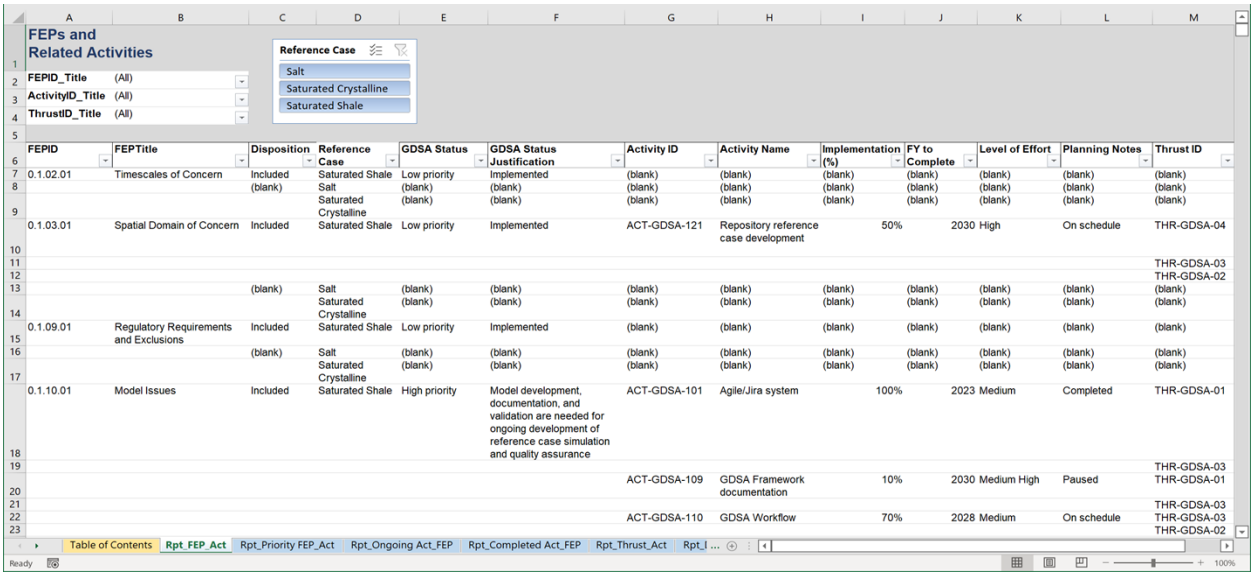

FEPs and Related Activities

Reference Case: Salt; Saturated Crystalline; Saturated Shale

FEPID_Title (All)
ActivityID_Title (All)
ThrustID_Title (All)

FEPID	FEPTitle	Disposition	Reference Case	GDSA Status	GDSA Status Justification	Activity ID	Activity Name	Implementation (%)	FY to Complete	Level of Effort	Planning Notes	Thrust ID
0.1.02.01	Timescales of Concern	Included	Saturated Shale	Low priority	Implemented	(blank)	(blank)	(blank)	(blank)	(blank)	(blank)	(blank)
		(blank)	Salt	(blank)	(blank)	(blank)	(blank)	(blank)	(blank)	(blank)	(blank)	(blank)
			Saturated Crystalline	(blank)	(blank)	(blank)	(blank)	(blank)	(blank)	(blank)	(blank)	(blank)
0.1.03.01	Spatial Domain of Concern	Included	Saturated Shale	Low priority	Implemented	ACT-GDSA-121	Repository reference case development	50%	2030	High	On schedule	THR-GDSA-04
												THR-GDSA-03
												THR-GDSA-02
		(blank)	Salt	(blank)	(blank)	(blank)	(blank)	(blank)	(blank)	(blank)	(blank)	(blank)
			Saturated Crystalline	(blank)	(blank)	(blank)	(blank)	(blank)	(blank)	(blank)	(blank)	(blank)
0.1.09.01	Regulatory Requirements and Exclusions	Included	Saturated Shale	Low priority	Implemented	(blank)	(blank)	(blank)	(blank)	(blank)	(blank)	(blank)
		(blank)	Salt	(blank)	(blank)	(blank)	(blank)	(blank)	(blank)	(blank)	(blank)	(blank)
			Saturated Crystalline	(blank)	(blank)	(blank)	(blank)	(blank)	(blank)	(blank)	(blank)	(blank)
0.1.10.01	Model Issues	Included	Saturated Shale	High priority	Model development, documentation, and validation are needed for ongoing development of reference case simulation and quality assurance	ACT-GDSA-101	Agile/Jira system	100%	2023	Medium	Completed	THR-GDSA-01
												THR-GDSA-03
						ACT-GDSA-109	GDSA Framework documentation	10%	2030	Medium High	Paused	THR-GDSA-01
												THR-GDSA-03
						ACT-GDSA-110	GDSA Workflow	70%	2028	Medium	On schedule	THR-GDSA-03
												THR-GDSA-02

Table of Contents | Rpt_FEP_Act | Rpt_Priority FEP_Act | Rpt_Ongoing Act_FEP | Rpt_Completed Act_FEP | Rpt_Thrust_Act | Rpt_I ...

Ready 100%

Fig. B-3 Example Database Report

During FY2023, the team developed eleven potential reports:

- FEPs and Related Activities
- Priority FEPs and Related Activities
- Ongoing Activities and Related FEPs
- Completed Activities and Related FEPs
- Thrusts and Related Activities
- Dispositions Conflicting with Suggested Dispositions
- Current Dispositions Compared to Historical Dispositions
- Dispositions Conflicting with Historical Dispositions
- FEPs without Activities
- Activities with ≤10% Implementation and Related FEPs
- Identified GAPs by FEPs and Activities

Each report occupies a single worksheet. Given that the list of reports is expected to change and grow as the tracking tool evolves, the team created a Table of Contents on the first worksheet of Integration.xlsx to facilitate navigation. The Table of Contents identifies the worksheet (i.e., tab) name, the worksheet type (i.e., database report or Excel table), and the name of the report or table along with providing a hyperlink to the worksheet.

B.4 Future Work

Future work will include enhancements to the SharePoint environment that houses the tool, population of the tables with activities and supporting information from all technical areas, mapping of FEPs and associated processes or subFEPs to a wider selection of GDSA reference cases, and use of the synthesized information to enhance program development. In addition, there will be an effort to identify and implement additional steps to enhance database integrity, including consideration of entity integrity, referential integrity, and domain integrity. Plans for the tracking tool also call for its eventual migration to a cloud environment.

The tool is currently in the developmental phase and will evolve. However, the basic architecture presented in Section B.2 is not expected to change. Comments and inputs from the technical staff are expected to lead to improvements making the tool more useful. Comments and inputs from management will also be sought.

Libraries for all technical areas are planned to be available for the FY2025 planning effort. Inputs from the technical staff during that planning effort will allow testing of the functionality of the entire tool. Significant improvements to the tool are expected to result from this planning effort.

The synthesis of the information provided by the technical staff has the potential to enhance program development. The status of the GDSA model can be clearly documented. The strengths and weaknesses of the model can be assessed. This information can be used to sharpen program thrusts and enhance the next Roadmap Update effort.

B.5 References

Freeze, G., P. Mariner, J.A. Blink, F.A. Caporuscio, J.E. Houseworth, J.C. Cunnane. 2011. *Disposal System Features, Events and Processes (FEPs): FY11 Progress Report.* FCRD-USED-2011-000254; SAND2011-6059P. Albuquerque, NM: Sandia National Laboratories.

Hansen, F.D., E.L. Hardin, R.P. Rechard, G.A. Freeze, D.C. Sassani, P.V. Brady, C.M. Stone, M.J. Martinez, J.F. Holland, T. Dewers, K.N. Gaither, S.R. Sobolik, and R.T. Cygan. 2010. *Shale Disposal of U.S. High-Level Radioactive Waste*. SAND2010-2843. Albuquerque, NM: Sandia National Laboratories.

Mariner, P.E., J.H. Lee, E.L. Hardin, F.D. Hansen, G.A. Freeze, A.S. Lord, B. Goldstein, and R.H. Price. 2011. *Granite Disposal of U.S. High-Level Radioactive Waste*. SAND2011-6203. Albuquerque, NM: Sandia National Laboratories.

Sassani, D., J. Birkholzer, R. Camphouse, G. Freeze, E. Stein. 2021. *SFWST Disposal Research R&D 5-Year Plan – FY2021 Update.* M2SF-21SN010304054. Albuquerque, NM: Sandia National Laboratories.

Sevougian, S.D., G.A. Freeze, M.B. Gross, J. Lee, C.D. Leigh, P. Mariner, R.J. MacKinnon, and P. Vaughn. 2012. *TSPA Model Development and Sensitivity Analysis of Processes Affecting Performance of a Salt Repository for Disposal of Heat-Generating Nuclear Waste*. FCRD-UFD-2012-000320, Rev. 0. Albuquerque, NM: Sandia National Laboratories.

Sevougian, S.D., P.E. Mariner, L.A. Connolly, R MacKinnon, R.D. Rogers, D.C. Dobson, J.L. Prouty. 2019. *DOE SFWST Campaign R&D Roadmap Update.* M2SF-19SN010304042, Rev. 1; SAND2019-9033 R. Albuquerque, NM: Sandia National Laboratories.

(This page is intentionally blank.)

Appendix C. FUEL MATRIX DEGRADATION PROCESS MODEL CODE DEVELOPMENT IN FORTRAN

FUEL MATRIX DEGRADATION PROCESS MODEL CODE DEVELOPMENT IN FORTRAN

C.1 Introduction

Herein we describe the efforts undertaken in FY2023 to complete the implementation of the Fuel Matrix Degradation (FMD) model in Fortran. The FMD model is designed to determine the rate of radionuclide release in a compromised waste package container. Surrogate models are trained from the data generated from the FMD model and are used in performance assessment simulations. The current implementation of the FMD model in MATLAB is slow, generates unphysical results, and is difficult to update or add new processes. Developing a Fortran version will alleviate these pressures and make the FMD model more user-friendly across the Spent Fuel and Waste Science and Technology (SFWST) campaign. Conversion of the MATLAB FMD model to Fortran was completed this year, however a few technical challenges remain before broad adoption can begin.

C.2 FMD Process Model

The FMD process model has been discussed in numerous reports and manuscripts (Jerden et al. 2012, Jerden et al. 2014, Jerden et al. 2015, Jerden et al. 2017). Briefly, the model encompasses a 1D reactive transport domain consisting of a fuel interface, bulk aqueous phase, and canister interface. The specific reactions that occur in each region are listed in the tables below. In addition to these reactions, H_2O_2 is produced via an alpha radiolysis process, and precipitation and dissolution of three uranium solid phases can occur. The full set of reactions is displayed in Tab. C-1 and Tab. C-2.

Tab. C-1 List of aqueous chemistry reactions incorporated in the FMD model.

Aqueous Chemistry Reactions
$UO_2^{2+} + 2OH^- + H_2O \rightarrow UO_3 \cdot 2H_2O$
$UO_2^{2+} + H_2O_2 + 4H_2O \rightarrow UO_4 \cdot 4H_2O + 2H^+$
$UO_2(CO_3)_2^{2-} + 2OH^- + H_2O \rightarrow UO_3 \cdot 2H_2O + 2CO_3^{2-}$
$UO_3 \cdot 2H_2O + 2CO_3^{2-} \rightarrow UO_2(CO_3)_2^{2-} + 2OH^- + H_2O$
$H_2O_2 + 2Fe^{2+} + 4OH^- \rightarrow 3H_2O + Fe_2O_3$
$O_2 + 4Fe^{2+} + 8OH^- \rightarrow 4H_2O + 2Fe_2O_3$
$UO_2^{2+} + 2Fe^{2+} + 6OH^- \rightarrow UO_{2,(aq)} + 3H_2O + Fe_2O_3$
$UO_2(CO_3)_2^{2-} + 2Fe^{2+} + 6OH^- \rightarrow UO_{2,(aq)} + 2CO_3^{2-} + 3H_2O + Fe_2O_3$
$H_2O_2 \rightarrow H_2O + \frac{1}{2}O_2$
$UO_{2,(s)} \rightarrow UO_{2,(aq)}$
$UO_{2,(aq)} \rightarrow UO_{2,(s)}$

Tab. C-2 Electrochemical reactions incorporated into the FMD model at the fuel, fuel noble metal particle (NMP), and steel (canister) interface. The steel reactions are included in the MATLAB FMD model but excluded in the Fortran version.

Surface	Reactions
Fuel	$UO_2 \rightarrow UO_2^{2+} + 2e^-$ $UO_2 + 2CO_3^{2-} \rightarrow UO_2CO_3^{2-} + 2e^-$ $UO_2 \rightarrow UO_{2,(aq)}$ $H_2 + 2OH^- \rightarrow 2H_2O + 2e^-$ $H_2O_2 + 2OH^- \rightarrow O_2 + 2H_2O + 2e^-$ $H_2O_2 + 2e^- \rightarrow 2OH^-$ $O_2 + 2H_2O + 4e^- \rightarrow 4OH^-$
Fuel, NMP	$H_2 + 2OH^- \rightarrow 2H_2O + 2e^-$ $H_2O_2 + 2e^- \rightarrow 2OH^-$ $H_2O_2 + 2OH^- \rightarrow O_2 + 2H_2O + 2e^-$ $O_2 + 2H_2O + 4e^- \rightarrow 4OH^-$
Steel	$Fe \rightarrow Fe^{2+} + 2e^-$ $2H_2O + 2e^- \rightarrow H_2 + 2OH^-$

C.3 Interfacial Reaction Region

The bulk of our efforts this year were spent implementing the fuel interfacial reactions. We excluded the steel interfacial reactions in the Fortran version because steel degradation is assumed to be modeled by a separate coupled model. Of particular importance is the formation of Fe^{2+} and H_2 at the steel interface. Hydrogen is significant because it oxidizes much more readily than the fuel and therefore slows the fuel oxidation process (Jerden 2015). Instead, an environmental concentration of H_2 is set at a bulk water boundary as a function of time by the user (eventually, it may be provided by a coupled model, e.g., a steel corrosion model). The MATLAB FMD model utilizes a logarithmic spatial discretization that generates cells that are closer together near the fuel and steel interfaces. By removing the steel interface reaction, the Fortran version simply implements a logarithmic spatial discretization away from the fuel surface only (i.e., the cells continuously get larger moving away from the fuel interface).

The fuel interface redox reactions are separated into half reactions that contribute to an electrical current such that currents offset each other:

$$i_{anode} - i_{cathode} = 0. \tag{C-1}$$

The current produced by each reaction typically takes on the form of

$$i^{UO_2,1} = nF\varepsilon k_{UO_2,1} exp\left[\frac{\alpha_{UO_2,1}F}{RT}\left(E_{corr}^{UO_2} - E_{UO_2,1}^{0}\right)\right] \tag{C-2}$$

where n is the number of transferred electrons, F is Faraday's constant, ε is the porosity of fuel or steel corrosion layers, $k_{UO_2,1}$ is the reaction rate constant, $\alpha_{UO_2,1}$ is the electrochemical transfer coefficient, R is the universal gas constant, T is the temperature, $E_{corr}^{UO_2}$ is the corrosion potential of the fuel, and $E_{UO_2,1}^{0}$ is the standard potential. The specific equation represented in Eq. C-2 is for reaction 1 in Tab. C-2. Other reactions also have a concentration dependence (Jerden et al. 2012, Jerden et al. 2014, Jerden et al. 2015, Jerden et al. 2017, Shoesmith et al. 2003). The unknowns for this set equations are the concentrations and corrosion potentials.

In the MATLAB FMD code these equations are solved iteratively using a recursive function that calls itself. The Fortran version creates two separate subroutines, one that solves for the corrosion potentials given the current concentration of the species and another that updates the concentrations given the new corrosion potential. These two subroutines pass their outputs back and forth until the solution for the concentrations essentially stabilizes. While these subroutines operate iteratively, as in the MATLAB version, the readability of the code is vastly improved without the recursive call of the same routine from itself. The corrosion potential is calculated using a separate Newton-Raphson solver from the concentration Newton-Raphson solver.

C.4 Corrosion Layer Thickness

The last remaining process incorporated into the Fortran version is the corrosion layer thickness. The corrosion layer is formed by precipitation of solid uranium phases via reactions 1, 2, and 11 in Tab. C-1. The thickness of this layer is determined by numerically integrating the concentration, multiplying by the molecular weight of the species, and dividing by the species density to yield a distance. Any grid cell that is less than this distance is modeled to be part of the corrosion layer. The corrosion layer retards diffusion and partially blocks access to the fuel surface thereby slowing the kinetics of the oxidation reactions. Both the rate of diffusion slowdown and fuel surface coverage are user input values.

C.5 Comparison of Fortran to MATLAB Results

Using the Fortran implementation of the FMD model we show brief comparisons to the MATLAB version results. Fig. C-1 depicts the concentration of $[UO_2]^{2+}$ as a function of time for three locations within the 1D domain. Results are shown for the Fortran version with and without the corrosion layer thickness turned on. A similar plot is shown in Fig. C-2 for the $[UO_2(CO_3)]^{2-}$. Comparisons between the MATLAB and Fortran versions are favorable.

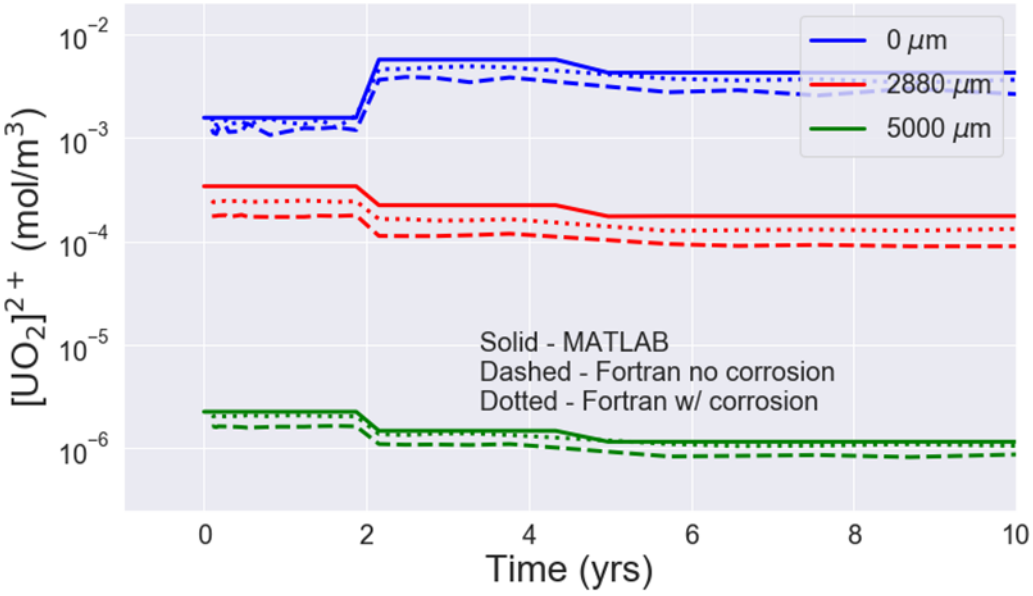

Fig. C-1 **The concentration of $[UO_2]^{2+}$ as a function of time at 0 (blue), 2880 (red), and 5000 μm (green) representing distances at the fuel interface, the middle of the 1D domain, and the farthest point in the simulation. Results for the MATLAB (solid), Fortran code without the corrosion layer thickness turned on (dash), and Fortran code with the corrosion layer thickness (dotted) are shown.**

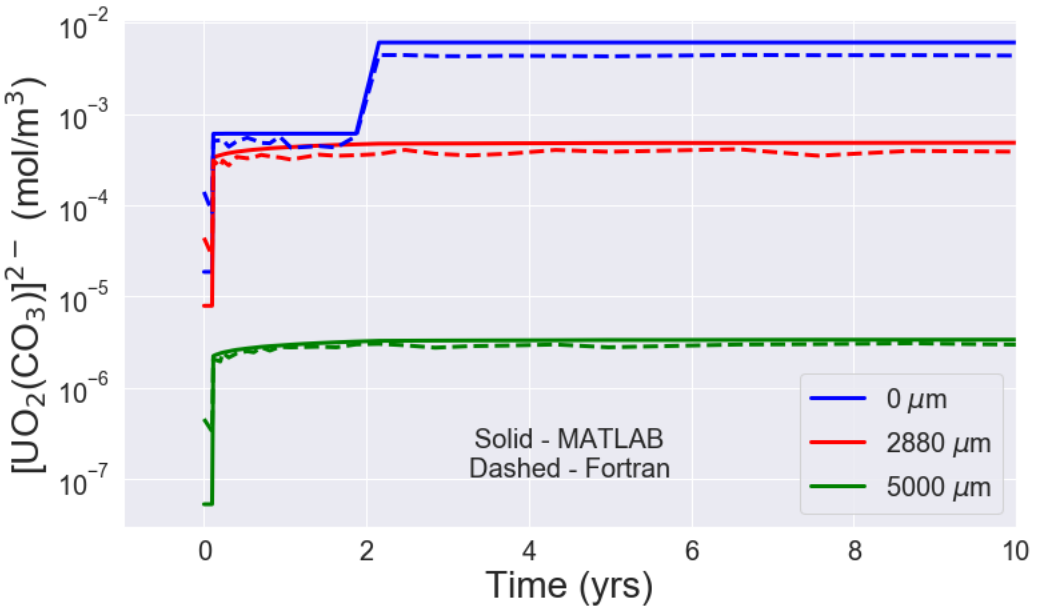

Fig. C-2 The concentration of $[UO_2(CO_3)]^{2-}$ as a function of time at 0 (blue), 2880 (red), and 5000 μm (green) representing distances at the fuel interface, the middle of the 1D domain, and the farthest point in the simulation. Results for the MATLAB (solid), Fortran code without the corrosion layer thickness turned on (dash), and Fortran code with the corrosion layer thickness (dotted) are shown.

C.6 FMD Time Stepping Challenge

The MATLAB code uses a fixed logarithmic time step algorithm to determine all time points at which to update the concentrations. The total number of time steps chosen by the user can cause simulations to fail. Sometimes failures can be avoided by increasing the number of grid cells, but it is also possible that the logarithmic time stepping algorithm causes important chemical transitions to be missed.

In the Fortran version an adaptive time stepping routine is implemented. If the number of Newton Raphson iterations required to update the concentrations exceeds a user-fixed tolerance, the time step is cut in half and the concentrations are reset to the previous solve. In this way, the timestep is allowed to adapt, on the fly, for difficult to converge points within the concentration profile. If concentrations are changing slowly and the number of iterations needed is low, then the time step is increased by a percentage depending on the number of iterations needed.

The adaptive time stepping routine is (in part) currently preventing simulation times from going more than several years. On a per time step basis the Fortran version is ~10 times faster than the MATLAB version which is encouraging for future development of surrogate models. However, the time step never reaches large values, typically remaining below 1 hour. Therefore, the Fortran version requires too many time steps for long time simulations. We believe this problem may be resolved by log transforming the concentrations as we discuss below.

C.7 Environmental Concentrations

The environment concentrations of all non-solid species (i.e., UO_2^{2+}, $UO_2(CO_3)_2^{2-}$, $UO_{2,(aq)}$, H_2O_2) at the bulk water boundary of the 1D domain are fixed at near-zero concentrations, 10^{-20} mol/m^3. For CO_3^{2-}, O_2, Fe^{2+}, and H_2, environmental concentrations in the test case are set by the user to 10^{-3}, 10^{-6}, 10^{-6}, and 10^{-6} mol/m^3 respectively. The effect of the near-zero concentrations at the bulk water boundary is to drive diffusion of the uranium species and H_2O_2 away from the fuel surface and out of the system.

Many of the reaction rates are 5th order on the concentrations. This causes reactions involving reactants with near-zero concentrations to proceed very slowly. Numerically, instabilities arise as the range of concentrations between species increases. Our next step is to implement a log formulation for the solver. In this context the Newtown Raphson algorithm is updated on the log values of the concentrations. The log formulation is expected to operate more smoothly when there are large differences in the magnitudes of the concentrations.

C.8 Conclusions

This year the fuel interface reactions and the corrosion layer thickness routine were added to the Fortran FMD code. These additions complete the implementation of all processes in the MATLAB code. Adding the interfacial reactions required implementation of two routines, one to solve for the concentrations and one to solve for the corrosion potentials.

Initial comparison between the models is favorable; however due to time stepping challenges the Fortran code takes too long to run long time simulations. Although the Fortran code is orders of magnitude faster than the MATLAB version on a per step basis, the adaptive time stepping routine causes the time steps to remain short, typically less than an hour. On-going work is focused on implementing a log-transformed formulation of the concentrations to feed to the solvers.

C.9 References

Jerden, J., Frey, K., Cruse, T., Ebert, W. (2012), Waste Form Degradation Model Status Report: Electrochemical Model for Used Fuel Matrix Degradation Rate, FCRD-UFD-2012-000169, Argonne National Laboratory.

Jerden, J., Frey, K., Copple, J.M., Ebert, W. (2014), ANL Mixed Potential Model for Used Fuel Degradation: Application to Argillite and Crystalline Rock Environments, FCRD-UFD-2014-000490, Argonne National Laboratory.

Jerden, J., Copple, J.M., Frey, K.E., Ebert, W. (2015), Mixed Potential Model for Used Fuel Dissolution – Fortran Code, FCRD-UFD-2015-000159, Argonne National Laboratory.

Jerden, J., Frey, K., Ebert, W., (2017) “Spent Fuel Matrix Degradation and Canister Corrosion: Quantifying the Effect of Hydrogen”, SFWD-SFWST-2017-000039, Argonne National Laboratory.

Jerden, J., Gattu, V.K., Ebert, W. (2018), Update on Validation and Incorporation of a New Steel Corrosion Module into Fuel Matrix Degradation Model, M4SF-18AN010301017, Argonne National Laboratory.

Shoesmith, D.W., Kolar, M., King, F. (2003), A Mixed-Potential Model to Predict Fuel (Uranium Dioxide) Corrosion within a Failed Nuclear Waste Container, Corrosion, 59:802-816.

Appendix D. SURROGATE MODELING OF THE FUEL MATRIX DEGRADATION (FMD) PROCESS MODEL WITH NEURAL ORDINARY DIFFERENTIAL EQUATIONS

SURROGATE MODELING OF THE FUEL MATRIX DEGRADATION (FMD) PROCESS MODEL WITH NEURAL ORDINARY DIFFERENTIAL EQUATIONS

D.1 Introduction

As discussed earlier in this report, the Geologic Disposal Safety Assessment (GDSA) Framework is an open source repository simulation software built around the massively-parallel multi-physics code PFLOTRAN. An important short-term goal of the development of the GDSA Framework (pa.sandia.gov) is to perform probabilistic repository simulations to identify sources of uncertainty to help prioritize future R&D. To achieve this short-term goal with current computer resources, developers must consider ways to include the effects of expensive process models in total system simulations.

High fidelity prediction of waste package and waste form degradation processes for thousands of waste packages in a probabilistic repository performance assessment calculation is expensive. With thousands of waste packages, thousands of time steps, and hundreds of realizations in a simulation to allow for uncertainty quantification, these process models may need to be called a billion times per simulation.

One way to reduce computational expense is to develop response surface surrogate models that can rapidly emulate the mechanistic process models. An ideal response surface surrogate model runs orders of magnitude faster than its parent mechanistic model and provides outputs identical to those of the mechanistic model within a specified range of the model inputs.

Over the past few years, a team of modelers and mathematicians at Sandia National Laboratories has been developing surrogate models for the UO_2 flux that is predicted by the Fuel Matrix Degradation (FMD) process model (Jerden et al., 2015a). The FMD process model has been coupled with PFLOTRAN (Mariner et al., 2015), but the coupled model runs too slowly for a set of probabilistic repository-scale simulations. The surrogate modeling work has examined Machine Learning (ML) approaches such as tabulation with tree-based lookup methods and artificial neural networks (Debusschere et al. 2023). This appendix describes the advances made over the past year into another surrogate approach: neural Ordinary Differential Equations (nODEs).

We next describe the FMD process model used to generate results for this appendix followed by a discussion of our general approach for surrogate modeling and the process for generating training data. Then, we review some prior results from surrogates using k-nearest neighbor regression and artificial neural network approaches and explore the use of surrogate models of neural ordinary differential equations, along with preliminary results.

D.2 Fuel degradation process model

The FMD process model used for the results in this appendix is a mechanistic spent fuel dissolution model coded in MATLAB and developed at Argonne National Laboratory and Pacific Northwest National Laboratory. The model calculates spent fuel dissolution rates as a function of radiolysis, alteration layer growth, diffusion of reactants through the alteration layer, temperature, and interfacial corrosion potential (Jerden et al., 2015b). It employs a one-dimensional (1D) reactive transport model to simulate diffusion and chemical reactions across this layer over time. The 1D domain, depicted in Fig. D-1, extends 0.05 m from the fuel surface to the bulk water. It is divided into as many as 100 cells with increasing length toward the bulk water boundary cell.

To couple the FMD model with PFLOTRAN, a "coupled" FMD process model was coded in Fortran (Mariner et al. 2015). At each time step, PFLOTRAN calls the coupled FMD model to obtain a new dissolution rate. Coupling requires PFLOTRAN to keep track of the 1D chemical profiles across the domain from the previous time step. It also requires relevant inputs from the main PFLOTRAN simulation, such as temperature, time, and environmental concentrations in the boundary cell. Dose rate is calculated in the coupled FMD model from time and burnup. A full list of FMD model inputs and outputs available for surrogate modeling is presented in Tab. D-1.

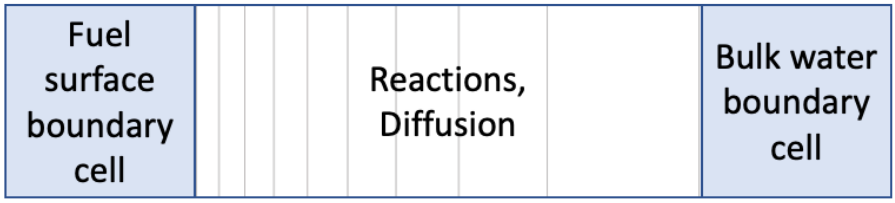

Fig. D-1 FMD Model Domain

Tab. D-1 Inputs/Outputs of FMD Model

Available Inputs	Outputs
• Initial concentration profiles across 1D corrosion/water layer (UO_2(s), UO_3(s), UO_4(s), H_2O_2, UO_2^{2+}, UCO_3^{2-}, UO_2, CO_3^{2-}, O_2, Fe^{2+}, and H_2) • Initial corrosion layer thickness • Dose rate at fuel surface (= f (time, burnup)) • Temperature • Time and time step length • Environmental concentrations (CO_3^{2-}, O_2, Fe^{2+}, and H_2)	• Concentration profiles across 1D corrosion/water layer • Corrosion layer thickness • Fuel dissolution rate (UO_2 flux)

The Fortran FMD model was tested on a problem involving a two-dimensional flow field containing 4 rows of 13 breached spent fuel waste packages. The model successfully simulated fuel degradation for each of the waste packages over 100 time steps (Mariner et al., 2015). Of the 45 minutes of computational time required to run the simulation, 30 minutes were used calculating the fuel dissolution rates in the FMD model.

D.3 Surrogate modeling

It is often useful to construct a surrogate model to use in uncertainty and sensitivity analysis of a computational physics model when it is computationally demanding. A surrogate model (sometimes called meta-model, emulator, or response surface model) is an inexpensive input-to-output mapping that replaces a process model. Once constructed, this meta-model is relatively inexpensive to evaluate so it is often used as a surrogate for the physics model in uncertainty propagation, sensitivity analysis, or optimization problems that may require thousands to millions of function evaluations (Simpson et al., 2008).

There are many different types of surrogate models, including neural networks (Pedregosa et al., 2011; Ben-David et al., 2014), k-Nearest Neighbor regression (Ben-David et al., 2014), and polynomial chaos expansions (Xiu, 2010; Ghanem & Spanos, 2002). Another popular approach in the literature is to develop an emulator that is a stationary smooth Gaussian process (Rasmussen & Williams, 2006; Santner et al., 2003). The popularity of Gaussian processes is due to their ability to model complicated functional forms and to provide an uncertainty estimate of their predicted response value at a new input point. There are many good overview articles that compare various meta-model strategies. Various smoothing predictors and nonparametric regression approaches are compared elsewhere (Simpson et al., 2008, Santner et al., 2003, Storlie et al., 2009). Simpson et al. provides an excellent overview not just of various statistical meta-model methods but also approaches that use low-fidelity models as surrogates for high-fidelity models. Haftka and his students developed an approach that uses ensembles of emulators or hybrid emulators (Viana et al., 2009).

Three ML surrogate modeling approaches are used in this work to predict the UO_2 flux resulting from fuel degradation: A k-nearest-neighbors regression (kNNr) surrogate model, an Artificial Neural Network (ANN), and a neural Ordinary Differential Equation (nODE). K-nearest neighbors models interpolate between points in a high-dimensional lookup table generated by sampling the FMD model. Artificial Neural Networks fit a nonlinear functional representation to the FMD process model data, and neural Ordinary Differential Equations fit a Neural Network to the time-derivative of the FMD process model data. All approaches require a sufficient amount of training data from the FMD process model. The kNNr and ANN approaches have been described in (Debusschere et al., 2023 and Mariner et al., 2022), but some of the theory and results are repeated here to set the context for the nODE developments.

D.3.1 k-Nearest Neighbor Regression

The k-Nearest Neighbors regressor (kNNr) is a supervised, non-parametric machine learning method that tabulates data points inside of a domain X with labels Y. The label for a point within the domain but not in the "table" is obtained as a weighted average of the labels of the k nearest neighbors of this new point, where $k \geq 1$ is fixed. The definition of nearest depends on the metric function one uses, though a typical choice is the Minkowski metric $\left(\sum_{i=1}^{d} |x_i - y_i|^p\right)^{\frac{1}{p}}$, with $p \geq 1$. The case of $p = 2$ is the popular Euclidean metric, which is used in this work. For efficient look-up in high-dimensional data sets, a K-D Tree tabulation method is used (Pedregosa et al., 2011). The inverse distances from the nearest-neighbor table points to the query point are used as the weight in the interpolation, so that points further away from the query point have less influence than more nearby points.

One of the attractive aspects of kNNr is that it makes predictions based on local information only, and therefore does not require global smoothness over the input space. As each prediction is a weighted average of known table points, the approach is also highly interpretable. On the other hand, the approach requires a sufficiently dense table to get good predictive accuracy, and the cost of table look-ups increases as the table density increases.

For model development and metaparameter tuning, we employed the kNNr implementation from the Python Scikit-Learn module (Pedregosa et al., 2011). For coupling to PFLOTRAN reservoir simulations, we relied on the open source FORTRAN code KDTREE 2 (Kennel, 2004).

D.3.2 Artificial Neural Network

Artificial Neural Network (ANN) models are commonly employed by the machine learning community for regression and classification problems. They can be described as intricate networks of "artificial neurons" that are essentially weighted combinations of (usually simple) nonlinear functions. One motivation for the development of neural networks (Pedregosa et al., 2011; Ben-David et al., 2014; Rasmussen & Williams, 2006) was to create a regression approach for complex functions that avoids the combinatorial growth of the parameter space that occurs in polynomial regression models as more inputs are added.

ANN can be more accurate than kNNr using fewer training data as its functional representation helps to interpolate in areas where fewer training data are available. However, ANN models are not as readily interpretable as kNNr models, and care must be taken to avoid overfitting.

The ANN surrogate was developed in Python using the Tensorflow/Keras module (Abadi et al, 2016). A feed-forward neural network structure was selected with the popular rectified linear unit (ReLU) activation function. All training and metaparameter tuning were done in Python. For coupling to PFLOTRAN reservoir simulations, a Fortran ANN evaluator was written specifically for the selected network configuration. This evaluator reads in the ANN weights that were determined offline in the Python training and tuning scripts.

D.3.3 Neural Ordinary Differential Equations

Neural Ordinary Differential Equations (nODEs) use neural networks to approximate the derivative of a system state (Chen et al., 2018). Then, to evaluate the system state itself, the neural network, initial conditions, other parameters, and desired output time points are fed into an ODE solver. This approach leverages the fact that the evolution of the fuel cask internal state is a dynamic system. The time-dependency requires sequential training data as well as initial conditions for any quantities of interest.

Since backpropagation through the ODE solver during training introduces computational challenges, our method of training a neural ODE surrogate follows that of Raissi et al. (Raissi et al., 2018), which uses a linear multistep method for the ODE solver. Specifically, we use a one-step Adams-Moulton approach to train the neural ODE with the following expression for the training error:

$$-u_{n+1} + u_n + \frac{\Delta t}{2}\left[f(u_{n+1},\lambda_{n+1}) + f(u_n,\lambda_n)\right] = w$$

where u_n is the system state at a time, λ_n are the parameters, Δt is the timestep, f is the derivative of the system state as approximated by the neural network, and w is the error between the approximated system state and the actual system state. While we use Adams-Moulton here, other multistep methods could be substituted. Any multistep method, however, requires data at equidistant timesteps.

The neural ODE surrogate was developed in Python using nn.Module in PyTorch. The neural network architecture comprises a series of fully-connected layers with equal numbers of neurons, separated by hyperbolic tangent activation functions. The weights for the fully connected layers are initially taken randomly from a normal distribution (with a mean of 0 and a standard deviation of 0.1) and the bias is set to 0. A learning rate of 0.01 for the training of the network is appropriate. During evaluation, we use the odeint solver from scipy.integrate.

D.4 Training Data

We used a standalone MATLAB implementation of the FMD process model to generate training data by randomly sampling the inputs to the model. The training data itself can be very large. For example, we may have millions of samples of FMD, where each sample involves a multi-dimensional vector sample of inputs such as the environmental concentrations, temperature, burnup, etc. (the left-hand quantities in Tab. D-1). The output is also extensive, since each FMD run involves a hundred timesteps with lots of information about the fuel cask state reported at every time step (e.g., the right-hand quantities in Tab. D-1). Note that in this work, we focus on predicting the fuel dissolution rate (UO_2 flux), although the other two output quantities could be treated with a surrogate in a similar manner.

A Latin hypercube sampling (LHS) study was performed to generate training and validation data for regression from the standalone FMD process model. LHS is a stratified sampling technique that generates "well-spaced" samples; it typically gives lower variance statistical estimators than plain Monte Carlo sampling (Helton & Davis, 2003). The six-dimensional sample space contained the parameters initial temperature, burnup, and the environmental concentrations of CO_3^{2-}, O_2, Fe^{2+}, and H_2. The probability distributions for each parameter are given in Tab. D-2.

Tab. D-2 Input parameters and their distributions

Parameter	Distribution	Min.	Max.
Init. Temp. (K)	Uniform	300	400
Burnup (Gwd/MTU)	Uniform	40	65
Env. CO_3^{2-} (mol/m^3)	Log-uniform	10^{-3}	2×10^{-2}
Env. O_2 (mol/m^3)	Log-uniform	10^{-7}	10^{-5}
Env. Fe^{2+} (mol/m^3)	Log-uniform	10^{-3}	10^{-2}
Env. H_2 (mol/m^3)	Log-uniform	10^{-5}	2×10^{-2}

The temporal discretization in each problem consists of 101 logarithmically-spaced (base 10) points in time from 0 to 10^5 years. Some FMD runs need to be filtered out if they either get stuck in infinite loops and never finish or if they show unphysical results, such as the UO_2 surface flux stagnating after 10^4 years, or the Corrosion Layer Thickness (CLT) growing beyond the computational domain of 0.05m.

To assess the accuracy of the models for a specific training data size, we analyzed the normalized root mean squared error ($nrmse$), which is computed over the data set as:

$$nrmse = \frac{\sqrt{\frac{1}{N}\sum_{i=1}^{N}(y_{pred,i} - y_{true,i})^2}}{\frac{1}{N}\sum_{i=1}^{N} y_{true,i}} \quad \text{(D-1)}$$

where N is the total number of data points. In other words, the $nrmse$ is the root mean squared error normalized by the mean of the true data. Another metric is the mean absolute percentage error ($mape$), which is computed as:

$$mape = \frac{1}{N}\sum_{i=1}^{N}\left|\frac{y_{pred,i} - y_{true,i}}{y_{true,i}}\right| \times 100 \quad \text{(D-2)}$$

The $mape$ error, due to its relative nature, does a good job of treating the approximations in all quantities, large or small, with equal importance. On the other hand, the $mape$ can be sensitive to numerical noise,

for example when reasonable errors get divided by very small quantities in absolute value. Also, for some applications, the approximation of the larger values is the most important criterion. For these situations, the $nrmse$ is a good overall measure of goodness. For a data set where the Quantity of Interest (QoI) spans many orders of magnitude, it is good to consider both metrics.

D.5 Prior Results with k-nearest neighbors and artificial neural networks

Early work with the kNNr and ANN surrogate models (Debusschere et al., 2023) used only environmental concentrations, the dose rate, and temperature as inputs. While the results with these inputs were encouraging, the accuracy of the surrogates is not superb. In this section, we show the potential of getting more accurate surrogate models by incorporating additional information about the internal fuel cask state, such as the Corrosion Layer Thickness (CLT), as covered in Mariner et al., 2022. Since the CLT is not readily available without running a detailed FMD process model, a dual surrogate model approach is followed.

A first surrogate model predicts the CLT at the current time, using the CLT at the previous time step and the time step size as inputs, in addition to the inputs in Tab. D-1. A second surrogate predicts the UO_2 flux, using this same expanded input set. After advancing to the next time step, the CLT predicted by the surrogate in the previous time step becomes part of the inputs for the next time step.

This dual surrogate approach was implemented for the kNNr surrogate, using dose rate, temperature, and the concentrations of CO_3^{2-} and H_2 along with CLT at the previous time step and the time step size as inputs. The surrogate was trained using a data set of 1 million FMD Matlab runs sampled from the distributions listed in Tab. D-2. After removing unphysical runs, 15% of the data was split off as validation data and 10% was split off as testing data, resulting in about 9.4 million validation data points, 6.3 million testing data points, and 47 million training data points. Following (Debusschere et al., 2023), the training data was down-sampled by randomly selecting a given number of samples from each FMD time trajectory.

Based on the trends in preliminary tuning of the kNNr meta parameters, both the CLT and UO_2 flux are best predicted using about 8 – 12 nearest neighbors with as much training data as possible. Based on these tuning results, a kNNr configuration of 10 nearest neighbors using all available training data (all 23 million samples from the data set that was downsampled to 50 samples per FMD process model run) was selected to predict the testing data. This testing data has not been used in any of the training and tuning of the kNNr surrogate.

Fig. D-2 and Fig. D-3 below compare the kNNr predictions of the CLT and UO_2 flux to the testing data for 50 randomly sampled trajectories of the FMD process model. Note that in this comparison, each data point in the time trajectories was predicted on its own, using the inputs provided by the testing data. In a practical PFLOTRAN repository simulation, the CLT value at the previous time step would not be readily available as the PFLOTRAN model does not track CLT independently. This CLT value would therefore need to be approximated by the same surrogate operating on the inputs from the prior time step. As such, if Fig. D-2 had been generated with a true time integration approach, where only the initial values of the CLT were specified, errors in the successive surrogate approximations for the CLT would have compounded over time, and might have caused the trajectories to diverge from the MATLAB model predictions over time. The analysis shown here is still useful as it shows where such errors are most likely to originate.

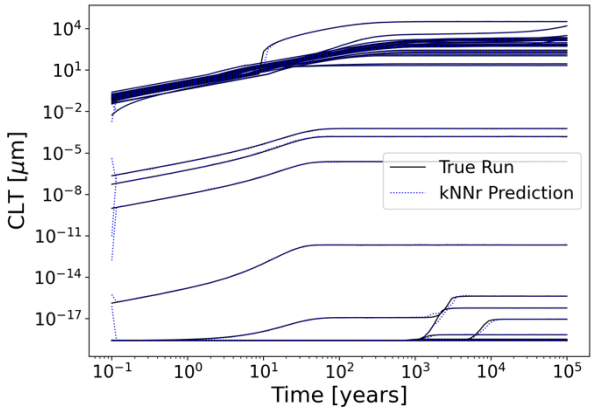

Fig. D-2 Comparison of the True and kNNr prediction of the CLT for 50 randomly selected runs in the testing data.

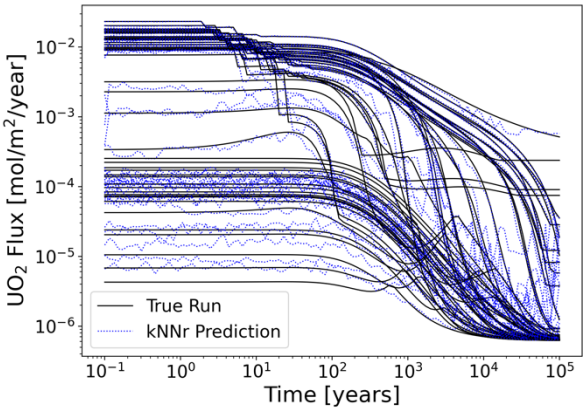

Fig. D-3 Comparison of the True and kNNr prediction of the UO_2 flux for 50 randomly selected runs in the testing data.

Aside from some deviations early in time, the kNNr predictions of the CLT in Fig. D-2 are very close to the true values in the testing data. This graph also illustrates the very wide range in CLT values.

The predictions of the UO_2 fluxes in Fig. D-3 show good agreement with the test data, although the agreement is not as good as for the CLT predictions. As observed also in (Debusschere et al., 2023), the kNNr prediction is noisy as it is a local prediction, drawing information only from 10 nearest neighbors to each query point in the training sample space.

Overall, with this kNNr configuration of 10 nearest neighbors and 23 million training samples, the prediction of the UO_2 flux in the testing data shows an $nrmse$ error of 0.11, and a $mape$ error of 29%.

Fig. D-4 and Fig. D-5 below compare the ANN predictions of the CLT and UO_2 flux to the testing data for 50 randomly sampled trajectories of the FMD process model. Also, in this comparison, each data point in the time trajectories was predicted on its own, using the inputs provided by the testing data.

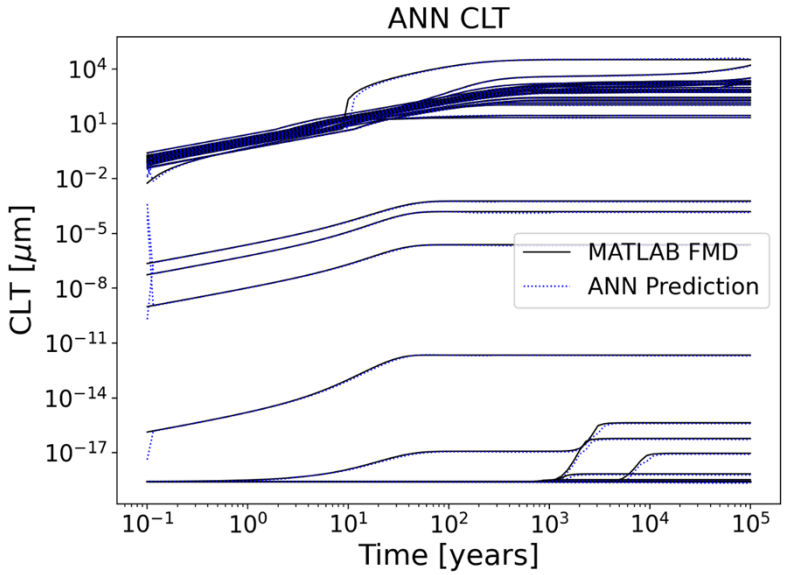

Fig. D-4 Comparison of the True and ANN prediction of CLT for 50 randomly selected runs in the testing data.

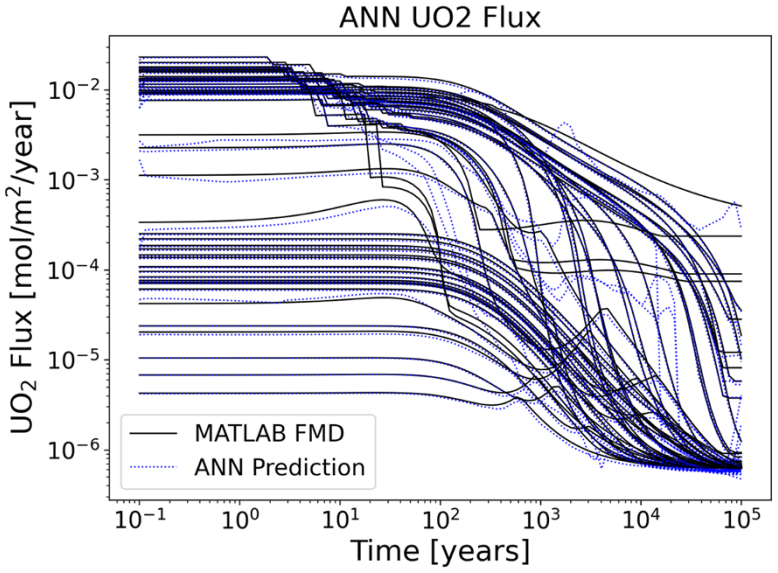

Fig. D-5 Comparison of the True and ANN prediction of the UO_2 flux for 50 randomly selected runs in the testing data.

Overall, with the ANN configuration of 2 layers and 64 nodes per layer and 23 million training samples, the prediction of the UO_2 flux in the testing data shows an $nrmse$ error of 0.12, and a $mape$ error of 14%. A summary of the surrogate results when CLT is used as an input is in Tab. D-3.

Tab. D-3 Error metrics for kNNr and ANN surrogates on UO_2 flux testing data for the case where CLT information is used along with the environmental information as an input

Surrogate	nrmse	mape
kNNr	0.11	29%
ANN	0.12	14%

D.6 Preliminary Results with Neural Ordinary Differential Equations

D.6.1 Surrogates Using Training Data with 100 Time Steps

With the same data set from training and testing as the kNNr and ANN trials, we use the following inputs for the neural ODE: the environmental concentrations of CO_3 and H_2, the temperature, the dose rate, the current corrosion layer thickness (CLT), and the current UO_2 flux. (Since CLT and UO_2 are the quantities of interest, we require them both to be inputs since initial conditions are required for solving an ODE.) Then, using this information, we predict the CLT and UO_2 flux at the next time step. Because of the time-dependent nature of this approach whole trajectories of 100 time points are used as training data. Taking the logarithm of time ensures data points are equidistant in time, as required for the multistep scheme used in the loss function for the neural network training.

During hyperparameter tuning, we consider the number of training epochs, the number of layers in the neural network, the number of neurons per layer, and the amount of training data to use. We use ten folds for cross-validation for each of these hyperparameters.

The loss (for which we use mean absolute error) for a surrogate of four layers and 16 neurons per layer trained with 200 trajectories of data converges by 20,000 epochs (as seen in the Fig. D-6 below). So, for the rest of the tuning, we will use 20,000 epochs for training.

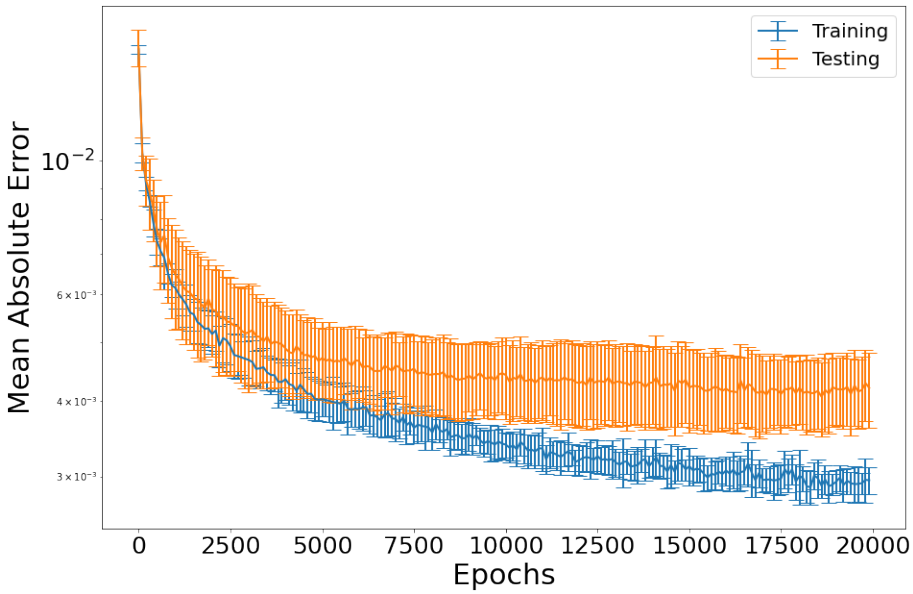

Fig. D-6 The mean absolute error for the combined prediction of CLT and UO_2 flux as a function of the number of epochs of training.

Varying the number of layers (each with 16 neurons) in the neural network shows that more layers decreases the mean absolute error, but by 4 layers, adding additional layers does not increase accuracy (Fig. D-7). Similarly, increasing the number of neurons per layer (while keeping the 4 layers) decreases the mean absolute error, but increasing beyond 16 layers does not increase accuracy (Fig. D-8). In the tuning of the network's architecture, we find that the mean absolute error converges by 500 trajectories of training data.

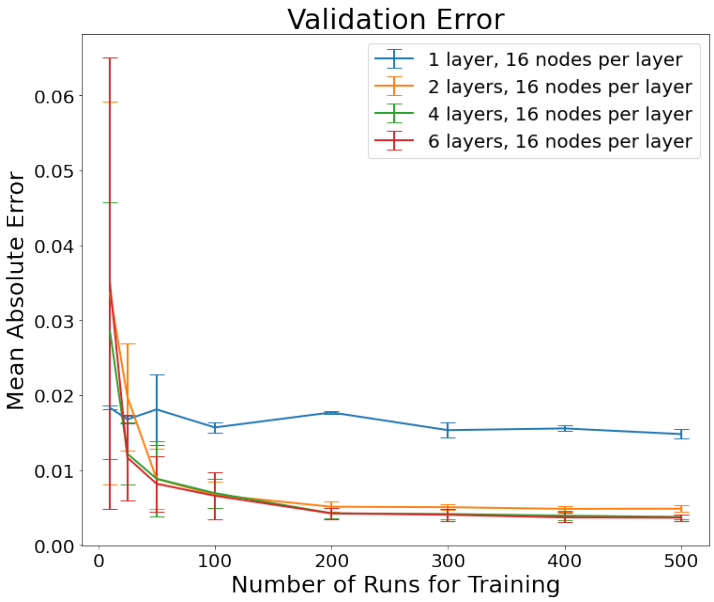

Fig. D-7 The mean absolute error for the combined prediction of CLT and UO_2 flux as a function of the amount of training trajectories for different numbers of neural network layers.

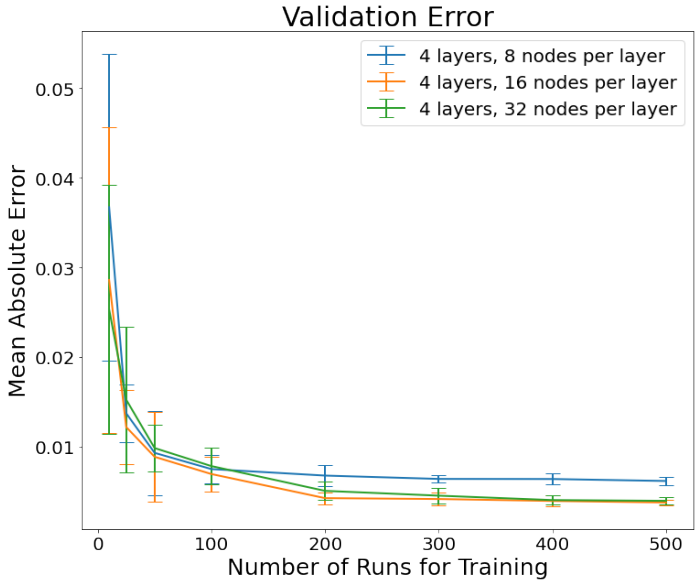

Fig. D-8 The mean absolute error for the combined prediction of CLT and UO_2 flux as a function of the amount of training trajectories for different numbers of neurons per neural network layer.

Based on the tuning results, we use a model of 4 layers, 16 neurons per layer, trained with 500 trajectories of training data for 20,000 epochs to predict the testing data. This testing data has not been used in any of the training and tuning of the surrogate. We predict each point on its own from the testing data at the previous timestep. Fig. D-9 and Fig. D-10 below compare the neural ODE surrogate's predictions of CLT and UO_2 flux to the testing data for 50 randomly-sampled trajectories of the FMD process model. The predictions for both CLT and UO_2 flux follow the actual trajectories quite closely and smoothly.

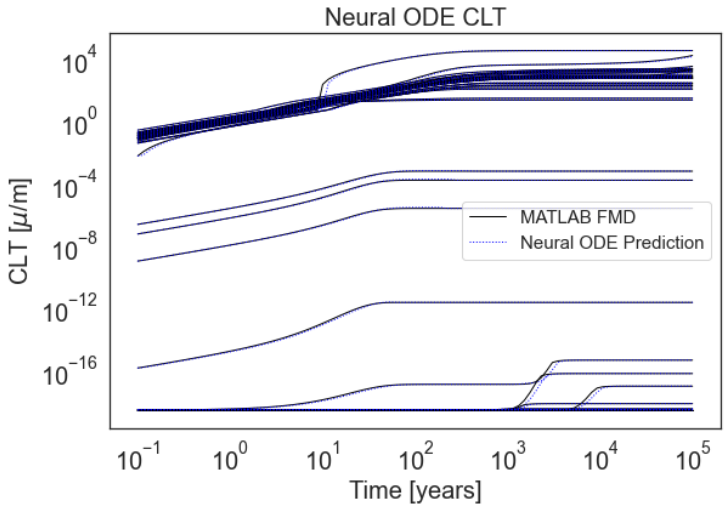

Fig. D-9 Comparison of the true and neural ODE prediction of the corrosion layer thickness for 50 randomly selected runs in the testing data.

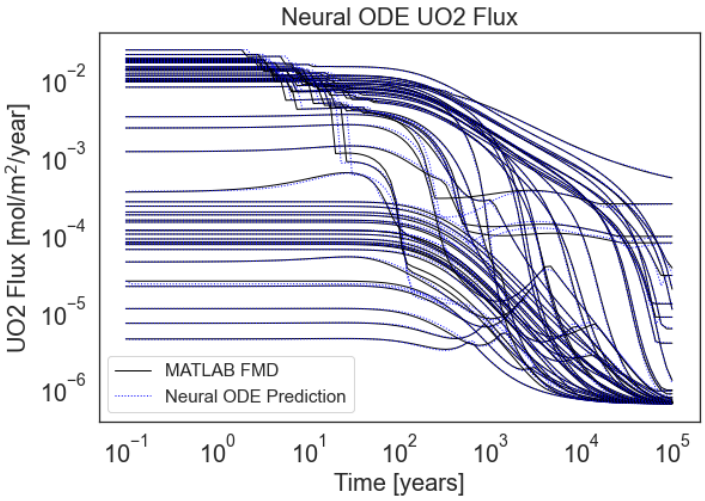

Fig. D-10 Comparison of the true and neural ODE prediction of the UO_2 flux for 50 randomly selected runs in the testing data.

Over all of the UO_2 flux testing data, a neural ODE surrogate with 4 layers of 16 neurons per layer, trained with 500 trajectories for 20,000 epochs yields a normalized root mean square error of 0.086 and a mean absolute percentage error of 1.9%. These are lower errors than those of the kNNr and ANN methods, as shown in Tab. D-4. However, it should be noted that the neural ODE surrogate uses UO_2 flux as an input, while the other surrogate methods do not. Using the UO_2 flux as an input in this way needs to be investigated since this flux is prone to rapid changes between times steps and could engage in a positive feedback loop. This is the subject of ongoing work.

Tab. D-4 Error metrics for the 3 surrogate modeling approaches on testing data based on training data with 100 time steps

Surrogate	nrmse	mape
kNNr	0.11	29%
ANN	0.12	14%
nODE	0.086	1.9%

D.6.2 nODE Surrogates with Finer Time Steps

To explore the impact of time step size, we generated a new training data ensemble using various time step sizes. As with the other training and testing set, we used a standalone MATLAB implementation of the FMD process model to generate training data by randomly sampling the inputs to the model.

A Latin hypercube sampling (LHS) study was performed to generate training and validation data for regression from the standalone FMD process model. To incorporate the impact of waste packages breaching at different times, we also sampled over the delay time in the Matlab FMD model. In the Matlab FMD model input file, we set the decay time (time between the moment spent fuel is taken out of a reactor and emplacement in the repository) to zero, so that the delay time would represent the time till waste package breach. The seven-dimensional sample space thus contained the parameters initial temperature, burnup, delay time, and the environmental concentrations of CO_3^{2-}, O_2, Fe^{2+}, and H_2. The probability distributions and ranges for each parameter are given in Tab. D-5.

Tab. D-5 Input Parameters and Their Distributions for Ensembles with Various Time Step Sizes

Parameter	Distribution	Min.	Max.
Init. Temp. (K)	Uniform	300	600
Burnup (Gwd/MTU)	Uniform	40	80
Delay Time (years)	Log-uniform	100	10000
Env. CO_3^{2-} (mol/m^3)	Log-uniform	10^{-3}	2×10^{-2}
Env. O_2 (mol/m^3)	Log-uniform	10^{-7}	10^{-5}
Env. Fe^{2+} (mol/m^3)	Log-uniform	10^{-3}	10^{-2}
Env. H_2 (mol/m^3)	Log-uniform	10^{-5}	2×10^{-2}

Using these parameter samples, 1000 trajectories were generated for different temporal discretizations: 101, 201, 401, 801, and 1601 logarithmically-spaced (base 10) points in time from 0 to 10^5 years. Some of the FMD runs were filtered out if they either got stuck in an infinite loop and never finished or if they showed unphysical results, such as the UO_2 surface flux stagnating after 10^4 years, or the Corrosion Layer Thickness (CLT) growing beyond the computational domain of 0.05m. If a particular run was discarded in any of the five sets of time series, then this run was removed from all of them. Further, some runs followed vastly different paths between sets. Since these are likely where computational error was introduced, these runs were also removed from the data. In the end, 572 different trajectories were retained in the data set.

Using the data set with 1600 time steps, we assessed the impact of using different numbers of time points in the training on the accuracy of the trained neural ODE. We skipped every other point to emulate a set of 800 time steps, every four for a set of 400, and so on. Doubling the number of timesteps roughly doubles the accuracy for a neural ODE with 4 layers and 16 nodes, as seen in the cross-validation results in Fig. D-11.

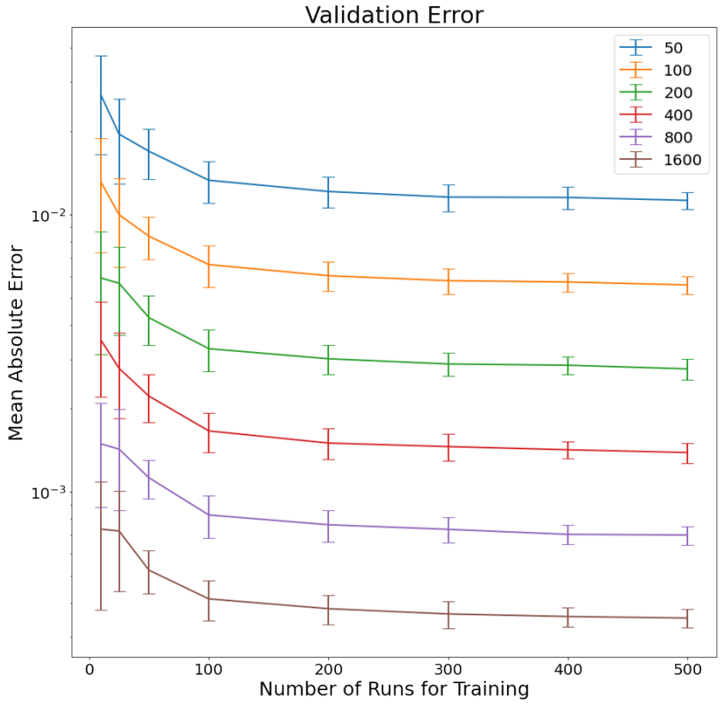

Fig. D-11 The mean absolute error for the combined prediction of CLT and UO_2 flux as a function of the amount of training trajectories for different numbers of time steps per run.

Inputs, outputs, and pre- and post-processing files for the work presented in this appendix are available in the GDSA Calculation Archive under CTN: 230814-FMDSURR-03.

D.7 Ongoing and Future Work

Ongoing work with the neural ODE surrogate further investigates the impact of the timestep size on the accuracy of the predictions. We are also exploring the number of steps used in the multistep scheme during neural ODE training. Note that all surrogate model results so far have focused on predictions of test data one time step at a time (with all inputs provided by test data). For a testing scenario that is closer to reality, we will also compare the methods on how they perform when integrating from the initial conditions all the way to the final state (without relying on testing data to provide the inputs for each time step).

D.8 Conclusions

Three machine learning surrogate models are under consideration to rapidly emulate the effects of the Fuel Matrix Degradation (FMD) process model in GDSA Framework. One is a k-Nearest Neighbors regressor (kNNr) method that operates on a lookup table, another is an Artificial Neural Network, and the final uses neural ordinary differential equations (nODEs). All approaches have a high degree of accuracy,

provided that enough training data are available with inputs that are informative of the UO_2 flux that results from the fuel dissolution.

While earlier work used kNNr and ANN methods, the current work explored the use of neural ODEs to predict both Corrosion Layer Thickness (CLT) and UO_2 Flux. Our results show that this approach improves accuracy relative to the previous surrogate methods. In addition, using more data points in each run also improves accuracy. Ongoing work involves continuing to investigate the size of the timestep between data points and how many previous data points to use in predictions.

The aim of these surrogate models is to enable GDSA Framework to simulate spent fuel dissolution for each individual breached spent fuel waste package in a probabilistic repository simulation. Having the ability to emulate spent fuel dissolution in probabilistic PA simulations will have the added capability of allowing uncertainties in spent fuel dissolution to be propagated and sensitivities in FMD inputs to be quantified and ranked against other inputs.

D.9 References

Abadi, M., et al. (2016). “TensorFlow: A System for Large-Scale Machine Learning”, 12th USENIX Conference on Operating Systems Design and Implementation (OSDI’16), Savannah, GA, November 2–4

Ben-David, S. and S. Shalev-Shwartz (2014). Understanding Machine Learning: From Theory to Algorithms. Cambridge, United Kingdom, Cambridge University Press.

Chen, R. T. Q., Y. Rubanova, J. Bettencourt, D. Duvenaud (2018). “Neural Ordinary Differential Equations,” https://doi.org/10.48550/arXiv.1806.07366

Debusschere, B.J., D.T. Seidl, T.M. Berg, K.W. Chang, R.C. Leone, L.P. Swiler, P.E. Mariner (2023), “Machine Learning Surrogates of a Fuel Matrix Degradation Process Model for Performance Assessment of a Nuclear Waste Repository”, Nuclear Technology, 209(9), pp. 1295-1318, https://doi.org/10.1080/00295450.2023.2197666

Ghanem, R. and P. Spanos (2002). *Stochastic Finite Elements: A Spectral Approach*. New York, New York: Springer Verlag.

Helton, J. C. and F. J. Davis (2003). "Latin hypercube sampling and the propagation of uncertainty in analyses of complex systems." Reliability Engineering & System Safety 81(1): 23-69.

Jerden, J., G. Hammond, J. M. Copple, T. Cruse and W. Ebert (2015b). Fuel Matrix Degradation Model: Integration with Performance Assessment and Canister Corrosion Model Development. FCRD-UFD-2015- 000550. Washington, DC, US Department of Energy.

Jerden, J., J. M. Copple, K. E. Frey and W. Ebert (2015a). Mixed Potential Model for Used Fuel Dissolution - Fortran Code. O. o. U. N. F. Disposition. FCRD-UFD-2015-000159. Washington, DC, US Department of Energy.

Kennel, M. B. (2004). KDTREE 2: Fortran 95 and C++ software to efficiently search for near neighbors in a multi-dimensional Euclidean space. https://arxiv.org/pdf/physics/0408067.pdf, Institute for Nonlinear Science, University of California.

Mariner, P. E., W. P. Gardner, G. E. Hammond, S. D. Sevougian and E. R. Stein (2015). Application of Generic Disposal System Models. FCRD-UFD-2015-000126, SAND2015- 10037 R. Sandia National Laboratories, Albuquerque, New Mexico.

Mariner, P. E., B. J. Debusschere, D.E. Fukuyama, J.A. Harvey, T.C. La Force, R.C. Leone, F.V. Perry, L.P. Swiler, A.M. Taconi (2022), GDSA Framework Development and Process Model Integration FY2022, SAND2022-14304 R and M2SF-22SN010304093

Pedregosa, F., G. Varoquaux, A. Gramfort, V. Michel, B. Thirion, O. Grisel, M. Blondel, P. Prettenhofer, R. Weiss, V. Dubourg, J. Vanderplas, A. Passos, D. Cournapeau, M. Brucher, M. Perrot and E.

Duchesnay (2011). "Scikit-learn: Machine Learning in Python." Journal of Machine Learning Research 12: 2825-2830.

Raissi, M., P. Perdikaris, G. E. Karniadakis (2018). “Multistep Neural Networks for Data-driven Discovery of Nonlinear Dynamical Systems,” https://arxiv.org/abs/1801.01236.

Rasmussen, C. E. and C. K. I. Williams (2006). Gaussian Processes for Machine Learninged., MIT Press.

Santner, T., B. Williams and W. Notz (2003). The Design and Analysis of Computer Experimentsed. New York, New York, Springer.

Simpson, T. W., V. Toropov, V. Balabanov and V. F.A.C. (2008). Design and analysis of computer experiments in multidisciplinary design optimization: A review of how far we have come or not. Proceedings of the 12th AIAA/ISSMO Multidisciplinary Analysis and Optimization Conference, Victoria, British Columbia, Canada. AIAA Paper 2008-5802.

Storlie, C. B., L. P. Swiler, J. C. Helton and C. J. Sallaberry (2009). "Implementation and evaluation of nonparametric regression procedures for sensitivity analysis of computationally demanding models." Reliability Engineering & System Safety 94(11): 1735-1763.

Viana, F.A.C., R.T. Haftka, and V. Steffen (2009). "Multiple surrogates: how cross-validation errors can help us to obtain the best predictor," *Structural and Multidisciplinary Optimization*, 39(4), 439-457

Xiu, D. (2010) *Numerical Methods for Stochastic Computations: A Spectral Method Approach*. Princeton University Press.